

The Effects of Structure, Humidity and Aging  
on the Mechanical Properties of Polymeric Ionomers  
for Fuel Cell Applications

Julie Tammy Uan-Zo-li

Thesis submitted to the Faculty of the  
Virginia Polytechnic Institute and State University  
in partial fulfillment of the requirements for the degree of

MASTER OF SCIENCE

in

Materials Science and Engineering

Dr. Ronald G. Kander, Chairman

Dr. Brian J. Love

Dr. Douglas J. Nelson

December 2001

Blacksburg, Virginia

KEYWORDS: Fuel Cell, Proton Exchange Membrane,  
Nafion<sup>®</sup>, Dais<sup>®</sup>, Physical Aging, Diffusion Properties

Copyright 2001, Julie T. Uan-Zo-li

# The Effects of Structure, Humidity and Aging on the Mechanical Properties of Polymeric Ionomers for Fuel Cell Applications

Julie Tammy Uan-Zo-li

Ronald G. Kander, Advisory Chairman  
Materials Science and Engineering Department

## Abstract

The purpose of this work was to investigate the effects of structure, humidity and aging on the mechanical behavior of Nafion<sup>®</sup> and Dais<sup>®</sup> ionomers. It was determined that the majority of the properties of these membranes were controlled by the formation and growth of the ionic clusters that were the direct result of the ionic nature of these materials.

In the process of this study, the properties of Nafion<sup>®</sup> and sulfonated Dais<sup>®</sup> polymers were investigated by dynamic mechanical analysis and thermal gravimetric analysis and their water uptake and sorption and desorption isotherms were measured. A mastercurve and a shift factor plot were constructed for 60% sulfonated Dais<sup>®</sup> membrane.

It was determined that an increase in the degree of sulfonation raised the glass transition temperature of these materials by facilitating the formation of the ionic clusters which acted as physical crosslinks, thereby reducing the mobility of polymeric chains. Water was found to effectively plasticize the membranes, especially in the case of Dais<sup>®</sup> materials, by reducing the storage modulus and decreasing the structural integrity of the ionomers. The effect of pre-treatment of Nafion<sup>®</sup> was investigated and the glass transition temperature was found to increase as a function of the severity of the treatment procedure. The maximum water uptakes were determined for virgin and aged Nafion<sup>®</sup> and Dais<sup>®</sup> membranes and their vapor phase water sorption diffusion coefficients were

calculated. The sorption process was found to follow pseudo-Fickian behavior, while the movement of water out of the membranes during the desorption process was determined to be controlled by mechanisms other than diffusion. Lastly, the effect of exposure of Nafion<sup>®</sup> and 30% sulfonated Dais<sup>®</sup> membranes to the saturated environment at elevated temperatures was investigated and found to result in the increase in the glass transition temperature of the materials. Results of the exposure effects on the diffusion properties of Nafion<sup>®</sup> and Dais<sup>®</sup> were inconclusive. Preliminary findings attributed the changes in the properties of the materials to the counteractive actions of physical aging and the growth of the ionic clusters.

## ACKNOWLEDGEMENTS

I would like to express my sincere gratitude to the members of my committee: my advisor, Dr. Ronald G. Kander, Dr. Brian J. Love and Dr. Douglas J. Nelson for the technical advice and moral support.

I would like to thank the Graduate Automotive Technology Education (GATE) Center of Virginia Tech for providing the financial support for this research project by awarding me with a GATE fellowship.

A lot of thanks to the following people for the help with this thesis. Michael Quah of DuPont Corporation and Dr. Glenn Doell of Dais-Analytic Corporation for providing me with the materials for this study. Ashish Aneja and Dr. Wilkes for the use of their DMA unit and Steve McCartney for performing the SEM experiments. Dr. Sean Corcoran and Dr. William Reynolds for the helpful technical discussions. Special thanks to Dr. Patricia Dolez for setting up the environmental chamber with the continuous data acquisition system and for a lot of help around the lab.

Thanks to Mrs. Susette Sowers for always getting all the organizational things done around the lab. Thank you very much to my colleagues and friends for their technical advice, English advice, life advice and just fun times: Dr. Mitchell Jackson, Dr. Jennifer McPeak, Sumitra Subrahmanyam, Derek Klinedinst, Dr. Julie Martin, Scott Trenor, Dan Esterly, David Brooks, Allison Suggs, Jeff Schultz and Michelle Jensen.

I would like to thank our mini -“Russian Community”: Ksenia, Phil, Irina, Zara, Gleb, Vitya, Vova and Vlada for always being there to distract me from doing the boring things, keeping me company when I was feeling down and offering me advice when I needed it.

I would also like to thank my family: my parents, Tamara and Mike, Rima, my brother Joe and sisters, Anna and Rachel, without whom this work would never be possible.

And finally, I would like to thank my husband, Alex Uan-Zo-li, for sharing with me all the good and the bad times, for the endless discussions and lectures about life, literature, music, economics, politics, morals and world in general, for tolerating my mood swings and panic attacks, but most importantly for always making me feel that no matter what happens, I will always have something to fall back on to, my own little fortress where I am always welcome. Spasibo, Solnsce.

# TABLE OF CONTENTS

<b>1</b>	<b>INTRODUCTION.....</b>	<b>1</b>
<b>2</b>	<b>BACKGROUND .....</b>	<b>3</b>
2.1	FUEL CELLS .....	3
2.2	PEMFC MEMBRANE MATERIALS.....	6
2.3	PHYSICAL AGING OF POLYMERS .....	9
2.4	TIME-TEMPERATURE SUPERPOSITION .....	12
2.5	WATER PLASTICIZATION.....	15
2.6	MOISTURE UPTAKE.....	16
2.7	SULFONATION EFFECT .....	19
2.8	THERMAL STABILITY .....	20
2.9	DYNAMIC MECHANICAL ANALYSIS .....	22
<b>3</b>	<b>EXPERIMENTAL.....</b>	<b>24</b>
3.1	MATERIALS.....	24
3.2	METHODS: DMA.....	26
3.3	METHODS: DSC.....	30
3.4	METHODS: TGA .....	32
3.5	METHODS: FTIR.....	33
3.6	METHODS: WATER UPTAKE .....	35
3.7	METHODS: SEM .....	36
<b>4</b>	<b>RESULTS .....</b>	<b>37</b>
4.1	DMA: NAFION <sup>®</sup> MEMBRANES.....	37
4.2	DMA: DAIS <sup>®</sup> MEMBRANES .....	47
4.3	TGA: NAFION <sup>®</sup> MEMBRANES .....	58
4.4	TGA: DAIS <sup>®</sup> MEMBRANES.....	59
4.5	FTIR: DAIS <sup>®</sup> MEMBRANES .....	65
4.6	WATER UPTAKE: NAFION <sup>®</sup> MEMBRANES .....	70

4.7	WATER UPTAKE: DAIS <sup>®</sup> MEMBRANES .....	71
4.8	WATER SORPTION KINETICS: NAFION <sup>®</sup> MEMBRANES.....	72
4.9	WATER SORPTION KINETICS: DAIS <sup>®</sup> MEMBRANES .....	74
4.10	WATER DESORPTION KINETICS: NAFION <sup>®</sup> MEMBRANES.....	76
4.11	WATER DESORPTION KINETICS: DAIS <sup>®</sup> MEMBRANES.....	77
4.12	SEM: NAFION <sup>®</sup> MEMBRANES .....	79
<b>5</b>	<b>DISCUSSION .....</b>	<b>80</b>
5.1	STRUCTURE, THERMAL DEGRADATION AND PLASTICIZATION OF NAFION <sup>®</sup> MEMBRANES.....	80
5.2	DIFFUSION PROPERTIES OF NAFION <sup>®</sup> MEMBRANES .....	83
5.3	PRE-TREATMENT OF NAFION <sup>®</sup> MEMBRANES .....	87
5.4	AGING OF NAFION <sup>®</sup> MEMBRANES .....	89
5.5	STRUCTURE, THERMAL DEGRADATION AND PLASTICIZATION OF DAIS <sup>®</sup> MEMBRANES.....	94
5.6	DIFFUSION PROPERTIES OF DAIS <sup>®</sup> MEMBRANES .....	100
5.7	AGING OF DAIS <sup>®</sup> MEMBRANES .....	105
<b>6</b>	<b>SUMMARY AND CONCLUSIONS.....</b>	<b>109</b>
<b>7</b>	<b>FUTURE WORK.....</b>	<b>112</b>
<b>8</b>	<b>REFERENCES.....</b>	<b>115</b>
	<b>VITA.....</b>	<b>118</b>

## LIST OF FIGURES

FIGURE 2.1.1 FUEL CELL STRUCTURE.....	4
FIGURE 2.1.2 FUEL CELL STACK <sup>7</sup> .....	4
FIGURE 2.1.3 FUEL CELL OPERATION.....	5
FIGURE 2.2.1 NAFION <sup>®</sup> IONIC PEM.....	6
FIGURE 2.2.2 DAIS IONIC PEM.....	6
FIGURE 2.2.3 ION TRANSPORT INSIDE THE PEM.....	7
FIGURE 2.2.4 FIVE REGIONS OF VISCOELASTIC BEHAVIOR.....	8
FIGURE 2.3.1 PHYSICAL AGING OF POLYMERS.....	10
FIGURE 2.3.2 NAFION <sup>®</sup> AGING DATA FROM S.H. DEALMEIDA AND Y.KAWANO <sup>20</sup> .....	12
FIGURE 2.4.1 MASTER CURVE FOR NAFION FROM YEO AND EISENBERG <sup>12</sup> .....	14
FIGURE 2.8.1 TGA TRACE OF NAFION <sup>®</sup> IN AIR FROM SAMMS ET AL <sup>45</sup> .....	20
FIGURE 2.8.2 TGA TRACE OF DAIS <sup>®</sup> IN AIR FROM WEISS ET AL <sup>18</sup> .....	20
FIGURE 2.9.1 DYNAMIC MECHANICAL STRESS-STRAIN RELATIONSHIP.....	22
FIGURE 2.9.2 DYNAMIC MECHANICAL BEHAVIOR.....	23
FIGURE 3.2.1 PERKIN ELMER DMA 7 TESTING GEOMETRIES.....	26
FIGURE 3.2.2 TEMPERATURE SWEEP OF NAFION <sup>®</sup> USING PARALLEL PLATES GEOMETRY.....	27
FIGURE 3.2.3 TEMPERATURE SWEEP OF NAFION <sup>®</sup> USING EXTENSION GEOMETRY.....	27
FIGURE 3.2.4 PERKIN ELMER DMA 7: A) ANALYZER, B) SAMPLE STAGE WITH THE SOLVENT SLEEVE <sup>48</sup> .....	28
FIGURE 3.3.1 DSC TRACE OF NAFION <sup>®</sup> FROM ALMEIDA <i>ET AL</i> <sup>46</sup> .....	31
FIGURE 3.3.2 DSC TRACE OF NAFION <sup>®</sup> .....	31
FIGURE 3.3.3 DSC TRACE OF DAIS <sup>®</sup> 30% SULFONATION.....	31
FIGURE 3.3.4 SUBAMBIENT DSC OF DAIS <sup>®</sup> 60% SULFONATION.....	32
FIGURE 3.3.5 AMBIENT DSC OF DAIS <sup>®</sup> 60% SULFONATION.....	32
FIGURE 3.4.1 TGA OF DAIS <sup>®</sup> 30% SULFONATION IN AIR.....	33
FIGURE 3.4.2 TGA OF NAFION <sup>®</sup> 117 IN AIR.....	33
FIGURE 3.5.1 FTIR SPECTRUM OF DAIS <sup>®</sup> 30% SULFONATION.....	34
FIGURE 3.6.1 ENVIRONMENTAL CONTROL CHAMBER WITH CONTINUOUS WEIGHT ACQUISITION SYSTEM..	35
FIGURE 4.1.1 NAFION <sup>®</sup> DMA SPECTRUM.....	37
FIGURE 4.1.2 AMBIENT DMA SCAN OF DRY NAFION <sup>®</sup> MEMBRANE.....	38
FIGURE 4.1.3 AMBIENT DMA SCAN OF SATURATED NAFION <sup>®</sup> MEMBRANE.....	38
FIGURE 4.1.4 COMPARISON OF DRY AND SATURATED NAFION <sup>®</sup> MEMBRANES.....	39

FIGURE 4.1.5 AMBIENT DMA SCAN OF SATURATED NAFION <sup>®</sup> FOR A RANGE OF FREQUENCIES .....	40
FIGURE 4.1.6 AMBIENT DMA SCANS OF DRY NAFION <sup>®</sup> FOR A RANGE OF FREQUENCIES .....	40
FIGURE 4.1.7 THE EFFECT OF THE PRE-TREATMENT ON NAFION <sup>®</sup> MEMBRANES .....	41
FIGURE 4.1.8 DMA SCAN OF THE NAFION <sup>®</sup> MEMBRANE PRE-TREATED BY METHOD 4: HEAT, HOLD AT 170°C, COOL, HEAT CYCLE .....	42
FIGURE 4.1.9 TAN $\delta$ PEAK POSITIONS OF NAFION <sup>®</sup> SAMPLES AGED IN DI WATER AT 90°C(EXPERIMENT 1)	43
FIGURE 4.1.10 TAN $\delta$ PEAK POSITIONS OF NAFION <sup>®</sup> SAMPLES AGED IN DI WATER AT 90°C (EXPERIMENT 2) .....	43
FIGURE 4.1.11 TAN $\delta$ PEAK POSITIONS OF NAFION <sup>®</sup> SAMPLES AGED IN DI WATER AT 90°C (EXPERIMENT 3) .....	44
FIGURE 4.1.12 DMA OF NAFION <sup>®</sup> MEMBRANE AGED FOR 60 DAYS IN DI WATER AT 90°C .....	45
FIGURE 4.1.13 DMA OF NAFION <sup>®</sup> MEMBRANE AGED FOR 80 DAYS IN DI WATER AT 90°C .....	45
FIGURE 4.1.14 DMA SCAN OF THE NAFION <sup>®</sup> MEMBRANE HEAT, HOLD AT 130°C, COOL, HEAT CYCLE .....	46
FIGURE 4.1.15 TAN $\delta$ PEAK POSITIONS OF NAFION <sup>®</sup> SAMPLES AGED IN DI WATER AT 65°C .....	46
FIGURE 4.2.1 DAIS <sup>®</sup> 30% SULFONATION DMA SPECTRUM .....	47
FIGURE 4.2.2 DAIS <sup>®</sup> 60% SULFONATION DMA SPECTRUM .....	48
FIGURE 4.2.3 AMBIENT DMA SCAN OF DRY DAIS <sup>®</sup> 30% SULFONATION MEMBRANE .....	49
FIGURE 4.2.4 AMBIENT DMA SCAN OF SATURATED DAIS <sup>®</sup> 30% SULFONATION MEMBRANE .....	49
FIGURE 4.2.5 COMPARISON OF DRY AND SATURATED DAIS <sup>®</sup> 30% SULFONATION MEMBRANE .....	50
FIGURE 4.2.6 THE EFFECT OF THE SCANNING RATE ON STORAGE MODULI OF THE SATURATED DAIS <sup>®</sup> 30% SULFONATION MEMBRANES .....	50
FIGURE 4.2.7 AMBIENT DMA SCAN OF DRY DAIS <sup>®</sup> 60% SULFONATION MEMBRANE .....	51
FIGURE 4.2.8 AMBIENT DMA SCAN OF SATURATED DAIS <sup>®</sup> 60% SULFONATION MEMBRANE, 10HZ .....	52
FIGURE 4.2.9 DMA SCAN OF DAIS <sup>®</sup> 30% SULFONATION MEMBRANE: HEAT, COOL, HEAT CYCLE .....	53
FIGURE 4.2.10 DMA SCAN OF DAIS <sup>®</sup> 30% SULFONATION MEMBRANE: HEAT, HOLD AT 160°C, COOL, HEAT CYCLE .....	53
FIGURE 4.2.11 SECOND HEATING OF DAIS <sup>®</sup> 60% SULFONATION MEMBRANE: HEAT, HOLD AT 170°C, HEAT CYCLE .....	54
FIGURE 4.2.12 DMA SCAN OF DAIS <sup>®</sup> 60% SULFONATION MEMBRANE: HEAT TO 235°C, COOL, HEAT CYCLE .....	54
FIGURE 4.2.13 DMA SCAN OF DAIS <sup>®</sup> 60% SULFONATION MEMBRANE: HEAT, HOLD AT 235°C, COOL, HEAT CYCLE .....	55
FIGURE 4.2.14 FREQUENCY SHIFTS DMA DATA FOR DAIS <sup>®</sup> 60% SULFONATION MEMBRANE .....	56
FIGURE 4.2.15 TAN $\delta$ PEAK POSITIONS OF DAIS <sup>®</sup> 30% SULFONATION MEMBRANE AGED IN DI WATER AT 90°C (EXPERIMENT 1) .....	56

FIGURE 4.2.16 TAN $\delta$ PEAK POSITIONS OF DAIS <sup>®</sup> 30% SULFONATION MEMBRANE AGED IN DI WATER AT 90°C (EXPERIMENT 2).....	57
FIGURE 4.2.17 DMA SCANS OF THE VIRGIN AND 1390HRS AGED DAIS <sup>®</sup> 30% SULFONATION MEMBRANE ..	57
FIGURE 4.3.1 TGA OF NAFION <sup>®</sup> MEMBRANE IN AIR.....	58
FIGURE 4.3.2 TGA OF NAFION <sup>®</sup> MEMBRANE IN N <sub>2</sub> .....	58
FIGURE 4.3.3 THE EFFECT OF PRE-TREATMENT ON TGA OF NAFION <sup>®</sup> MEMBRANES.....	59
FIGURE 4.4.1 TGA SCAN OF DAIS <sup>®</sup> 30% SULFONATION MEMBRANE IN AIR .....	60
FIGURE 4.4.2 TGA SCAN OF DAIS <sup>®</sup> 30% SULFONATION MEMBRANE IN N <sub>2</sub> .....	61
FIGURE 4.4.3 TGA SCAN OF DAIS <sup>®</sup> 60% SULFONATION MEMBRANE IN AIR .....	61
FIGURE 4.4.4 TGA SCAN OF DAIS <sup>®</sup> 60% SULFONATION MEMBRANE IN N <sub>2</sub> .....	62
FIGURE 4.4.5 THE EFFECT OF DRYING DAIS <sup>®</sup> 60% SULFONATION MEMBRANE IN THE VACUUM OVEN OVERNIGHT (TGA IN AIR) .....	62
FIGURE 4.4.6 TGA SCAN IN AIR OF 30% SULFONATED DAIS <sup>®</sup> MEMBRANE: EQUILIBRATED AT RT CONDITIONS, DRIED IN VACUUM OVEN AND AGED FOR 168HRS IN DI WATER AT 90°C (WEIGHT %)	63
FIGURE 4.4.7 TGA SCAN IN AIR OF 30% SULFONATED DAIS <sup>®</sup> MEMBRANE: EQUILIBRATED AT RT CONDITIONS, DRIED IN VACUUM OVEN AND AGED FOR 168HRS IN DI WATER AT 90°C (DERIVATIVE WEIGHT %).....	63
FIGURE 4.4.8 THE EFFECT OF THE TGA HEATING RATE IN AIR ON 30% SULFONATED DAIS <sup>®</sup> MEMBRANE (WEIGHT %) .....	64
FIGURE 4.4.9 THE EFFECT OF THE TGA HEATING RATE IN AIR ON 30% SULFONATED DAIS <sup>®</sup> MEMBRANE (DERIVATIVE WEIGHT %).....	64
FIGURE 4.5.1 FTIR OF 30% VS. 60% SULFONATED DAIS <sup>®</sup> MEMBRANES.....	65
FIGURE 4.5.2 FTIR OF RANDOM SAMPLES OF 30% SULFONATED DAIS <sup>®</sup> MEMBRANES (LOW WAVELENGTHS) .....	66
FIGURE 4.5.3 FTIR OF RANDOM SAMPLES OF 30% SULFONATED DAIS <sup>®</sup> MEMBRANES (HIGH WAVELENGTHS) .....	66
FIGURE 4.5.4 FTIR OF 30% SULFONATED DAIS <sup>®</sup> MEMBRANE: THE EFFECT OF HEATING (LOW WAVELENGTHS).....	67
FIGURE 4.5.5 FTIR OF 30% SULFONATED DAIS <sup>®</sup> MEMBRANE: THE EFFECT OF HEATING (HIGH WAVELENGTHS).....	67
FIGURE 4.5.6 FTIR OF 60% SULFONATED DAIS <sup>®</sup> MEMBRANE: THE EFFECT OF HEATING (LOW WAVELENGTHS).....	68
FIGURE 4.5.7 FTIR OF 60% SULFONATED DAIS <sup>®</sup> MEMBRANE: THE EFFECT OF HEATING (HIGH WAVELENGTHS).....	68
FIGURE 4.5.8 FTIR OF 30% SULFONATED DAIS <sup>®</sup> MEMBRANE: THE EFFECT OF AGING (LOW WAVELENGTHS) .....	69

FIGURE 4.5.9 FTIR OF 30% SULFONATED DAIS <sup>®</sup> MEMBRANE: THE EFFECT OF AGING (HIGH WAVELENGTHS)	69
.....	
FIGURE 4.6.1 MAXIMUM WATER UPTAKE OF NAFION <sup>®</sup> MEMBRANES	70
FIGURE 4.6.2 EFFECT OF DRYING NAFION <sup>®</sup> MEMBRANES IN THE OVEN AT 160°C	71
FIGURE 4.7.1 MAXIMUM WATER UPTAKE OF DAIS <sup>®</sup> MEMBRANES	72
FIGURE 4.8.1 VAPOR PHASE WATER SORPTION STUDIES OF VIRGIN NAFION <sup>®</sup> MEMBRANES	73
FIGURE 4.8.2 VAPOR PHASE WATER SORPTION STUDIES OF AGED NAFION <sup>®</sup> MEMBRANES	73
FIGURE 4.9.1 VAPOR PHASE WATER SORPTION STUDIES OF 30% DAIS <sup>®</sup> MEMBRANES	74
FIGURE 4.9.2 VAPOR PHASE WATER SORPTION STUDIES OF 60% DAIS <sup>®</sup> MEMBRANES	75
FIGURE 4.9.3 VAPOR PHASE WATER SORPTION STUDIES OF AGED 30% DAIS <sup>®</sup> MEMBRANES	75
FIGURE 4.10.1 WATER DESORPTION STUDIES OF NAFION <sup>®</sup> MEMBRANES	76
FIGURE 4.10.2 WATER DESORPTION STUDIES OF AGED NAFION <sup>®</sup> MEMBRANES	76
FIGURE 4.11.1 WATER DESORPTION STUDIES OF 30% SULFONATED DAIS <sup>®</sup> MEMBRANES	77
FIGURE 4.11.2 WATER DESORPTION STUDIES OF 60% SULFONATED DAIS <sup>®</sup> MEMBRANES	78
FIGURE 4.11.3 WATER DESORPTION STUDIES OF AGED 30% SULFONATED DAIS <sup>®</sup> MEMBRANES	78
FIGURE 4.12.1 SEM IMAGE OF UNTREATED NAFION <sup>®</sup> MEMBRANE	79
FIGURE 4.12.2 SEM IMAGE OF NAFION <sup>®</sup> MEMBRANE BOILED IN DI WATER FOR 1HR	79
FIGURE 4.12.3 SEM IMAGE OF NAFION <sup>®</sup> MEMBRANE BOILED 1HR IN H <sub>2</sub> O AND 1HR IN H <sub>2</sub> O <sub>2</sub>	79
FIGURE 5.2.1 VAPOR PHASE SORPTION BEHAVIOR OF NAFION <sup>®</sup> MEMBRANES	85
FIGURE 5.2.2 LOG-LOG PLOT OF INITIAL 1,225 S OF NAFION <sup>®</sup> SORPTION DATA (SAMPLE A)	86
FIGURE 5.2.3 WATER DESORPTION BEHAVIOR OF NAFION <sup>®</sup> MEMBRANES	87
FIGURE 5.4.1 90°C AGING DATA FOR NAFION <sup>®</sup> MEMBRANES (EXPERIMENT 1)	89
FIGURE 5.4.2 90°C AGING DATA FOR NAFION <sup>®</sup> MEMBRANES (EXPERIMENT 3)	89
FIGURE 5.4.3 90°C AGING DATA FOR NAFION <sup>®</sup> MEMBRANES (EXPERIMENT 2)	89
FIGURE 5.4.4 65°C AGING DATA FOR NAFION <sup>®</sup> MEMBRANES	89
FIGURE 5.4.5 VAPOR PHASE SORPTION BEHAVIOR OF NAFION <sup>®</sup> MEMBRANES AGED AT 65°C	91
FIGURE 5.4.6 WATER DESORPTION BEHAVIOR OF NAFION <sup>®</sup> MEMBRANES AGED AT 65°C	91
FIGURE 5.4.7 RESULTS OF THE NAFION <sup>®</sup> AGING EXPERIMENTS (90°C)	93
FIGURE 5.4.8 RESULTS OF THE NAFION <sup>®</sup> AGING EXPERIMENTS (65°C)	93
FIGURE 5.5.1 ISOTHERMAL FREQUENCY DATA FOR 60% SULFONATED DAIS <sup>®</sup> MEMBRANE	97
FIGURE 5.5.2 MASTERCURVE OF 60% SULFONATED DAIS <sup>®</sup> MEMBRANE	97
FIGURE 5.5.3 SHIFT FACTOR PLOT FOR 60% SULFONATED DAIS <sup>®</sup> MEMBRANE (A: RELAXATION OF ETHYLENE/BUTYLENE BLOCK, T: INTERMEDIATE TRANSITION REGION, B: RELAXATION OF STYRENE BLOCK)	98
FIGURE 5.6.1 LOG-LOG PLOT OF INITIAL 1,225 S OF 30% SULFONATED DAIS <sup>®</sup> SORPTION DATA (SAMPLE A)	101
.....	

FIGURE 5.6.2 LOG-LOG PLOT OF INITIAL 1,225 s OF 60% SULFONATED DAIS <sup>®</sup> SORPTION DATA (SAMPLE A)	101
.....	
FIGURE 5.6.3 VAPOR PHASE SORPTION BEHAVIOR OF 30% SULFONATED DAIS <sup>®</sup> MEMBRANE .....	102
FIGURE 5.6.4 VAPOR PHASE SORPTION BEHAVIOR OF 60% SULFONATED DAIS <sup>®</sup> MEMBRANE .....	102
FIGURE 5.6.5 WATER DESORPTION BEHAVIOR OF 30% SULFONATED DAIS <sup>®</sup> MEMBRANE.....	104
FIGURE 5.6.6 WATER DESORPTION BEHAVIOR OF 60% SULFONATED DAIS <sup>®</sup> MEMBRANE.....	104
FIGURE 5.7.1 RESULTS OF 30% SULFONATED DAIS <sup>®</sup> AGING EXPERIMENTS .....	105
FIGURE 5.7.2 VAPOR PHASE SORPTION BEHAVIOR OF AGED 30% SULFONATED DAIS <sup>®</sup> MEMBRANE .....	107
FIGURE 5.7.3 WATER DESORPTION BEHAVIOR OF AGED 30% SULFONATED DAIS <sup>®</sup> MEMBRANE .....	107

## LIST OF TABLES

TABLE 2.6.1 RESULTS OF NAFION <sup>®</sup> WATER UPTAKE STUDIES .....	16
TABLE 2.8.1 RESULTS OF NAFION <sup>®</sup> TGA STUDIES .....	21
TABLE 3.1.1 PROPERTIES OF NAFION <sup>®</sup> MEMBRANES .....	24
TABLE 3.1.2 NAFION <sup>®</sup> PRE-TREATMENT PROCEDURES .....	25
TABLE 3.2.1 INITIAL FORCES FOR DMA 7 ISOCHRONAL SCANS .....	29
TABLE 4.1.1 THE EFFECT OF THE PRE-TREATMENT ON THE POSITION OF TAN $\delta$ PEAK.....	42
TABLE 4.4.1 THE TEMPERATURE POSITIONS OF THE CHARACTERISTIC FEATURES OF DAIS <sup>®</sup> TGA SCANS ...	60
TABLE 5.4.1 DIFFUSION PROPERTIES OF VIRGIN AND AGED NAFION <sup>®</sup> MEMBRANES .....	92
TABLE 5.6.1 DIFFUSION PROPERTIES OF NAFION <sup>®</sup> AND DAIS <sup>®</sup> MEMBRANES .....	100
TABLE 5.7.1 DIFFUSION PROPERTIES OF VIRGIN AND AGED DAIS <sup>®</sup> MEMBRANES.....	106

# 1 INTRODUCTION

In recent years, the demand for environmentally friendly and cost effective alternatives to traditional power sources has significantly grown. As a result, many industries have invested considerable resources in finding and implementing new methods of power production. One of the new technologies under consideration is a Proton Exchange Membrane Fuel Cell (PEMFC).

The main components of a PEMFC are two metal electrodes separated by a polymeric Proton Exchange Membrane (PEM), which is permeable to positively charged particles. A detailed description and the principles of fuel cell operation are addressed in Section 2.1.

To date, most of the research done by the scientific community has concentrated on the design and performance modeling of the PEMFCs. Studies, that have been conducted to mathematically predict long-term performance of the cells,<sup>1, 2, 3, 4</sup> have, for the most part, relied on the time-independent virgin properties of the polymeric materials employed in the PEMFCs. However, PEM properties can significantly change as functions of time and exposure to elevated temperatures due to degradation and/or aging (Section 2.3 and 2.8). This provides numerous motivations for the current research.

This work focuses on the effects of a series of variables defined below on properties of virgin and aged PEMs. The two materials chosen for this study are Nafion<sup>®</sup> membranes manufactured by DuPont Corporation and Dais<sup>®</sup> membranes manufactured by Dais-Analytic Corporation. Nafion<sup>®</sup> is currently one of the leading choices for PEMs and most of the research done on fuel cell membranes has focused on this material. Dais<sup>®</sup> is a new membrane that was created for low cost residential and commercial applications, and only a few studies that address its properties have been published. While both materials are used in fuel cells, their applications and, consequently, their properties are very different (Section 2.1 and 3.1).

The studies of the time-dependence of mechanical properties of Nafion<sup>®</sup> are especially of interest if PEM operational range and common pre-treatment temperatures

are considered in light of the glass transition temperature ( $T_g$ ) of this material (Section 2.5).

Since both membranes examined in this study, have to be saturated in order to achieve their peak performance, it is also extremely important to consider the properties of the virgin and aged materials in saturated environments (Section 2.5). For the same reason, examination of the moisture uptake and drying for these polymers becomes critical (Section 2.6).

In order to establish the stability of both materials, degradation behavior of Nafion<sup>®</sup> and Dais<sup>®</sup> membranes is addressed in this study, and the results are correlated to data that exist in the literature (Section 2.8).

Another important aspect under consideration, which can be effectively demonstrated on the example of Dais<sup>®</sup> membranes, is the effect of sulfonation on the properties of PEMs (Section 2.7). Since changes in the level of sulfonation lead to dramatic changes in the physical properties of the material, the results of this study are relevant for material selection purposes.

In light of the discussion above, the purpose of this thesis was to investigate the effects of structure, humidity, and aging on properties of ionic PEMs. In the course of this study, the effect of the saturated high temperature environments on the materials was examined and thermal stability and diffusion properties of the fuel cell membranes were determined.

## 2 BACKGROUND

### 2.1 Fuel Cells

Over the past 20 years, one of the most important challenges facing industry has been the search for a solution to the energy crisis. As natural resources become scarcer and the environmental constraints on industry grow tighter, it is imperative to find an environmentally friendly and cost effective alternative to the traditional power production methods. Fuel cell technology has been around for a long time; for example, NASA has been using fuel cells in the space program since the 1950s. However, only lately has this technology received appropriate attention from the scientific community as a candidate for an alternative power source. The features that brought fuel cells to the forefront of research efforts for the automotive industry include high power density, significantly reduced emissions, fast room temperature start up, elimination of corrosion problems, noise free operation, and lower operating cost.<sup>1, 2, 5</sup>

A fuel cell is an electrochemical device that operates on the principle of converting the chemical energy of the fuel and an oxidant to electrical energy.<sup>6</sup> The common types of fuel cells, characterized by electrolyte, are Alkaline (AFC), Proton Exchange Membrane (PEMFC), Phosphoric Acid (PAFC), Molten Carbonate (MCFC), and Solid Oxide (SOFC). This work focuses on PEMFC.

PEMFC consists of two bipolar graphite plates that hold a Membrane Electrode Assembly (MEA). Each MEA is a set of two electrodes made of thin porous graphite papers with platinum catalyst deposited on them and with PEM sandwiched between them (Figure 2.1.1). Individual cells are connected in series to form a stack (Figure 2.1.2).

The basic electrochemical principles of PEMFC operation can be summarized as follows. The polymeric membrane, held between two metal electrodes, is permeable to positively charged particles. Hydrogen and oxygen gases are supplied to the anode

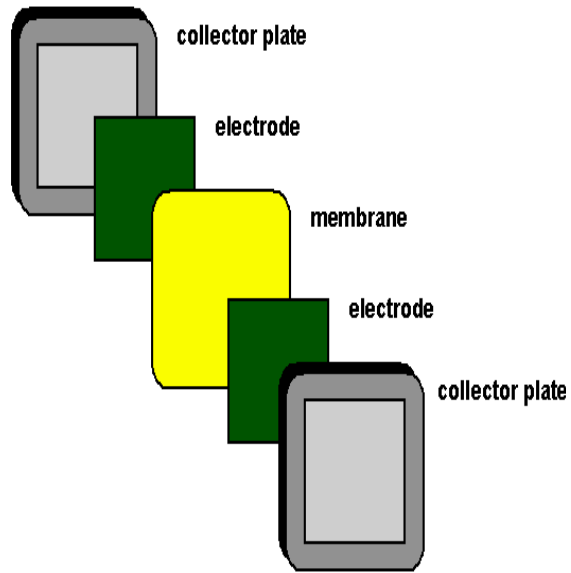


Figure 2.1.1 Fuel Cell Structure<sup>7</sup>

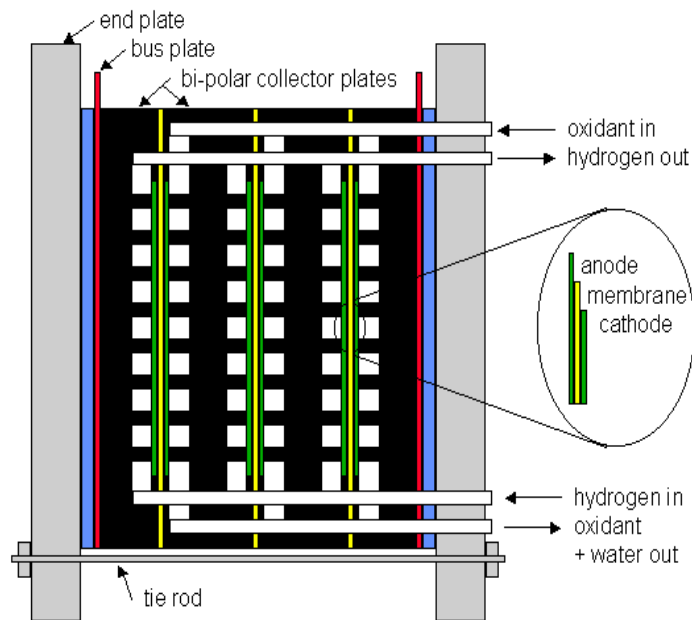


Figure 2.1.2 Fuel Cell Stack<sup>7</sup>

and the cathode, respectively. Hydrogen oxidation reaction occurs at the anode producing hydrogen ions and free electrons. At the cathode, free electrons are pulled through the external circuit producing oxygen anions. The protons then diffuse through the membrane to the other side where hydrogen ions combine with oxygen anions to form water<sup>2</sup> (Figure 2.1.3).

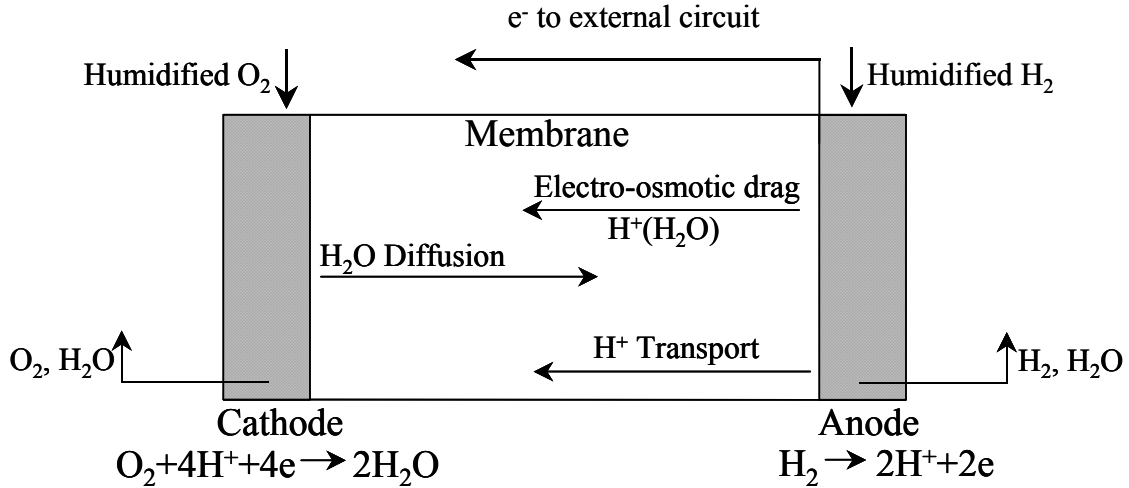


Figure 2.1.3 Fuel Cell Operation

According to M.Verbrugge *et al.*,<sup>8</sup> the ion transport inside of the membrane can be described using the modified Nernst-Planck equation:

$$N_i = \underbrace{-D_i \nabla c_i}_{\text{Diffusion}} - \underbrace{z_i F u_i c_i \nabla \Phi}_{\text{Migration}} + \underbrace{c_i v}_{\text{Convection}} \quad \text{Equation 2.1.1}$$

where  $N$  is the ionic species flux,  $D$  is the species diffusion coefficient,  $c$  is the molar concentration,  $z$  is the charge number,  $F$  is the Faraday constant,  $u$  is the species mobility coefficient,  $\Phi$  is the electric potential, and  $v$  is the pore-fluid velocity. Based on the equation 2.1.1, the flux of each species through the membrane consists of three terms: diffusion due to concentration gradients, migration due to electric gradients and convection due to electric and pressure gradients.

## 2.2 PEMFC Membrane Materials

The two materials chosen for the present study are Nafion<sup>®</sup> and Dais<sup>®</sup> membranes. Although both of them are used as PEMs, they have different target market areas due to the difference in materials structure, properties and cost. Nafion<sup>®</sup> is widely used for automotive applications, where the required operational range is from 80°C to 110°C. It has a high power density (Section 3.1) and is well known in industry. However, this material is expensive and might not be cost effective for use in home and small business applications. Dais<sup>®</sup> was created to fill in this gap. It has an operational range from 35°C to 70°C, which is lower than that for Nafion<sup>®</sup>, but this material is considerably cheaper and as result, offers an affordable alternative for lower cost room temperature uses. Dais<sup>®</sup> market is portable electronics and other low power applications.

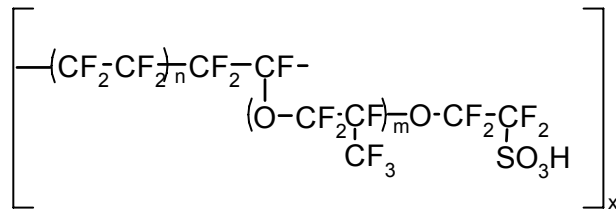


Figure 2.2.1 Nafion<sup>®</sup> Ionic PEM

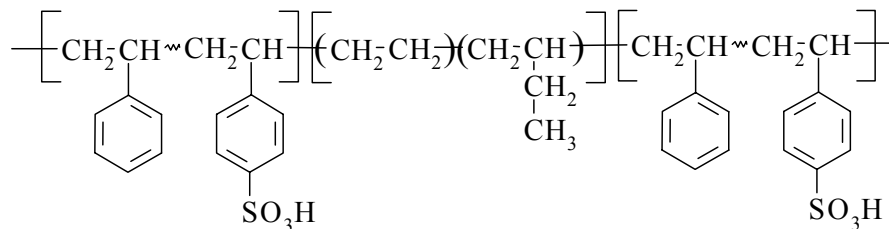
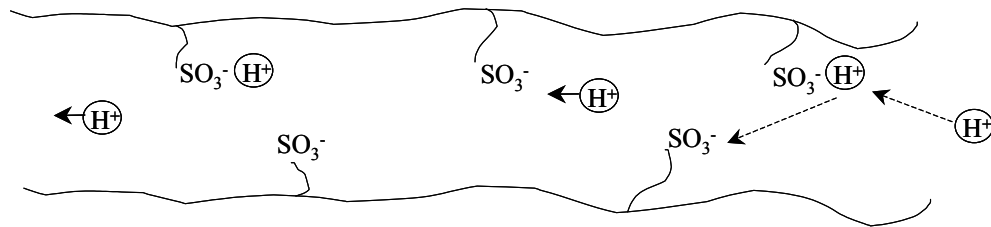


Figure 2.2.2 Dais Ionic PEM

The reason that Nafion<sup>®</sup> and Dais<sup>®</sup> are chosen for fuel cell applications is their ability to selectively pass through them positively charged particles, a distinctive characteristic made possible because of their structure. While these materials have

different backbones (Figure 2.2.1 and Figure 2.2.2), they have one important feature in common: they both have sulfonic acid side groups, which play a key role in ion transport.

While the exact nature of ion transport in ionic PEMs is not well understood, the following explanation is accepted in the literature.<sup>9</sup> It was determined that for operational efficiency, membranes need to be saturated by water.<sup>10,11</sup> As a result of hydration, negatively charged sulfonate sites are formed (Figure 2.2.3) and positive ions, such as protons created by hydrogen oxidation reaction (Section 2.1), can “jump” from site to site permeating through the membrane.



**Figure 2.2.3 Ion Transport inside the PEM**

Nafion<sup>®</sup> and Dais<sup>®</sup> have structurally different backbones: Nafion<sup>®</sup> is a homopolymer with a polytetrafluoroethylene (PTFE) backbone and Dais<sup>®</sup> is a styrene-ethylene/butylene-styrene tri-block copolymer (Figure 2.2.1 and Figure 2.2.2). In order to explain the distinction between the two, a short discussion of the morphological and viscoelastic behavior of these polymers is required.

Linear amorphous materials exhibit five regions of viscoelastic behavior: a glassy region, a glass-rubber transition, a rubbery plateau, a rubbery flow region and a liquid flow region (Figure 2.2.4). In the glassy region, only short range rotations and vibrations of the molecular chains take place. The glass-rubber transition is characterized by initiation of long range molecular motions (10-50 atoms) and this is where the glass transition temperature,  $T_g$ , is defined. In the rubbery plateau region, polymeric chains have mostly elastic behavior that is combined with the flow behavior in the rubbery flow region, and, finally, is changed to the behavior of a viscous liquid in the liquid flow region.

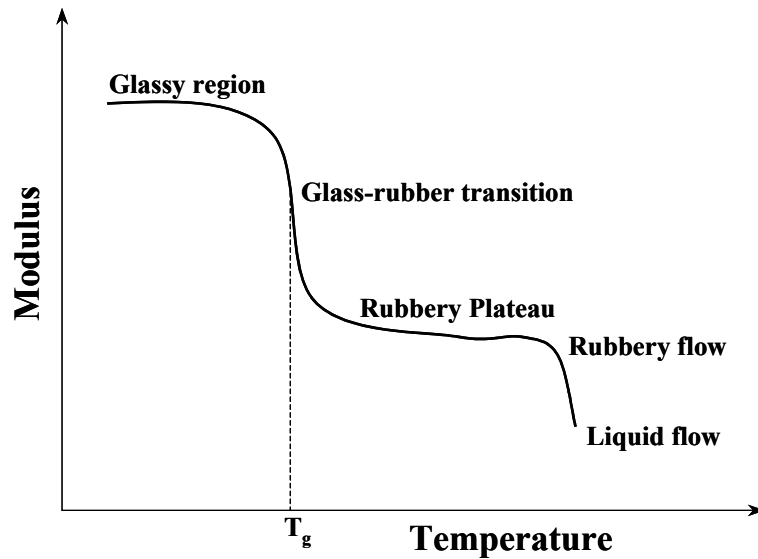


Figure 2.2.4 Five Regions of Viscoelastic Behavior

Since Nafion<sup>®</sup> is a homopolymer, it exhibits one  $T_g$ . While studying Nafion<sup>®</sup>'s viscoelastic behavior, Yeo and Eisenberg<sup>12</sup> identified three transitions: an  $\alpha$  transition at 111°C due to the movement of the PTFE backbone, a  $\beta$  transition at 23°C due to the relaxation of ionic regions and a  $\gamma$  transition at -100°C due to local short range motions of fluorocarbons in the backbone. Since the fluorocarbon matrix is hydrophobic, polar water molecules are not expected to have a drastic effect on its glass transition. Data collected by these authors suggests that an  $\alpha$  transition is not influenced by the water content of the material, while the position of a  $\beta$  transition strongly depends on the amount of water present inside of the membrane. Based on this evidence, Yeo and Eisenberg assigned  $\alpha$  and  $\beta$  transitions to the relaxations of the matrix and the ionic regions, respectively. In contrast to this, a later study by Kyu and Eisenberg<sup>13</sup> suggests that the assignment of  $\alpha$  and  $\beta$  peaks be reversed and the  $\beta$  peak be assigned to represent matrix relaxation. They base this decision on the new evidence of the sensitivity of  $\alpha$  peak to the change in the water content of the membrane. In this work, the term “ $T_g$ ” will refer to the upper  $\alpha$  transition.

Dais<sup>®</sup> membrane, as described previously, is a tri-block copolymer. It consists of two separate microphases: a styrene phase and an ethylene/butylene phase.<sup>14</sup> Microphase separation in the block copolymers occurs when the entropy of mixing of individual

blocks is small and there is an excess of free energy contributions due to structural difference between the blocks.<sup>15</sup> An increase in the size of the blocks leads to a further decrease in the entropy of mixing and an increase in the driving force for phase separation; however, since the blocks are covalently connected to each other, the macrophase separation does not occur. Each phase has its own  $T_g$  at the temperature where the  $T_g$  of its homopolymer constituent would occur. In the case of the ethylene/butylene random copolymer, no phase separation takes place and there is only one  $T_g$  associated with that block. The  $T_g$  of the ethylene/butylene copolymer can be approximated using the Fox equation:<sup>16</sup>

$$\frac{1}{T_g} = \frac{M_1}{T_{g1}} + \frac{M_2}{T_{g2}} \quad \text{Equation 2.2.1}$$

where  $M$  is the mass fraction of the component. The expected temperature value of the glass transition of ethylene/butylene block is discussed in Section 5.2.

The  $T_g$  of polystyrene is reported to be 100°C;<sup>17</sup> however, according to Weiss *et al.*,<sup>18</sup> the  $T_g$  of the styrene block in Dais<sup>®</sup> material is measured at a much higher temperature and the reasons for this phenomenon are discussed in Section 2.7.

### ***2.3 Physical Aging of Polymers***

Nafion<sup>®</sup> and Dais<sup>®</sup> are viscoelastic polymeric materials, which means that their mechanical properties are time-dependent and they can be subject to physical aging.

Physical aging of polymers can be explained by invoking free volume theory, which states that, in order for molecular motion to occur, “holes” or free volume must be present between polymeric chain segments.<sup>16</sup> According to Sperling,<sup>16</sup> the amount of free volume at  $T_g$  is a constant for all viscoelastic polymers and is about 11%. However, when a polymeric material is in the glassy state, after being formed or quenched, the chains are not packed closely, especially in the case of chains having large branches or

inflexible components in the backbone, which give rise to steric hindrance. As a result, a substantial amount of free volume, in excess of 11%, is trapped between the elements of polymeric chains (Figure 2.3.1). As time passes, the chains rearrange themselves into a more closely packed conformation reducing free volume. In theory, given enough time, the amount of free volume should reach quasi-equilibrium, 11%. The process of free volume shrinkage is called physical aging. Physical aging is reversible: if a polymer is heated above  $T_g$  and is held in the rubbery state for a short period of time, all of its thermal history can be erased.

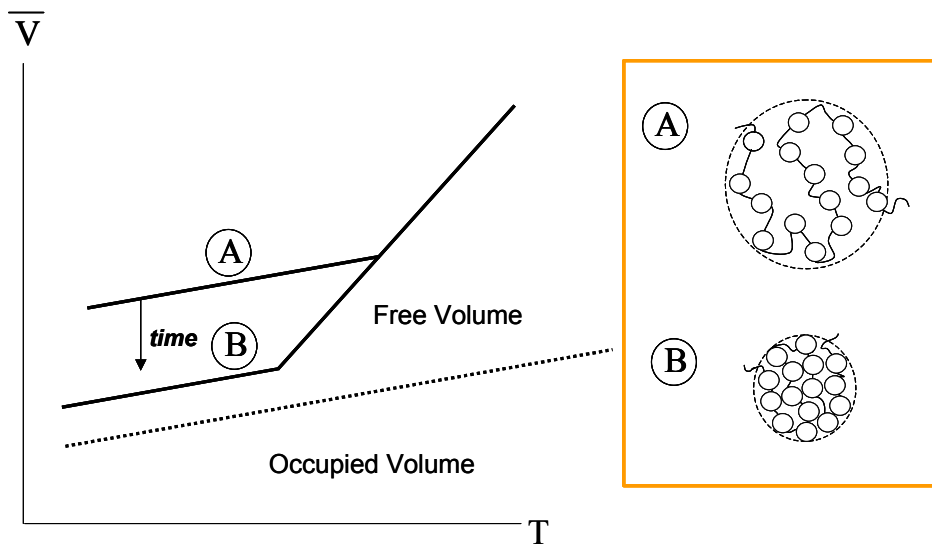


**Figure 2.3.1 Physical Aging of Polymers**

The amount of free volume present between the chains is directly related to the observed  $T_g$ . Since  $T_g$  is the temperature at which large scale molecular motions are initiated, the ease with which the molecule is able to move is directly linked to  $T_g$ . The amount of thermal energy that is necessary to move a closely packed chain is much larger than that required to move a chain with substantial free volume. As a result, virgin samples have lower  $T_g$ s at heating than do aged polymers and, consequently, their mechanical properties change as a function of time. This point is especially important if the temperature at which material is used is close to its  $T_g$ .

Since it is established that the properties of viscoelastic materials are time-

dependent, it is becoming evident that material behavior prediction should be done for both virgin and aged films. The problem of physical aging is extremely important for ionic membranes, such as Nafion<sup>®</sup> and Dais<sup>®</sup>, because their ability to pass protons through them may be intimately related to the structure. Since it has been assumed that ion transport depends on the degree of mobility of protons and water molecules between sulfonic sites, it could be argued that the amount of free volume is directly related to that mobility. As free volume collapses, the mobility of species within the chains should decrease and diffusion coefficients for water and proton transport should decrease as well.

To date, few studies that address aging in Nafion<sup>®</sup> have been published<sup>19,20</sup> and no data regarding aging in Dais<sup>®</sup> is available. In a study by Yeager and Steck,<sup>19</sup> as-received samples of Nafion<sup>®</sup> were stored for two years in dry form and diffusion coefficients for Cs<sup>+</sup> and Na<sup>+</sup> ions through the membrane were measured for virgin and aged samples. The self-diffusion coefficients for Cs<sup>+</sup> ions were found to increase significantly, while those for Na<sup>+</sup> ions remained almost the same. The authors have explained the dissimilarity between the two by assigning different diffusion paths for ions with different size and charge density. It is interesting to note that when newly manufactured virgin Nafion<sup>®</sup> material was analyzed, its diffusion properties were close to those of previously aged samples and did not match the values of original virgin membranes. In the study by deAlmeida and Kawano,<sup>20</sup> Nafion<sup>®</sup> samples were treated, hydrated and UV/Vis spectra were recorded for fresh and aged films (Figure 2.3.2). The samples were aged under atmospheric conditions. It was found that the intensity of the band around 200 nm has increased with aging time and the peak itself shifted slightly to a higher wavelength. The authors concluded that the change in the spectra with sample aging was irreversible due to the dehydration because time aging initiated conformational changes that were different from those induced by loss of water during heating.

The studies mentioned above raise several questions about aging of Nafion<sup>®</sup> membranes. First, by definition, physical aging is a reversible process that deals with the conformational changes of polymeric chains due to loss of free volume. Although some of the changes that deAlmeida and Kawano observed might be, in fact, due to changes in free volume, most of them are due to the effect of dehydration. Second, both aging

studies looked at the dry membranes stored at atmospheric conditions. There is no literature available that addresses the aging of these polymers at the conditions in which they are used, i.e. saturated in water at temperatures between 60°C and 90°C. A study that focuses on physical aging of Nafion® and Dais® membranes in the saturated state at high temperatures, is, therefore, expected to yield valuable functional results.

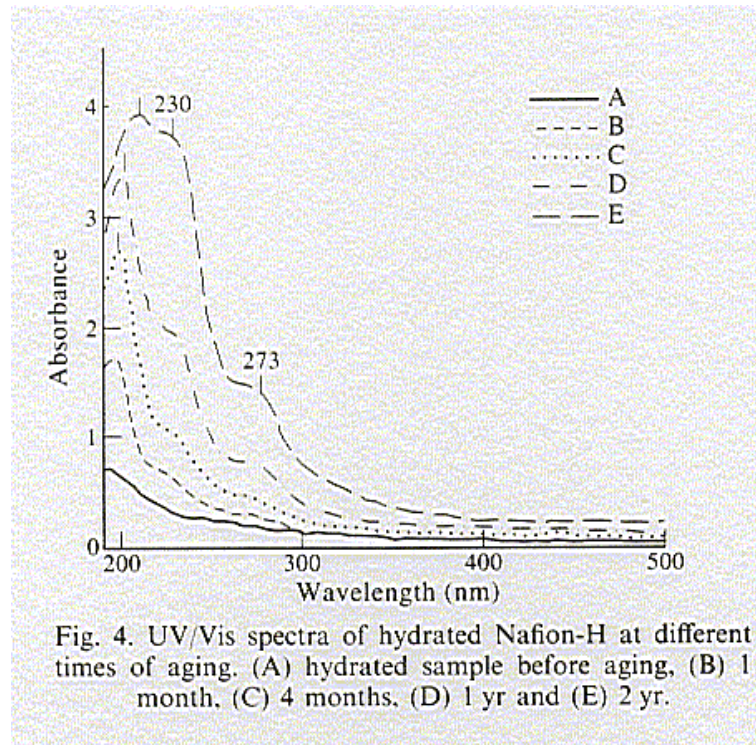


Figure 2.3.2 Nafion® Aging Data from S.H. deAlmeida and Y.Kawano<sup>20</sup>

## 2.4 Time-Temperature Superposition

As previously stated, properties of viscoelastic materials are time-dependent; however, relaxation time for some groups of polymers can be significantly long. This can make studies of long-term performance time consuming at best and, in some cases, unfeasible. Time-temperature superposition is a method used to predict long-term behavior of polymers in a relatively short experimental time frame.

Relaxation of the polymeric matrix requires the presence of a sufficient amount of free volume and is dictated by the ease with which polymeric chains are able to move. If the sample temperature is raised, the added kinetic energy provides chains with an extra mobility and shortens the time required for chain rearrangement to take place. Based on this argument, both time and temperature can be used to manipulate the speed of polymer relaxation. It was determined<sup>21</sup> that there is a logarithmic relationship between time and temperature that exists for viscoelastic polymeric materials. This relationship can be represented by the WLF equation:<sup>16</sup>

$$\ln A_T = -\frac{B}{f_0} \left[ \frac{(T - T_0)}{\frac{f_0}{\alpha_f} + (T - T_0)} \right] \quad \text{Equation 2.4.1}$$

where  $B$  is a constant,  $f$  is a fractional free volume at transition temperature  $T_0$ ,  $\alpha_f$  is the expansion coefficient of free volume and  $A_T$  is the reduced variable shift factor, which is defined as

$$\ln A_T = \ln \left( \frac{t}{t_0} \right) \quad \text{Equation 2.4.2}$$

where  $t_0$  is the transition time.

Time-temperature superposition follows from Equation 2.4.1 and states that data collected for viscoelastic materials as a function of frequency corresponds to the data collected as a function of temperature over a period of time. Technically, frequency scans collected over a range of temperatures can be shifted horizontally along a log time axis. This would result in an analogous plot as one recorded for a temperature sweep as a function of time. This type of curve, constructed using time-temperature superposition principle, is called a master curve and the temperature, about which the curves are shifted, is called the reference temperature. According to Sperling,<sup>21</sup> reference temperature is typically 25°C.

In the process of constructing a master curve, one more variable needs be taken into account. There is a change in the density of the material associated with a change in the temperature. Therefore, in order to obtain a more accurate master curve, in some cases, it is necessary to shift data vertically as well as horizontally to accommodate for a vertical shift factor  $T_0\rho_0/T\rho^{22}$ .

A master curve for Nafion<sup>®</sup> (marked as Nafion-H) constructed by Yeo and Eisenberg<sup>12</sup> is shown in Figure 2.4.1. The master curve was created from stress relaxation data taken for periods of time up to  $2 \times 10^4$  s.

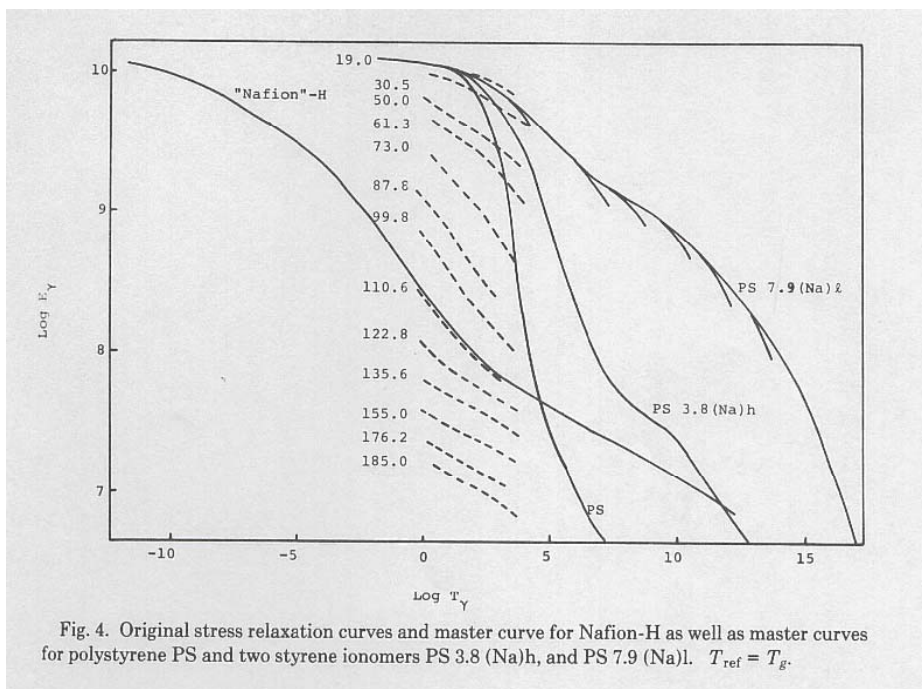


Fig. 4. Original stress relaxation curves and master curve for Nafion-H as well as master curves for polystyrene PS and two styrene ionomers PS 3.8 (Na)h, and PS 7.9 (Na)l.  $T_{ref} = T_g$ .

**Figure 2.4.1 Master Curve for Nafion from Yeo and Eisenberg<sup>12</sup>**

Based on the literature review of widely available sources, a master curve for Dais<sup>®</sup> materials has never been constructed. According to Sperling<sup>21</sup>, master curves can be constructed for individual constituents of block copolymers; however, combining them into a single plot requires further data manipulation. One goal of this thesis is the construction of a mastercurve for Dais<sup>®</sup> membrane in order to look at both its relaxation mechanisms: one, associated with the ethylene/butylene block, and the second, associated with the sulfonated styrene block.

## 2.5 Water Plasticization

Plasticizers are low molecular weight compounds that are usually added to soften rigid polymeric materials. They dissolve in the polymeric matrix and interfere with chain-to-chain secondary bonding.<sup>23</sup> As a result, chains acquire greater mobility and free volume increases, leading to decrease in the glass transition temperature of the material. The  $T_g$  of a plasticized system can be approximated using the Fox equation<sup>16</sup> (Equation 2.2.1).

It is apparent that the  $T_g$  of a plasticized system will be strongly dependent on the  $T_g$  of a plasticizer. Since water has a low  $T_g$  (estimated value at -130°C), it acts as a very good plasticizer even in small quantity. The concept of plasticization by water can be an important factor in studying properties of Nafion<sup>®</sup> and Dais<sup>®</sup> membranes, given that both are used in the saturated state. It is especially interesting with regard to Nafion<sup>®</sup> membranes since the temperature at which they are used is only 20-30°C below their  $T_g$ , so the  $T_g$  of saturated Nafion<sup>®</sup> might fall into the materials operational range.

Another area where the effect of water plasticization is an issue for Nafion<sup>®</sup> materials is sample pre-treatment. It was determined that electrical conductivity properties of Nafion<sup>®</sup> improve upon pre-treatment due to removal of low-molecular weight impurities left during processing and increase in the water content of the membrane.<sup>20</sup> The pre-treatment procedures involve boiling membrane samples in combinations of water, hydrogen peroxide, nitric or sulfuric acid solutions for various amounts of time (the exact procedure depends on the literature source) and is commonly used in a range of studies.<sup>11,24,25,26,27,28,29,30,31</sup> According to Zawodzinski *et al.*,<sup>26</sup> boiling Nafion<sup>®</sup> during the pre-treatment step promotes creation and growth of hydrated ionic clusters which leads to an increase in water content of the membrane. One more question that arises is if heating of the Nafion<sup>®</sup> sample above its  $T_g$  during the pre-treatment step erases possible effects of aging during sample storage, and if this membrane rejuvenation, along with the formation of ionic clusters, is responsible for the higher water content of pre-treated samples.

Yeo and Eisenberg<sup>12</sup> measured the  $T_g$  of a partly saturated Nafion<sup>®</sup> membrane and concluded that water strongly affects the  $\beta$  transition, shifting it to a lower temperature.

They have attributed this effect to the high polarity of ionic groups. They concluded that water has no effect on relaxation of the matrix because of the non-polar nature of PTFE backbone. The experimental procedure employed by Yeo and Eisenberg involved loading saturated Nafion<sup>®</sup> samples in the free vibrational torsional pendulum and then measuring their properties. The water content was determined after each measurement was completed and might not have accurately reflected the actual water content in the membrane during the course of the experiment. In this thesis, the mechanical properties of fully saturated Nafion<sup>®</sup> and Dais<sup>®</sup> membranes immersed in water will be measured and compared to those of the dry materials.

## 2.6 Moisture Uptake

Moisture uptake and drying behavior of Nafion<sup>®</sup> membranes have been extensively studied and the activation energies for these processes have been determined. The results of moisture absorption studies that have been conducted for Nafion<sup>®</sup> are summarized in Table 2.6.1.

**Table 2.6.1 Results of Nafion<sup>®</sup> Water Uptake Studies**

Source	Water Uptake Behavior	Activation Energy	Water Uptake at Saturation 23-25°C	Water Diffusion Coefficient (cm <sup>2</sup> /s)
Yeo and Eisenberg <sup>12</sup>	Arrhenius	4.8 kcal		sorption (liquid): $2.3 \times 10^{-6}$
Duplessix <i>et al</i> <sup>32</sup>		12kcal/mol@water<4.5% 4kcla/mol@water>7%	20%	
Hashimoto <i>et al</i> <sup>33</sup>			32%	
Kreuer <i>et al</i> <sup>34</sup>	Arrhenius			
Cappadonia <i>et al</i> <sup>35</sup>			20-25%	
Morris and Sun <sup>36</sup>				(vapor): $16.3 \times 10^{-7}$
Takamatsu <i>et al</i> <sup>37</sup>	Arrhenius	4.8 kcal		sorption (liquid): $1.8 \times 10^{-6}$ sorption (vapor): $2 \times 10^{-8}$ desorption: $1.1 \times 10^{-7}$

According to a study conducted by Zawodzinski *et al.*,<sup>26</sup> Nafion<sup>®</sup> water uptake depends on the drying method preceding the experiment. Samples that have been dried at room temperature achieved higher water content compared to samples dried at 105°C, whereas the time required to reach the equilibrium was roughly the same in both cases. The water uptake of the samples dried at high temperature increased with an increase in the temperature of the water bath in which the membranes were hydrated, while the water uptake of the samples dried at room temperature was independent of the temperature of the water bath. The authors explained this effect by ionic cluster formation and disintegration. When Nafion<sup>®</sup> was dried at high temperature, the ionic clusters were broken up and this process lead to a decrease in the overall water uptake of the membrane upon rehydration.

The water absorption behavior of Dais<sup>®</sup> membranes was studied by Weiss *et al.*<sup>18</sup> They determined that the equilibrium water uptake of the membranes with 5.2 mol% sulfonation was 0.40 wt% at 23°C and 10.7 wt% at 70°C and the equilibrium water uptake of the membranes with 11.9 mol% sulfonation was 2.35 wt% at 23°C and 11.07 wt% at 70°C. In a similar study conducted by Edmondson *et al.*<sup>38</sup> for 60% sulfonated Dais<sup>®</sup>, it was found that above 10% water uptake at room temperature, the rate at which samples absorb water increased compared to the rate below 10%. The swelling of the membranes was determined to be linearly proportional to the amount of water absorbed.

The molecular flux of the water molecules during water sorption/desorption experiments can be expressed by the following equation<sup>39</sup>:

$$J = -D \frac{d\mu}{dz} \quad \text{Equation 2.6.1}$$

where  $J$  is the flux,  $D$  is the constant,  $\mu$  is the chemical potential and  $z$  is the position. Fick's second law describes the changes in the species concentration with respect to time and position and can be described by the following differential equation:

$$\frac{\partial C}{\partial t} = \frac{\partial}{\partial z} \left( D \frac{\partial C}{\partial z} \right) \quad \text{Equation 2.6.2}$$

where  $C$  is the species concentration,  $t$  is the time, and  $D$  is the diffusion coefficient. The equation 2.6.2 assumes that the water behaves as an ideal solution and that, as result, Henry's law applies.

In the case of water sorption/desorption through Nafion<sup>®</sup> and Dais<sup>®</sup> membranes, the thickness of the membranes is infinitesimally small compared to the area of the film faces, so it can be assumed that transfer of water molecules does not occur through the edges of the material. If the assumption is made that the diffusion coefficient is only a function of temperature, the water concentration on the surface does not change, and there is no significant change in the sample dimensions, Fick's second law can be solved for semi-infinite slab geometry<sup>40</sup>:

$$\frac{\partial C}{\partial t} = D \left( \frac{\partial^2 C}{\partial z^2} \right) \quad \text{Equation 2.6.3}$$

The integration of the equation 2.6.3 over the sample volume results in the following expression<sup>41</sup>:

$$D = \pi \left( \frac{z_0}{4M_e} \right)^2 \left( \frac{M_2 - M_1}{\sqrt{t_2} - \sqrt{t_1}} \right)^2 \quad \text{Equation 2.6.4}$$

where  $M_e$  is an equilibrium moisture uptake and the term inside of the second brackets is the slope of the plot of mass uptake as a function of the square root of time. The equation 2.6.4 is used to determine the diffusion coefficients for the water sorption/desorption processes if the diffusion has Fickian or pseudo-Fickian character.

The diffusion through the polymer can be represented by the following expression<sup>41,42</sup>:

$$\frac{M_t}{M_e} = Kt^n \quad \text{Equation 2.6.5}$$

where  $M_t$  is the moisture uptake at time  $t$ , and  $K$  is a constant. If  $n$  is  $\frac{1}{2}$ , then the diffusion is Fickian and if  $\frac{1}{2} < n < 1$ , the diffusion is pseudo-Fickian. The equation 2.6.5 can be rearranged into a more convenient for use form:

$$\text{Log}\left(\frac{M_t}{M_e}\right) = \text{Log}(K) + n\text{Log}(t) \quad \text{Equation 2.6.6}$$

In this thesis, water absorption and desorption rates at room temperature will be determined and equilibrium water uptake will be calculated and compared to the results found in the literature. The diffusion coefficients will be determined for the sorption/desorption processes that follow the Fickian type of behavior.

## 2.7 Sulfonation Effect

Weiss *et al*<sup>18</sup> studied the effects of sulfonation in Dais<sup>®</sup> membranes. They compared the results of thermomechanical analysis of the styrene-ethylene/butylene-styrene (SEBS) samples and 5.2% and 11.9% sulfonated sodium and zinc salts of SEBS. The authors determined that  $T_g$  of the styrene block increased with the increase in the sulfonation level of the polymers due to the formation of ionic clusters that served as physical crosslinks. As reported previously, they also found that equilibrium water uptake increased with an increase in sulfonation level. Weiss *et al* attributed this effect to an enhanced hydrophilicity of the membranes caused by the introduction of polar sulfonic acid side-groups.

Hara *et al*<sup>43</sup> studied the effect of sulfonation on the mechanical properties of lightly sulfonated (up to 8.5 mol% sulfonation) polystyrene ionomers. They found that the  $T_g$  of the polystyrene increased linearly with the increase in the degree of sulfonation at the rate of about 3°C/mol%. They also attributed this effect to the formation of the ionic clusters.

In this thesis, water absorption and mechanical behavior of Dais<sup>®</sup> membranes with 30% and 60% sulfonation levels will be compared.

## 2.8 Thermal Stability

The thermal stability of Nafion<sup>®</sup> membranes has been studied by thermogravimetric analysis technique (TGA) (Section 3.4) in conjunction with mass spectrometry and differential thermal analysis. It was determined that Nafion<sup>®</sup> was stable up to 275-280°C. The detailed results of the studies of thermal stability of Nafion<sup>®</sup> are summarized in Table 2.8.1. A typical TGA trace of Nafion<sup>®</sup> in air is shown in Figure 2.8.1.

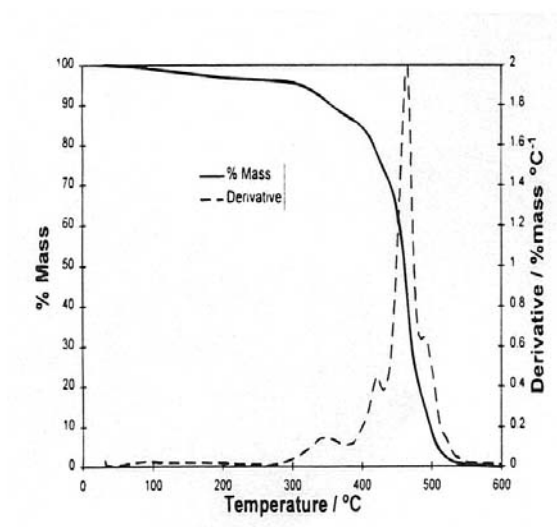


Figure 2.8.1 TGA Trace of Nafion<sup>®</sup> in Air from Samms et al<sup>45</sup>

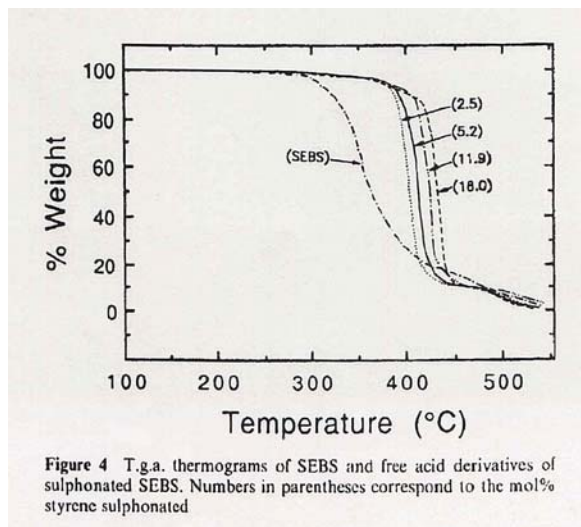


Figure 4 T.g.a. thermograms of SEBS and free acid derivatives of sulphonated SEBS. Numbers in parentheses correspond to the mol% styrene sulphonated

Figure 2.8.2 TGA Trace of Dais<sup>®</sup> in Air from Weiss et al<sup>18</sup>

The thermal stability of Dais<sup>®</sup> membranes was studied by Weiss *et al*<sup>18</sup> who performed TGA analysis of the material in air at the heating rate of 10°C/min (Figure 2.8.2). They found that thermal stability increased with an increase in the sulfonation level of the material. This effect might be due to the formation of ionic crosslinks as discussed in section 2.7. The analysis of the TGA traces lead to the conclusion that

sulfonated SEBS was stable up to the temperature of 360-380°C even though sulfonic side-groups are generally considered thermally unstable.

Table 2.8.1 Results of Nafion® TGA Studies

	Surowiec and Bogoczek <sup>44</sup>	Samms et al <sup>45</sup>		DeAlmeida and Kawano <sup>46</sup>
Conditions	Air atmosphere 10°C/min	N <sub>2</sub> 20°C/min	Air 20°C/min	N <sub>2</sub> 20°C/min
<b>Mass Loss region</b>				
<i>Temperature</i>	50-180°C	75-225°C	75-225°C	25-290°C
<i>Mass % lost</i>	4%	5%		6.4%
<i>Groups lost</i>	moisture	moisture	moisture	moisture
<b>Mass Loss region</b>				
<i>Temperature</i>	310-380°C	275-400°C	275-400°C	290-400°C
<i>Mass % lost</i>	7.7%	10%		
<i>Groups lost/ decomposition products</i>	Sulfonic groups	Sulfur dioxide	Sulfur dioxide	Desulfonation
<b>Mass Loss region</b>				
<i>Temperature</i>	420-590°C	400-600°C	400-500°C, 2 peaks	a) 400-470°C b) 470-560°C
<i>Mass % lost</i>	78%	75%		
<i>Groups lost/ decomposition products</i>	Perflurionated matrix	SO <sub>2</sub> , CO <sub>2</sub> , C <sub>x</sub> F <sub>y</sub>	SO <sub>2</sub> , CO <sub>2</sub> , C <sub>x</sub> F <sub>y</sub> , C <sub>x</sub> F <sub>y</sub> O <sub>z</sub>	a) Side-chain decomposition b) PTFE backbone decomposition

In this thesis, the thermal stability of Nafion® and Dais® membranes will be studied by means of TGA and the results will be compared to the results reported in the literature.

## 2.9 Dynamic Mechanical Analysis

The response of viscoelastic materials to an applied deformation consists of an elastic component (due to an elastic energy stored in the material) and a viscous component (due to viscous energy dissipation). When a sinusoidal stress  $\sigma$  with an angular frequency  $\omega$  is applied to the material, the response of the system is a strain,  $\epsilon$ , due to elastic component of the deformation. However, this strain is not instantaneous because the time lag exists between the initial stress application and the materials response due to viscous flow (Figure 2.9.1). The phase shift between the stress and strain curves is  $\delta$ .

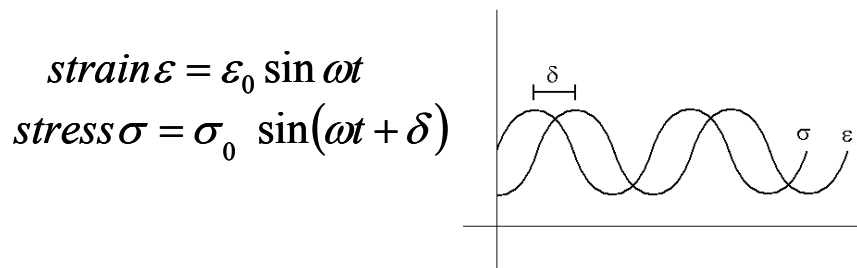


Figure 2.9.1 Dynamic Mechanical Stress-Strain Relationship

The phase shift  $\delta$  is related to the energy stored in the material by Equation 2.9.1 where  $E'$  is storage modulus (elastic component) and  $E''$  is loss modulus (viscous component). The graphical representation of this dependence is shown in Figure 2.9.2.

$$\tan \delta = \frac{E''}{E'} \quad \text{Equation 2.9.1}$$

From Figure 2.9.2 it is evident that the relative amounts of elastic and viscous components change as functions of temperature and time. Since the elastic component drastically decreases with the onset of long-range coordinated molecular motions while the viscous component reaches the maxima, Dynamic Mechanical Analysis (DMA) can be successfully employed to detect glass transition temperature(s). DMA is also capable

of detecting secondary transitions. For example, the relaxation of the side-chains ( $\beta$  transition) and short range movements of the atoms in the backbone ( $\gamma$  transition) will result in the small peaks in the  $\tan \delta$  curve.

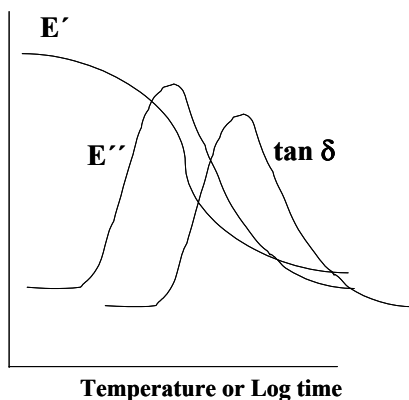


**Figure 2.9.2 Dynamic Mechanical Behavior**

From DMA data,  $T_g$  can be mechanically defined either as the peak in the loss modulus or  $\tan \delta$  peak (Figure 2.9.2). In this work, the later convention will be adopted for most cases with the exception of the aging experiment where  $T_g$  will be defined as an inflection point in the storage modulus (Section 4.2).

The position of the  $\tan \delta$  peak along the temperature axis depends on the rate at which the DMA trace is collected: the slower the scan rate, the larger the amount of time allowed for reorientation of polymeric chains. Therefore, the samples measured at slower rate or at lower frequency will have peak of the  $\tan \delta$  at lower temperature.

In this thesis DMA will be used to study the mechanical response of virgin and aged Nafion<sup>®</sup> and Dais<sup>®</sup> membranes in the dry and saturated state.

### 3 EXPERIMENTAL

#### 3.1 Materials

The chemical structures of Nafion<sup>®</sup> and Dais<sup>®</sup> membranes used in the study were shown in Figure 2.2.1 and Figure 2.2.2, while their chemical composition was discussed in Section 2.2.

**Table 3.1.1 Properties of Nafion<sup>®</sup> Membranes<sup>47</sup>**

Property	Typical Value
Water Uptake, % water <sup>i</sup>	35
Tensile Modulus, MPa 50% RH, 23°C water soaked, 23°C water soaked, 100°C	249 114 64
Tensile Strength, max, MPa 50% RH, 23°C water soaked, 23°C water soaked, 100°C	43 <sup>ii</sup> , 32 <sup>iii</sup> 34 <sup>ii</sup> , 26 <sup>iii</sup> 25 <sup>ii</sup> , 24 <sup>iii</sup>
Elongation at Break, % 50% RH, 23°C water soaked, 23°C water soaked, 100°C	225 <sup>ii</sup> , 310 <sup>iii</sup> 200 <sup>ii</sup> , 275 <sup>iii</sup> 180 <sup>ii</sup> , 240 <sup>iii</sup>
Density, g/cm <sup>3</sup>	2.0
Conductivity, S/cm	0.10

<sup>i</sup> Water uptake from dry membrane soaked in water at 100°C for 1 hour

<sup>ii</sup> Measured in machine direction

<sup>iii</sup> Measured in transverse direction

Nafion<sup>®</sup> membranes were donated by DuPont Corporation. The material was supplied in the form of a film with a thickness of 0.18 mm. Some relevant properties of the material are listed in Table 3.1.1. Prior to use, the membranes were pre-treated by boiling in deionized (DI) water for 2 hours. After the pre-treatment, the films were stored in DI water at room temperature until the subsequent testing.

For the aging experiments, the pre-treated Nafion<sup>®</sup> membranes were stored for various amounts of time in the deionized water in the oven at 60°C and 90°C.

For the experiment on the effects of the pre-treatment, Nafion<sup>®</sup> membranes were treated by the methods shown in Table 3.1.2. After pre-treatment, the films were stored in DI water at room temperature until the subsequent testing.

**Table 3.1.2 Nafion<sup>®</sup> Pre-Treatment Procedures**

<b>Method</b>	<b>Treatment Procedure</b>
1	Boil for 1 hr in DI water
2	Boil for 2 hrs in DI water
3	Boil for 1 hr in DI water Boil for 1 hr in 3% Hydrogen Peroxide (H <sub>2</sub> O <sub>2</sub> )
4	Boil for 1 hr in DI water Boil for 1 hr in 3% Hydrogen Peroxide (H <sub>2</sub> O <sub>2</sub> ) Boil for 1 hr in DI water

Dais 585 membranes were donated by Dais-Analytic Corporation. This material was supplied in the form of a film with the thickness of 0.127 mm and 0.038 mm. For all of the experiments (with the exception of Fourier Transform Infrared Analysis) 0.127 mm film was used. Two forms of the membranes were studied: one with 30% sulfonation and another with 60% sulfonation. The proton conductivity of Dais<sup>®</sup> membranes at 60% sulfonation was measured by Wnek *et al*<sup>14</sup> to be 0.08 S/cm. Data on the mechanical properties of these membranes were not found in the literature. Prior to testing, the materials were stored in the dry form in a dark drawer at room temperature.

For the aging studies of the Dais<sup>®</sup> membranes, 30% sulfonated Dais<sup>®</sup> films were stored in DI water in the oven at 90°C.

### 3.2 Methods: DMA

The majority of studies of the dynamic mechanical properties of Dais<sup>®</sup> and Nafion<sup>®</sup> membranes were performed using a Perkin Elmer DMA 7. The DMA 7 unit is capable of supporting three different geometries: 3-point bending assembly, extension assembly and parallel plates assembly (Figure 3.2.1).

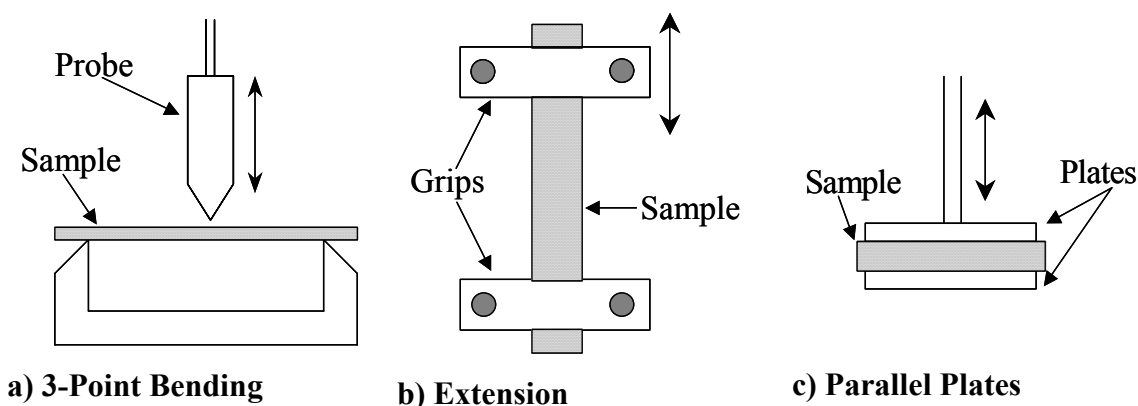


Figure 3.2.1 Perkin Elmer DMA 7 Testing Geometries

The 3-point bending assembly consists of a fixed base and a probe that oscillates in the vertical direction (Figure 3.2.1a). It is commonly used to measure dynamic mechanical response of crystalline and semicrystalline polymers. However, this assembly is often not suitable for testing flexible thin films, as in the case of Nafion<sup>®</sup> and Dais<sup>®</sup> membranes, because of the sample's inability to support the weight of the probe.

The parallel plates assembly consists of two parallel plates (Figure 3.2.1c) with the bottom plate fixed and the upper plate oscillating in the vertical direction. A characteristic data curve obtained for Nafion<sup>®</sup> using the parallel plates assembly is shown in Figure 3.2.2. The data was collected at the rate of 2°C/min at the frequency of 1Hz in a nitrogen atmosphere. It is possible to monitor the changes in the material response using this geometry: there is a clear peak in  $\tan \delta$  at 121°C and a drop in the storage modulus from  $1.0 \times 10^7$  Pa to  $3.8 \times 10^6$  Pa. However, the  $\tan \delta$  curve is noisy and the drop in the storage modulus is lower than expected. The expected drop in the storage modulus at the glass transition is at least one order of magnitude, but it can be lower in this case

since the sample is tested in the compression mode. If the thickness of the sample is increased, the results of the tests performed using the parallel plates assembly will improve; however, in this case the sample thickness is limited by the availability of the manufactured Nafion<sup>®</sup> and Dais<sup>®</sup> membranes.

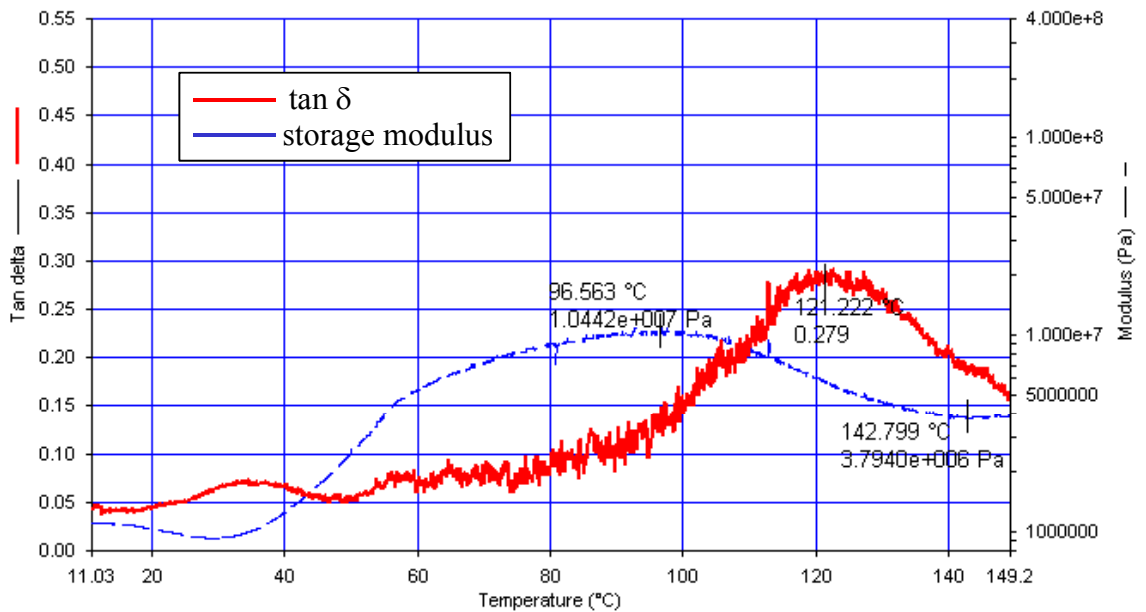


Figure 3.2.2 Temperature Sweep of Nafion<sup>®</sup> Using Parallel Plates Geometry

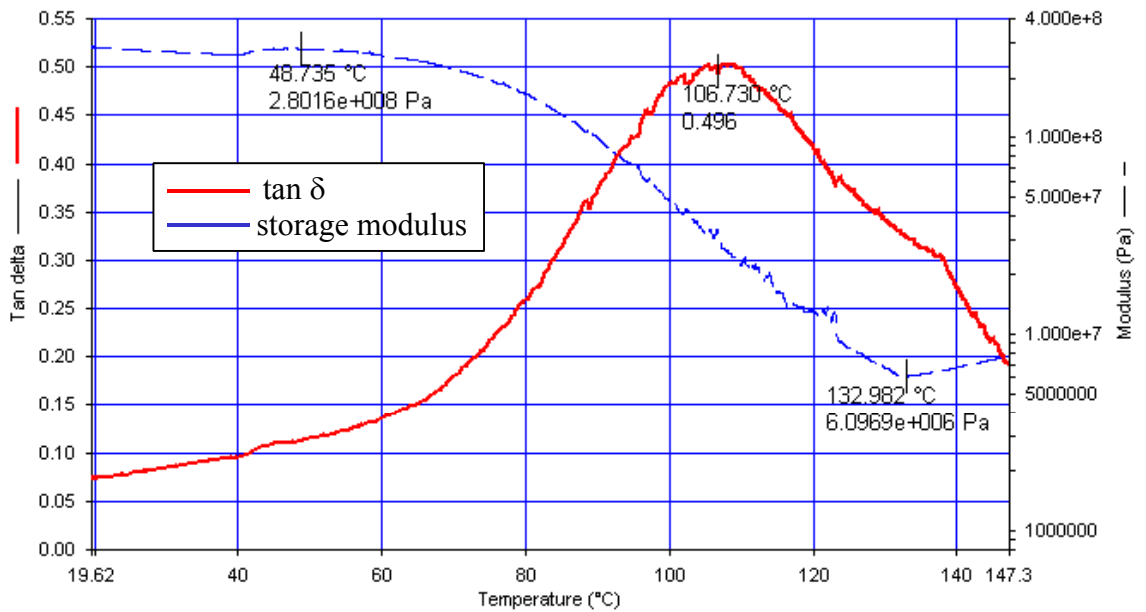


Figure 3.2.3 Temperature Sweep of Nafion<sup>®</sup> Using Extension Geometry

The extension assembly consists of two grips (Figure 3.2.1b). The bottom grip is fixed and the upper grip oscillates in the vertical direction. The sample is fixed between the grips and is held in place by four screws. A characteristic data curve obtained for Nafion<sup>®</sup> using the extension assembly is shown in Figure 3.2.3. The sample was tested using the same experimental settings (nitrogen atmosphere and a heating rate of 2°C/min) as the Nafion<sup>®</sup> membrane shown in Figure 3.2.2. However, the trace of the extension sample has significantly less noise and the drop in the storage modulus is more pronounced, despite being collected at the same conditions. The extension geometry was chosen over other assemblies for all dynamic mechanical tests performed using Perkin Elmer DMA 7.

In order to measure the dynamic mechanical response of the saturated Nafion<sup>®</sup> and Dais<sup>®</sup> membranes, a solvent sleeve, fitted for the DMA 7 by McPeak,<sup>48</sup> was used. The schematics of the Perkin Elmer DMA 7 and the water sleeve for 3-point bending geometry are shown in Figure 3.2.4. The sleeve filled with DI water fits inside of the DMA furnace opening and the sample stage with the sample are immersed inside. This set up allows for the measuring of the properties of the films while they are saturated by DI water.

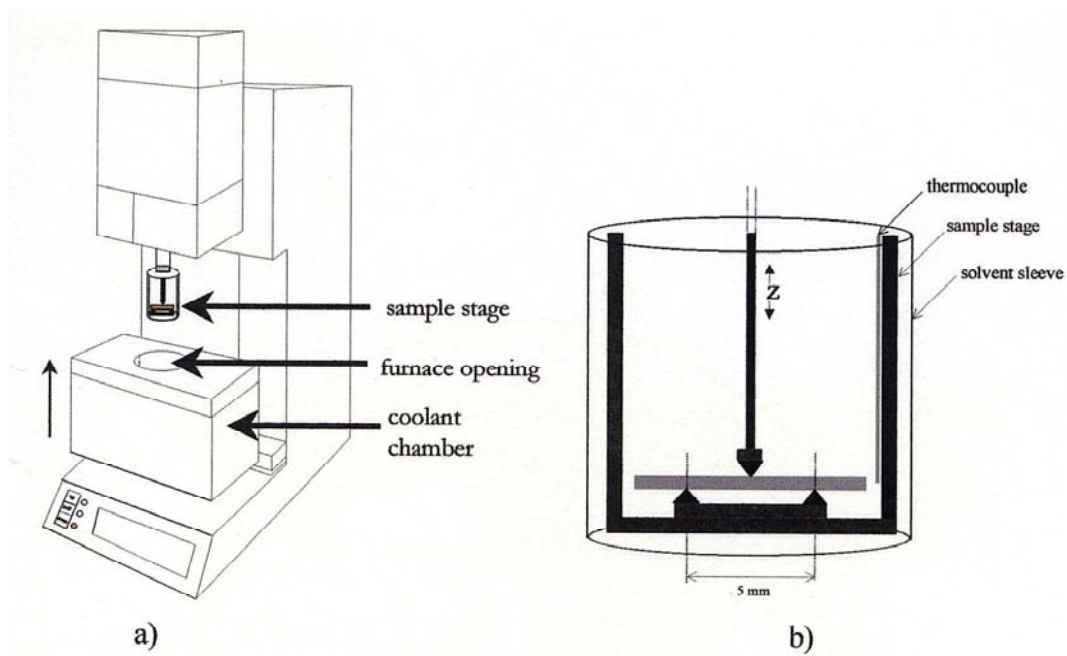


Figure 3.2.4 Perkin Elmer DMA 7: a) Analyzer, b) Sample Stage with the Solvent Sleeve<sup>48</sup>

Isochronal DMA scans were performed for Nafion<sup>®</sup> and Dais<sup>®</sup> membranes in order to determine their glass transition temperature at both dry and saturated states and to monitor the changes in  $T_g$  of the materials as a function of aging time. The samples were tested in a nitrogen atmosphere at a scanning rate of 2°C/min and a frequency of 1Hz. In order to demonstrate the effect of frequency on the response of the material, frequencies other than 1 Hz were also used in several runs. The initial forces applied to the samples are shown in Table 3.2.1. Both materials were run with the applied static force set at 110% of the applied tensile force. The dimensions of the samples varied between 3.5 mm and 5.5 mm in length and between 0.18 and 0.3 mm in width. The dimensions of the samples in each set of the experiments were kept approximately the same. The thickness of the films was 0.18 mm for Nafion<sup>®</sup> membranes and 0.127 mm for Dais<sup>®</sup> membranes.

**Table 3.2.1 Initial Forces for DMA 7 Isochronal Scans**

	<b>Static Force, mN</b>	<b>Dynamic Force, mN</b>
Nafion <sup>®</sup>	150	136
Dais <sup>®</sup>	50	45

Prior to DMA testing of the saturated membranes, the samples were immersed in DI water and allowed to equilibrate for 30min. In the case of aged Nafion<sup>®</sup>, saturated films were removed from the oven, blotted with Kimwipes and allowed to dry in air for 1 hr before the DMA testing. In the case of aged Dais<sup>®</sup> membranes, saturated films were removed from the oven, blotted and allowed to dry in air for 12 hours before testing. The drying times (1hr for Nafion<sup>®</sup> and 12 hours for the Dais<sup>®</sup> membranes) were determined in independent experiments to be sufficient time periods to assure that the samples are equilibrated at RT conditions. The DMA coupons in each separate aging experiment were cut from a single aging sample and the rest of the sample was returned to the ovens for further aging. For each aging time three samples were tested. Three experiments were carried out for aging of Nafion<sup>®</sup> membranes at 90°C, one experiment for aging of Nafion<sup>®</sup> membranes at 65°C and two experiments for aging of Dais<sup>®</sup> membranes at 90°C.

Initially, in order to construct a mastercurve for Dais<sup>®</sup> membranes with 60% sulfonation, the DMA 7 was used to obtain isothermal frequency scans of the films in the temperature range between  $-80^{\circ}\text{C}$  and  $250^{\circ}\text{C}$ . However, all scans that were obtained had a peak in the  $\tan \delta$  and an abrupt drop of the storage modulus in the range of 25-30 Hz due to the resonant frequency of the DMA unit and materials system. As a consequence, the data used to construct a mastercurve was collected using a Seiko DMS 210. The sample was tested using a horizontal extension fixture under nitrogen atmosphere with a scanning rate of  $2^{\circ}\text{C}/\text{min}$  in the temperature range between  $-80^{\circ}\text{C}$  and  $250^{\circ}\text{C}$ . The sample was cycled through the following range of frequencies: 0.05 Hz, 0.1Hz, 0.3Hz, 1Hz, 5Hz and 10Hz. The tested Dais<sup>®</sup> film was 10mm in length and 3.6mm in width.

In order to construct a mastercurve, storage modulus data at each frequency were plotted as a function of temperature and data for selected temperature values for each frequency was interpolated from these curves. The storage modulus curves were then plotted as a function of  $\text{Log}(1/\text{frequency})$  for each temperature selected in the previous step. Finally, the curves were shifted right and left of the  $25^{\circ}\text{C}$  curve, so that a continuous storage modulus plot versus  $\text{Log}(A/\text{Frequency})$  was obtained. The values of the shift factor  $A$  were then used to create a shift factor plot.

### **3.3 Methods: DSC**

Differential Scanning Calorimetry (DSC) is commonly used to detect transitions and sub-transitions such as melting point and  $T_g$  of the polymeric materials. It measures the difference between the energy absorbed or desorbed by the empty reference pan and a pan with the tested material in it.

A DSC trace obtained for Nafion<sup>®</sup> membrane by Almeida *et al*<sup>46</sup> is shown in Figure 3.3.1. The authors attributed the lower peak in Nafion-H at  $115^{\circ}\text{C}$  to order-disorder transition of ionic clusters and the higher peak at  $230\text{-}250^{\circ}\text{C}$  to the melting of microcrystalline regions in the material.

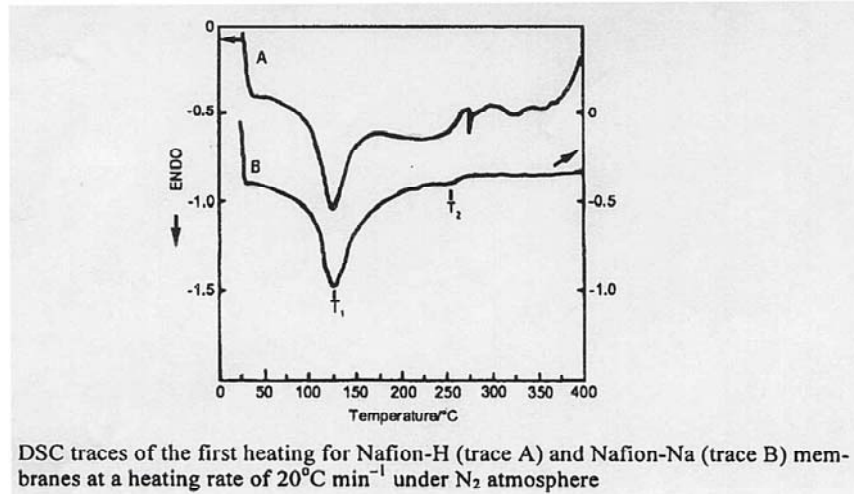


Figure 3.3.1 DSC trace of Nafion<sup>®</sup> from Almeida *et al*<sup>46</sup>

In this work, a Perkin Elmer Pyris 1 DSC was originally used to analyze the thermal behavior of the Nafion<sup>®</sup> and Dais<sup>®</sup> membranes at subambient temperatures and a Perkin Elmer DSC 7 was used to analyze the thermal behavior at ambient temperatures. The samples were tested under nitrogen atmosphere at a heating rate of  $5^{\circ}\text{C/min}$ . The sample size was  $16.5 \pm 0.2$  mg for Nafion<sup>®</sup> samples and  $10.6 \pm 0.2$  mg for Dais<sup>®</sup> samples. The sample traces for Nafion<sup>®</sup>, Dais<sup>®</sup> 30% sulfonation and Dais<sup>®</sup> 60% sulfonation membranes are shown in Figure 3.3.2, Figure 3.3.3, Figure 3.3.4 and Figure 3.3.5 respectively.

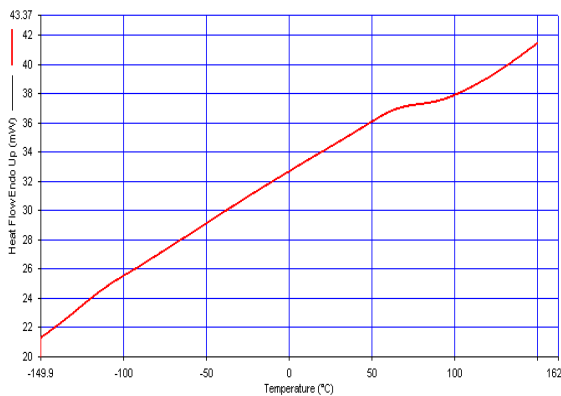


Figure 3.3.2 DSC Trace of Nafion<sup>®</sup>

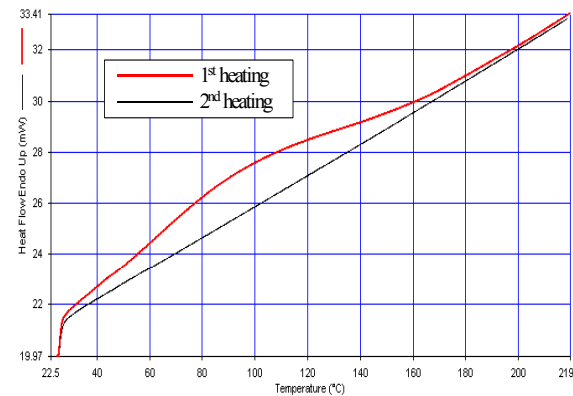
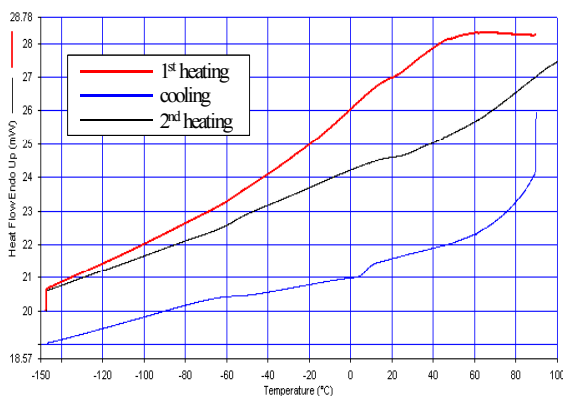
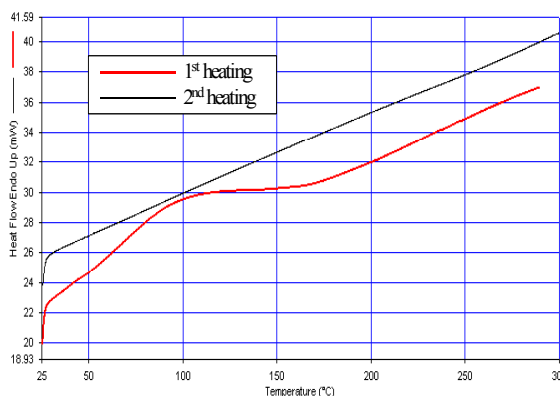


Figure 3.3.3 DSC Trace of Dais<sup>®</sup> 30% Sulfonation



**Figure 3.3.4 Subambient DSC of Dais® 60% Sulfonation**



**Figure 3.3.5 Ambient DSC of Dais® 60% Sulfonation**

Based on the results shown above, it is not possible to detect any transitions in Nafion® or Dais® using DSC. The effects that are seen on the first heating of the materials are absent on subsequent heating and are attributed to the residual water present in both membranes. Similar DSC results for Nafion® are also reported by Chen *et al.*<sup>49</sup> It is conceivable that the differences in the heat capacities of the materials above and below the glass transition are not very large and that is the reason why they are not detected by the DSC. As a result, the DSC results for both Nafion® and Dais® membranes will not be used in further discussions.

### **3.4 Methods: TGA**

Thermogravimetric Analysis (TGA) is commonly utilized to study thermal stability of polymeric materials. It measures weight loss as a function of temperature of a sample suspended inside of the furnace.

In this work a Perkin Elmer TGA 7 was used to study thermal degradation behavior of Nafion® and Dais® membranes. Samples were tested using nitrogen and air atmospheres at a heating rate of 20°C/min. Sample weight varied between 8.0 mg and 11.0 mg. The results were reported as weight % vs. temperature and the derivative of

weight % vs. temperature. Characteristic TGA traces of Nafion<sup>®</sup> and Dais<sup>®</sup> membranes are shown in Figure 3.4.1 and Figure 3.4.2.

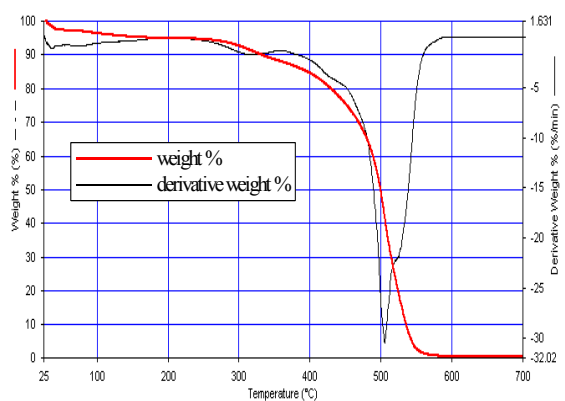


Figure 3.4.1 TGA of Dais<sup>®</sup> 30% Sulfonation in Air

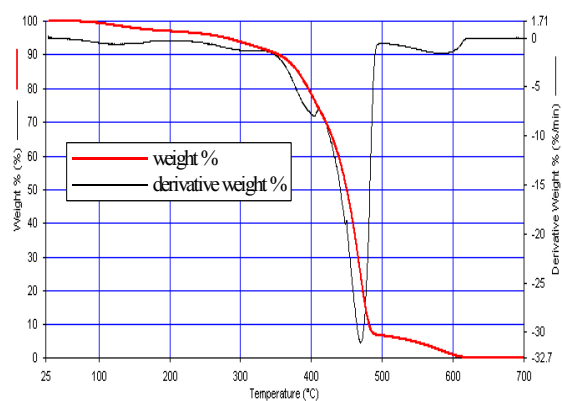
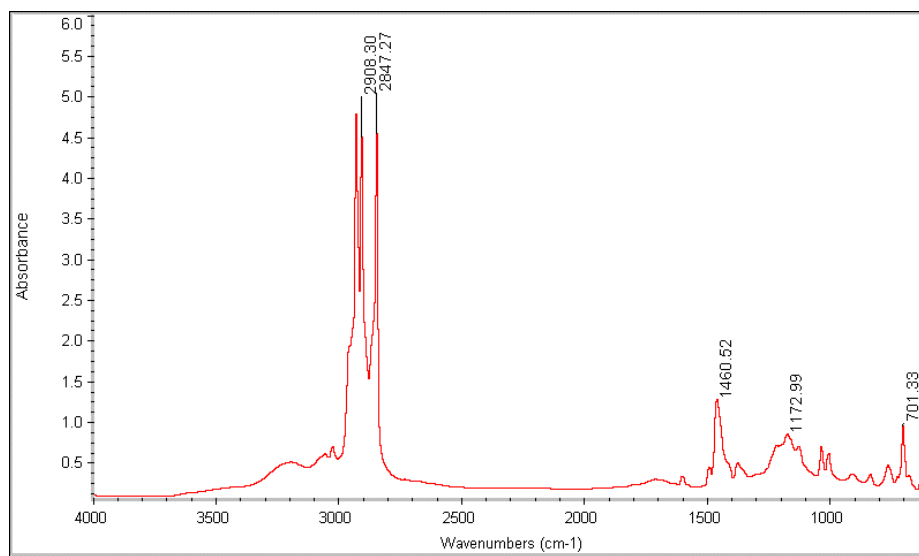


Figure 3.4.2 TGA of Nafion<sup>®</sup> 117 in Air

### 3.5 Methods: FTIR

Fourier Transform Infrared Spectroscopy (FTIR) is a technique that can be used to study the chemical structure of organic molecules and potential structural changes that occur as a result of the material's chemical treatment or degradation. FTIR measures the infrared radiation absorbed as a result of the change in the dipole moment due to the vibrational or rotational motions of the atoms.<sup>50</sup>

In this thesis a Midac M series FTIR with Midac Grams/32 software was used to collect FTIR spectra of the Dais<sup>®</sup> membranes. The measurements were taken in the absorbance mode using a film FTIR stage. The samples were tested in a nitrogen atmosphere and a total of 32 scans were collected for each spectrum. The samples were purged with nitrogen inside of the FTIR chamber for 10 min prior to the start of the scanning in order to minimize the effects of the residual water in the membranes. The thickness of the films studied was 0.038 mm. The FTIR data were analyzed using Omnic E.S.P. software. The characteristic spectrum of the Dais<sup>®</sup> membrane is shown in Figure 3.5.1.



**Figure 3.5.1 FTIR Spectrum of Dais® 30% Sulfonation**

FTIR analysis was used to investigate potential chemical changes that might occur as a result of heating or aging of Dais® membranes. In order to assure better reproducibility and accuracy of the measurements, the following procedure was implemented. Two samples of 30% sulfonated Dais® membrane and one sample of 60% sulfonated membrane were cut and each of them was fixed between two pieces of silicon rubber with a round opening in the middle. The initial spectrum of each sample was then taken and the samples were left for an appropriate treatment: the first 30% sulfonated membrane was immersed in DI water and placed in a 90°C oven for 150 hrs, the second one was placed in the oven at 160°C for 1hr and the 60% sulfonated sample was placed in the oven at 225°C for 1hr. The FTIR spectrum of the aged sample was measured at the end of the aging period and the spectra of the other two samples were taken every 15 min. The samples were never removed from the rubber silicon fixture and, as result, the spectra were taken at the same spot throughout each experiment; thereby, reducing the effect of sample inhomogeneity.

### 3.6 Methods: Water Uptake

The experiments in this section were divided into three parts: moisture uptake, sorption kinetics and desorption kinetics studies. For all three sets of the experiments, membranes were cut into  $21.7 \pm 0.9 \times 27.4 \pm 1$  cm rectangular pieces and, except where noted, a total of three measurements was taken for each kind of membrane.

In the moisture uptake experiments, the maximum amount of water absorbed by the membranes from the liquid phase was determined. In order to accomplish this, the samples were first equilibrated at room temperature conditions for 24 hrs and weighed. This weight is referred to as the “dry RT weight”. The samples were then placed in DI water at RT for 24 hrs, after which they were blotted with Kimwipes and weighed again. This weight is referred to as the “maximum uptake” weight.

The water absorption and desorption kinetics studies were carried out in an environmental chamber with a continuous weight acquisition system (Figure 3.6.1). The chamber model 518 was connected to ETS ultrasonic humidification system model 5612 and to a Drierite gas drying unit. A Denver Instrument Company A-200DS digital balance connected to the data acquisition computer was placed on top of the chamber and the sample was suspended from the bottom of the balance inside of the chamber by a wire with a shock absorber. The humidity in the chamber was measured by a Fisher Scientific digital hygrometer. The data was collected using LabView data acquisition software.

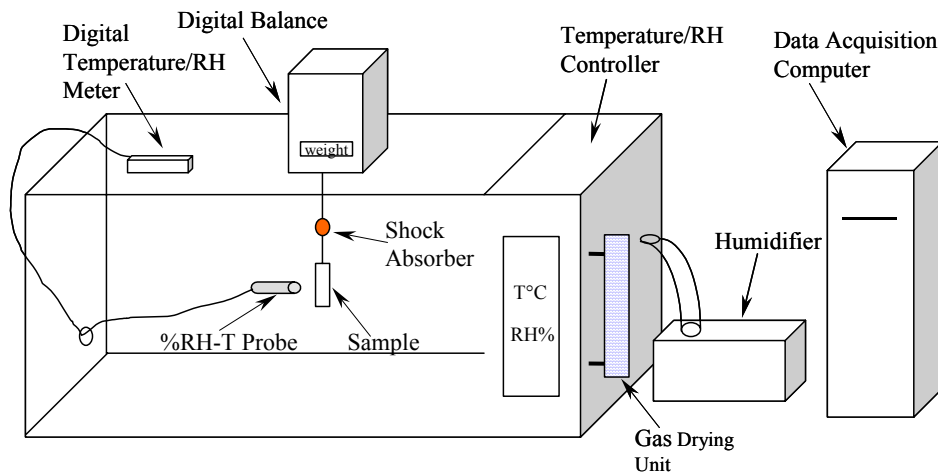


Figure 3.6.1 Environmental Control Chamber with Continuous Weight Acquisition System

In the sorption kinetics studies, the amount of water absorbed by the membranes from the vapor phase was determined. In order to accomplish this, the samples were equilibrated at RT conditions for 24 hours prior to the start of the experiment. They were then suspended inside of the chamber at  $98\pm 2\%$  RH and their weight uptake was recorded as a function of time.

For the desorption kinetics studies, the samples were equilibrated in DI water at RT for 24 hours prior to the start of the experiment. They were then suspended inside of the chamber at  $10\pm 2\%$  RH and their weight loss was recorded as a function of time.

### ***3.7 Methods: SEM***

Scanning electron microscopy (SEM) is a method commonly used to analyze the topology of the material surfaces on a submicrometer scale by sweeping the surface by a finely focused electron beam<sup>51</sup>.

In this thesis, LEO 1550 SEM with accelerating voltage of 5kV was used to compare the topology of untreated and pre-treated Nafion<sup>®</sup> membranes. Prior to the analysis, the membranes were coated with gold using BAL-TEC SCD 05 sputter coater.

## 4 RESULTS

### 4.1 DMA: Nafion<sup>®</sup> Membranes

A DMA spectrum of Nafion<sup>®</sup> is shown in Figure 4.1.1. It is evident that the storage modulus of the material exhibits two major drops: the first drop from  $1.8 \times 10^9$  Pa to  $3.4 \times 10^8$  Pa in the temperature region between  $-104^\circ\text{C}$  and  $0^\circ\text{C}$  and the second drop from  $3.4 \times 10^8$  Pa to  $4.9 \times 10^6$  Pa in the temperature region between  $50^\circ\text{C}$  and  $145^\circ\text{C}$ .  $\tan \delta$  shows two visible peaks: at  $-74^\circ\text{C}$  and at  $109^\circ\text{C}$ .

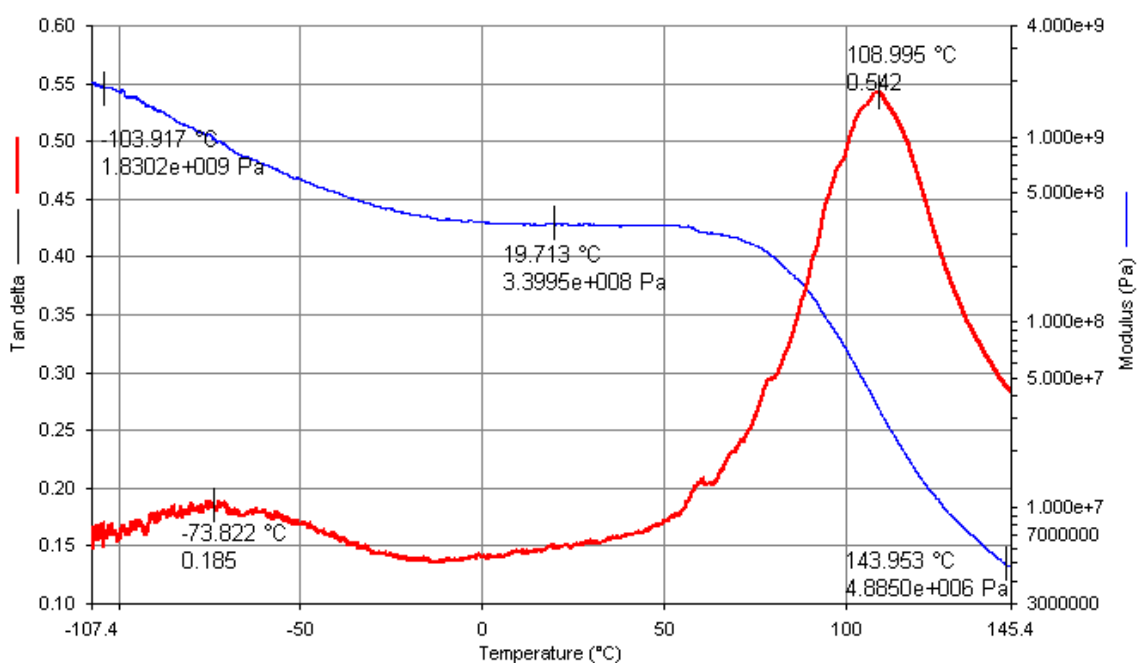


Figure 4.1.1 Nafion<sup>®</sup> DMA Spectrum

The results of the ambient scan of dry Nafion<sup>®</sup> membrane are shown in Figure 4.1.2. “Dry membrane” in this case is defined as the membrane that was equilibrated at the room temperature conditions. The results of the ambient scan of the saturated Nafion<sup>®</sup> membrane are shown in Figure 4.1.3.

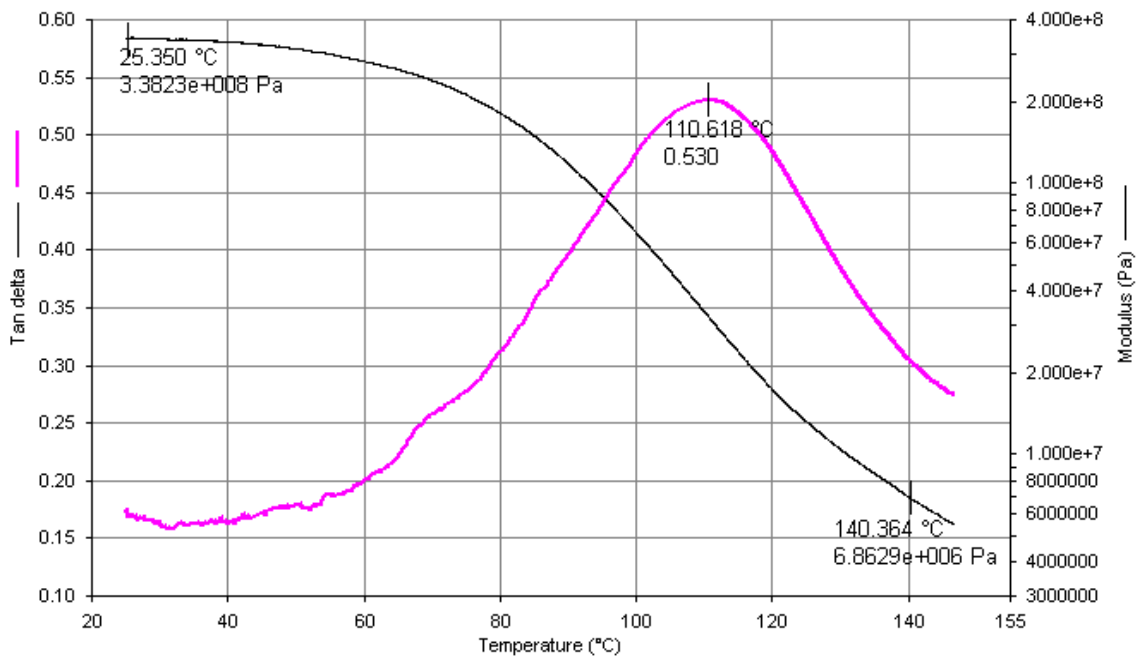


Figure 4.1.2 Ambient DMA Scan of Dry Nafion® Membrane

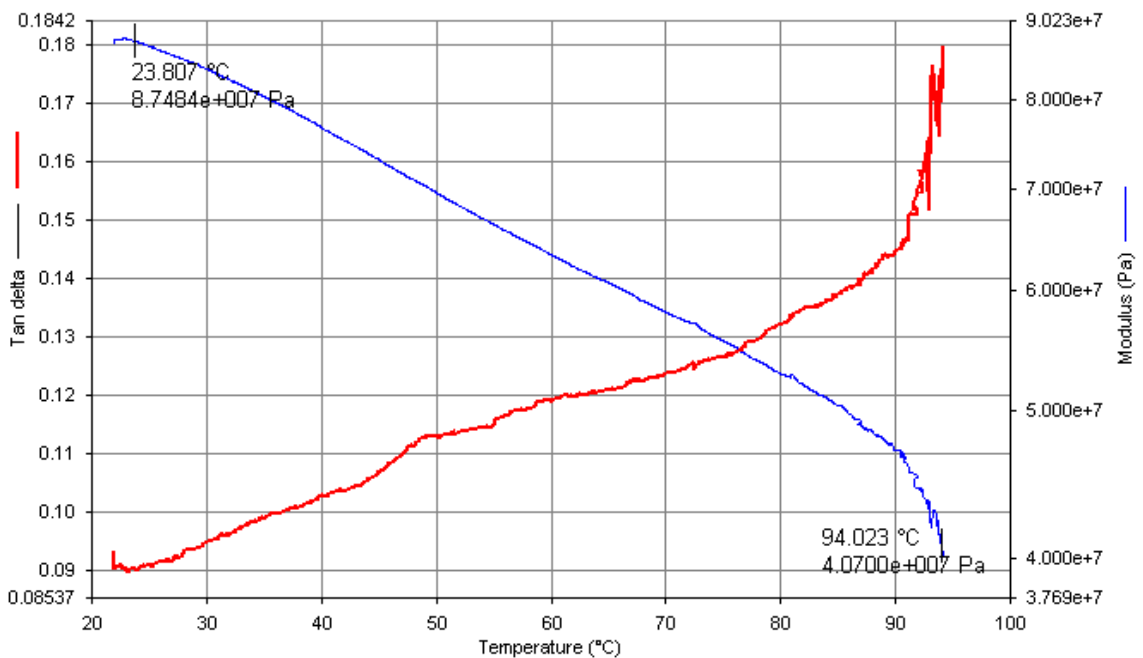
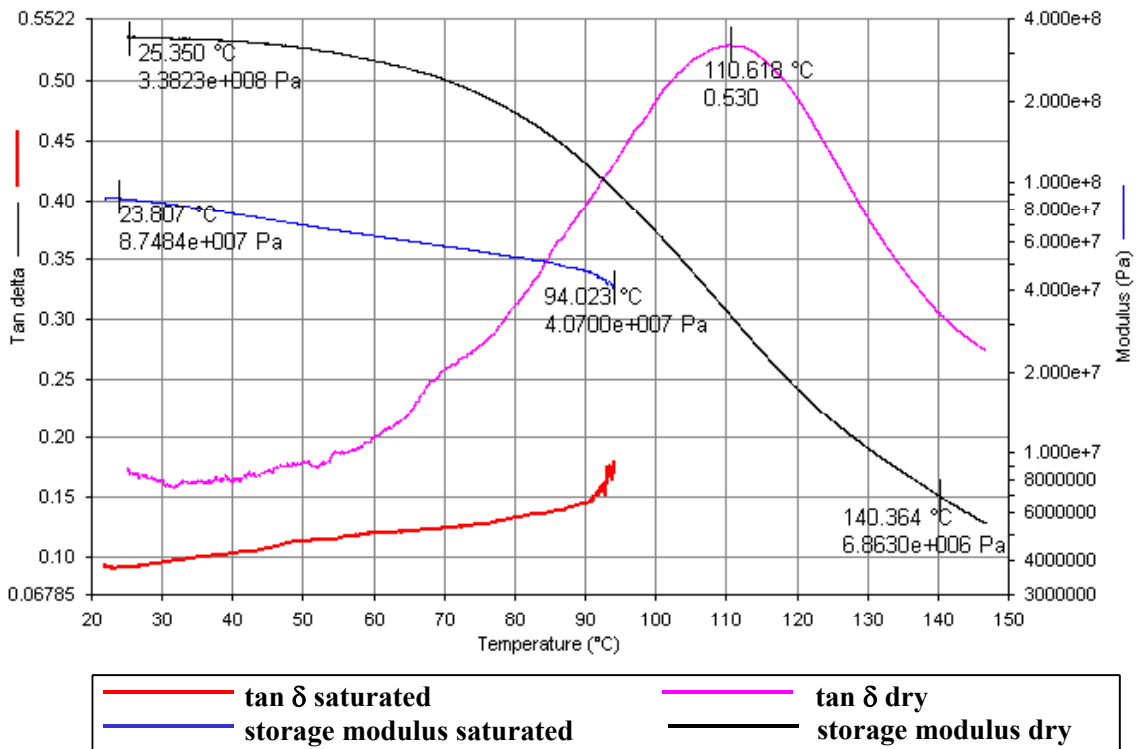


Figure 4.1.3 Ambient DMA Scan of Saturated Nafion® Membrane



**Figure 4.1.4 Comparison of Dry and Saturated Nafion® Membranes**

In order to compare the dry and saturated membranes, both dry and saturated scans are combined in Figure 4.1.4. The storage modulus of the dry sample drops by over an order of magnitude from  $3.38 \times 10^8$  Pa to  $6.9 \times 10^6$  Pa and tan  $\delta$  has a peak at 111°C. The storage modulus of the saturated sample starts at a much lower value of  $8.7 \times 10^7$  Pa and decreases to  $4.1 \times 10^7$  Pa without going through a well-pronounced drop. Tan  $\delta$  of the saturated membrane never reaches a peak.

The effect of frequency on the behavior of the saturated and dry membranes is shown in Figure 4.1.5 and Figure 4.1.6. For the saturated membranes there are no significant dissimilarities between the scans collected at different frequencies over the range examined. For the dry membranes, the tan  $\delta$  peak moved from 105°C for the scan collected at 0.5Hz to 122°C for the scan collected at 45Hz. There is also a noticeable shift to higher temperature with an increase in the frequency of the storage modulus curve for the dry Nafion®.

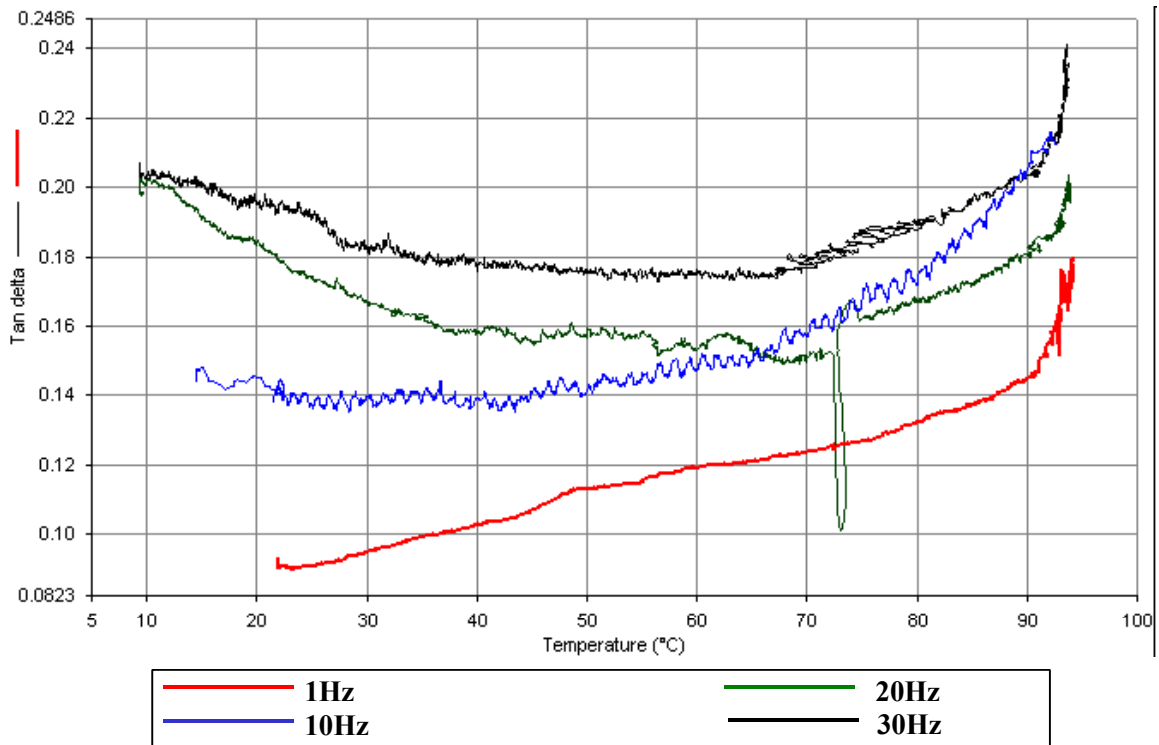


Figure 4.1.5 Ambient DMA Scan of Saturated Nafion® for a Range of Frequencies

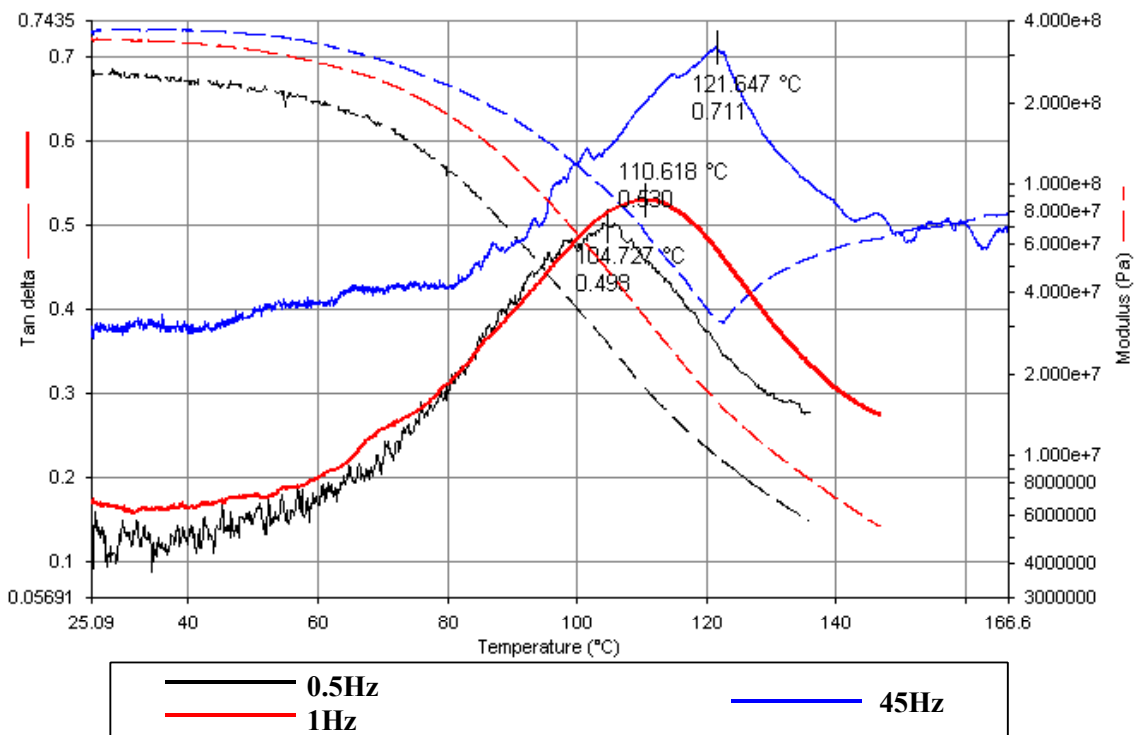


Figure 4.1.6 Ambient DMA Scans of dry Nafion® for a Range of Frequencies

The effect of various pre-treatment methods (Table 3.1.2) on the mechanical behavior of Nafion<sup>®</sup> membranes is shown in Figure 4.1.7 by the representative DMA scans. The complete results of the pre-treatment effect on the position of tan  $\delta$  peak are summarized in Table 4.1.1. The lowest tan  $\delta$  peak corresponds to the untreated Nafion<sup>®</sup> sample. The samples pre-treated in boiling DI water for 1hr and 2hr have tan  $\delta$  peaks at the same temperature, several degrees higher than do untreated samples. The membranes treated in aqueous solution of 3% H<sub>2</sub>O<sub>2</sub> have tan  $\delta$  peak at temperatures much higher than do untreated samples and those treated in DI water.

The effect of temperature cycling on the Nafion<sup>®</sup> membrane pre-treated by method 4 is demonstrated in Figure 4.1.8. After the sample has been heated to 170°C at 2°C/min, held at 170°C for 1hr, cooled down at 2°C/min to 50°C and heated at 2°C/min to 170°C, the position of the tan  $\delta$  peak remained at 144°C.

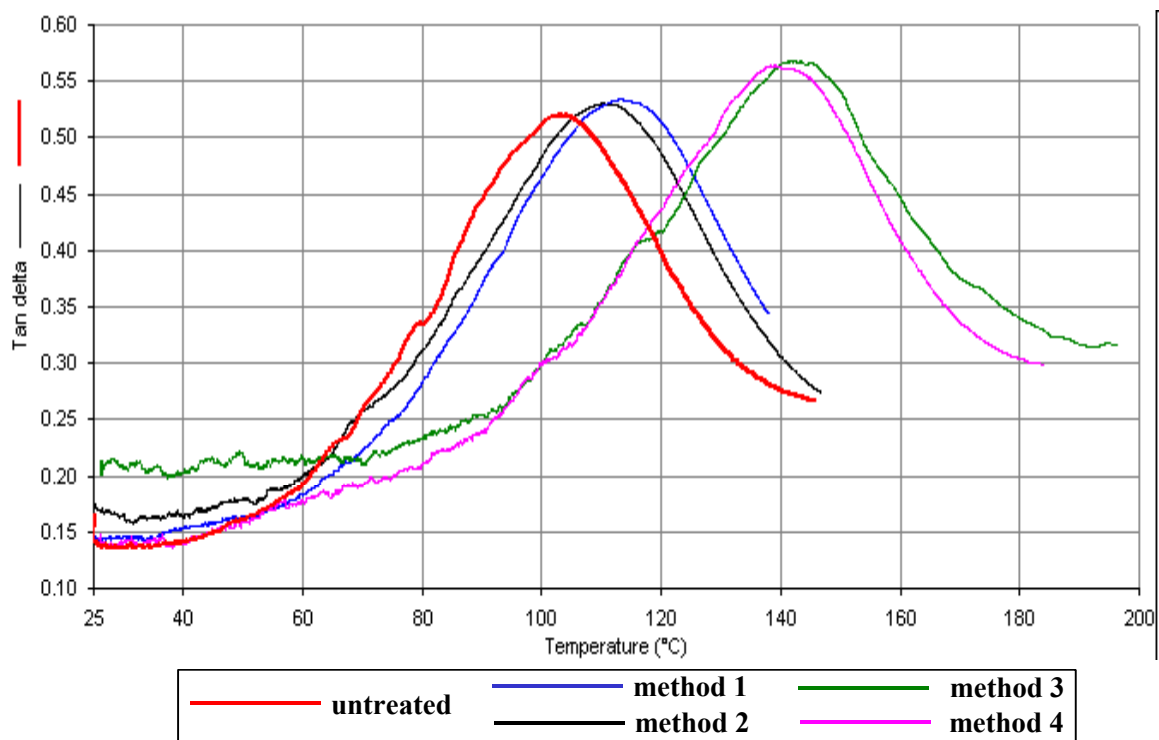
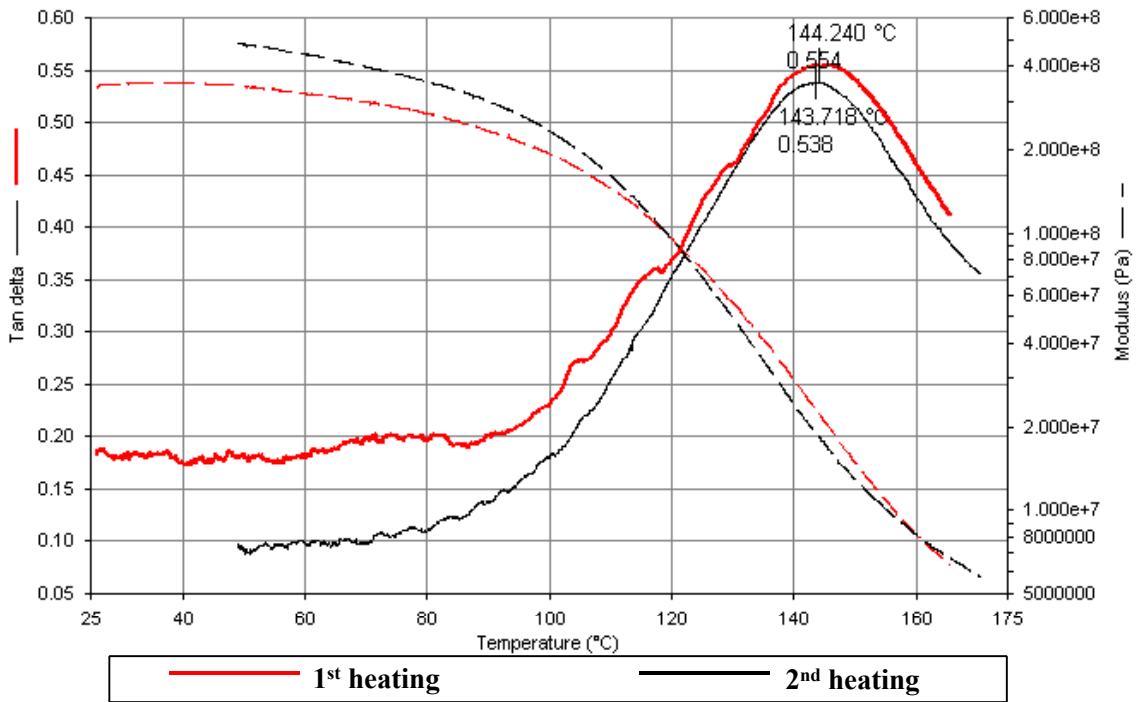


Figure 4.1.7 The Effect of the Pre-treatment on Nafion<sup>®</sup> Membranes

**Table 4.1.1 The Effect of the Pre-treatment on the Position of Tan  $\delta$  Peak**

Method	Tan $\delta$ Peak	
	Range	Position
untreated	103°C -106°C	104.8±1.4°C
1	111°C -114°C	112.3±1.7°C
2	110°C -113°C	112.4±1.0°C
3	137°C -145°C	141.6±3.8°C
4	136°C -141°C	138.5±2.7°C



**Figure 4.1.8 DMA Scan of the Nafion<sup>®</sup> Membrane Pre-Treated by Method 4: Heat, Hold at 170°C, Cool, Heat Cycle**

The results of the studies of Nafion<sup>®</sup> aged in DI water at 90°C are shown in Figure 4.1.9, Figure 4.1.10 and Figure 4.1.11. The  $T_g$  of the membranes in all three experiments increases as a function of aging time. The  $T_g$  of a virgin film in experiment 1 is higher than the  $T_g$  of the virgin membranes in experiments 2 and 3 because material 1 came from a different batch. The difference between the  $T_g$ s of the virgin membranes in

experiments 2 and 3 is due to different treatment batches. The error bars are absent in Figure 4.1.9 since only one sample was analyzed for each aging time in this experiment.

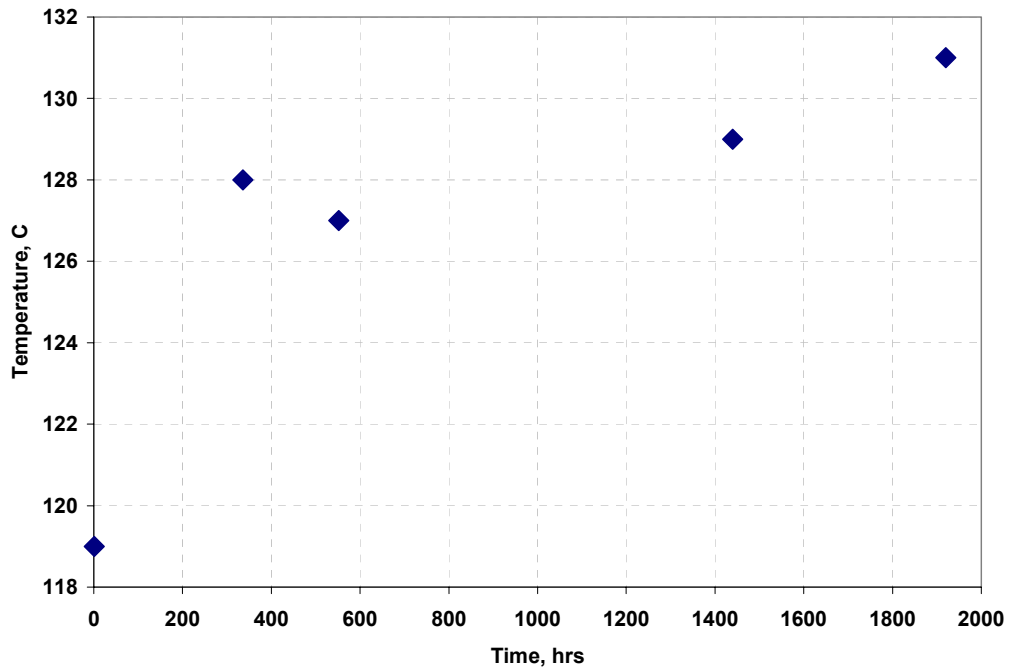


Figure 4.1.9 Tan  $\delta$  Peak Positions of Nafion<sup>®</sup> Samples Aged in DI Water at 90°C(Experiment 1)

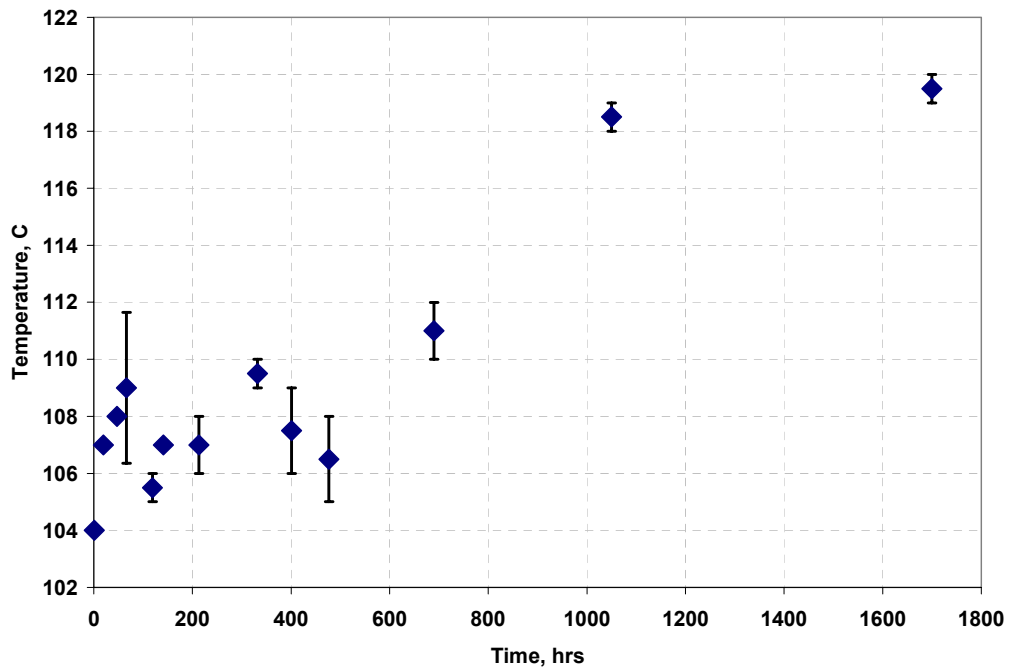
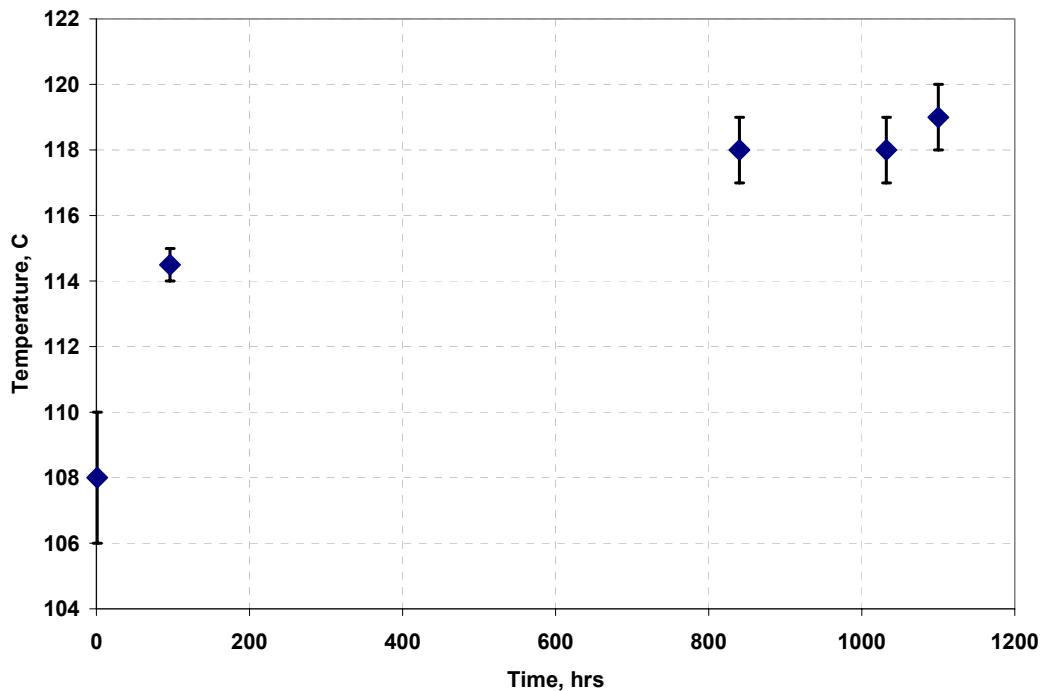


Figure 4.1.10 Tan  $\delta$  Peak Positions of Nafion<sup>®</sup> Samples Aged in DI Water at 90°C (Experiment 2)



**Figure 4.1.11 Tan  $\delta$  Peak Positions of Nafion<sup>®</sup> Samples Aged in DI Water at 90°C (Experiment 3)**

In order to determine whether the increase in  $T_g$  for the Nafion<sup>®</sup> samples aged in DI water at 90°C for 60 and 80 days is reversible, the appropriate aged Nafion<sup>®</sup> membranes were heated in the DMA at 2°C/min up to 160°C, held at 160°C for 1hr, and then cooled to 30°C at 2°C/min. This heat/hold/cool cycle was repeated twice for each aging time. The annealing results are shown in Figure 4.1.12 for the samples aged for 60 days and in Figure 4.1.13 for the samples aged for 80 days. In the first case, the tan  $\delta$  peak observed at 129°C on the first heating moved to 125°C on the second heating and to 124°C on the third heating. In the second case, the tan  $\delta$  peak observed at 131°C on the first heating moved to 124°C on the second heating and remained there on the third heating. For comparison, the annealing effect was also studied for virgin Nafion<sup>®</sup>. The membranes were heated in the DMA at 2°C/min up to 130°C, held at 130°C for 1hr, cooled to 30°C at 2°C/min and heated back up at 2°C/min. The tan  $\delta$  peak observed at 101°C on the first heating was measured at 99°C on the cooling and at 101°C on the second heating.

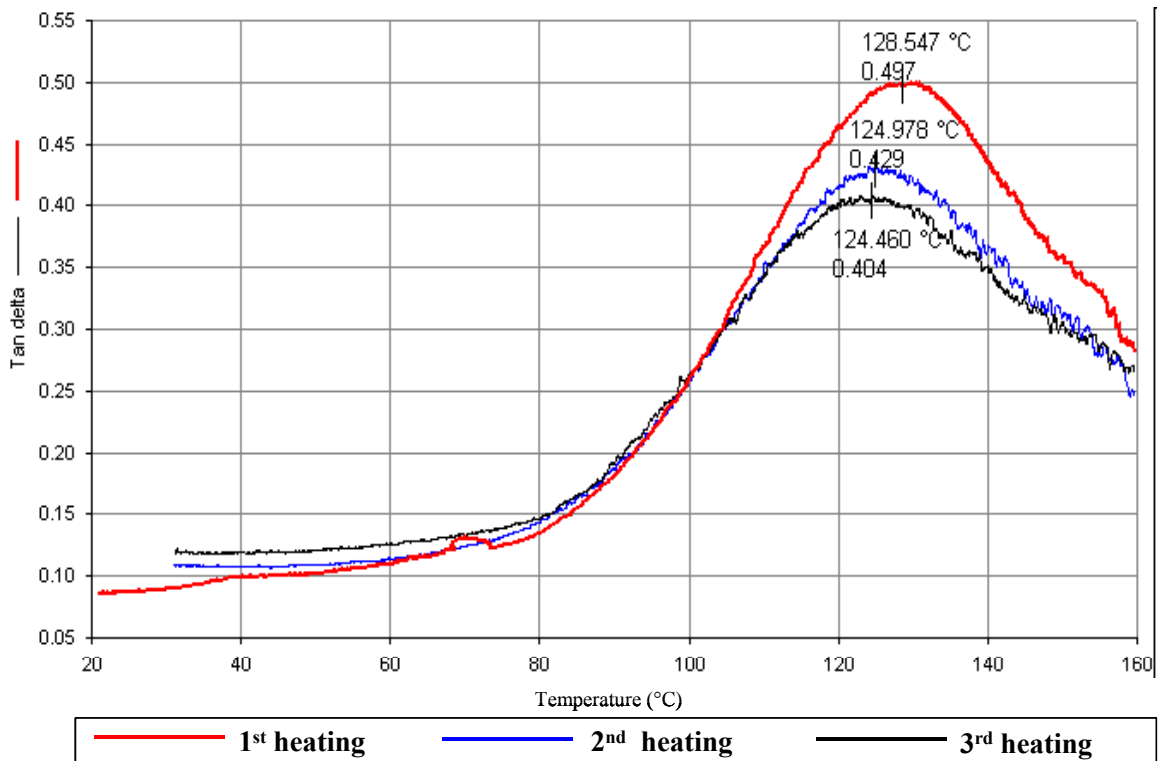


Figure 4.1.12 DMA of Nafion<sup>®</sup> Membrane Aged for 60 Days in DI Water at 90°C

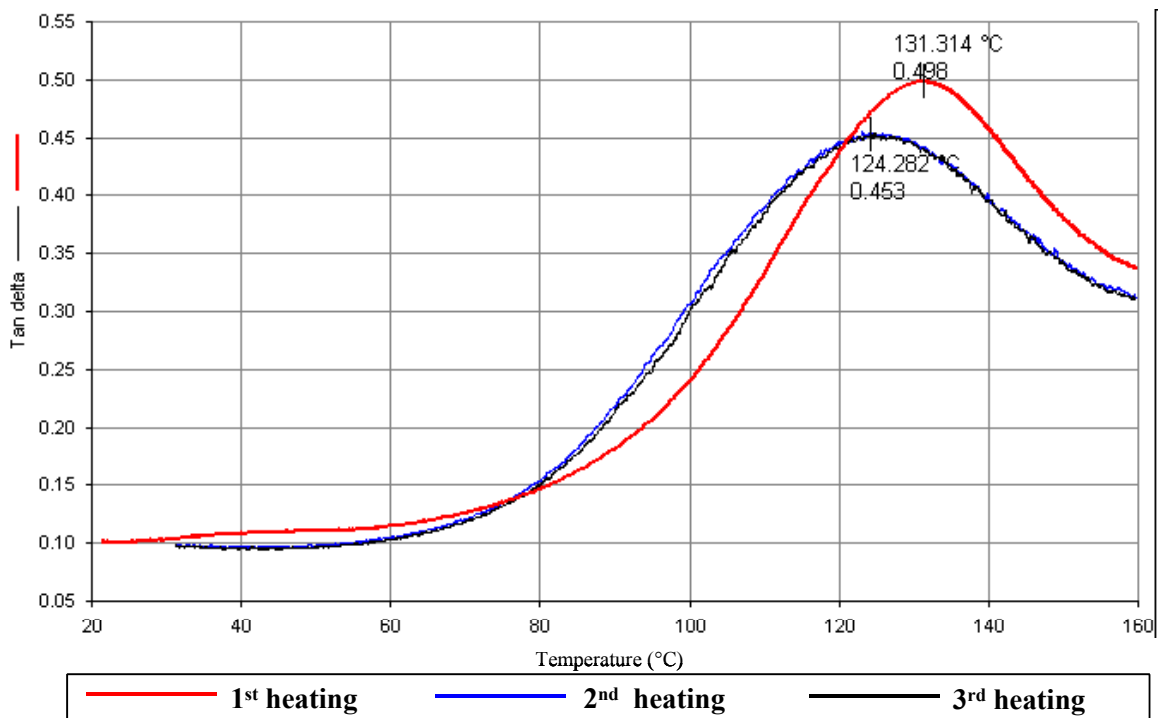


Figure 4.1.13 DMA of Nafion<sup>®</sup> Membrane Aged for 80 Days in DI Water at 90°C

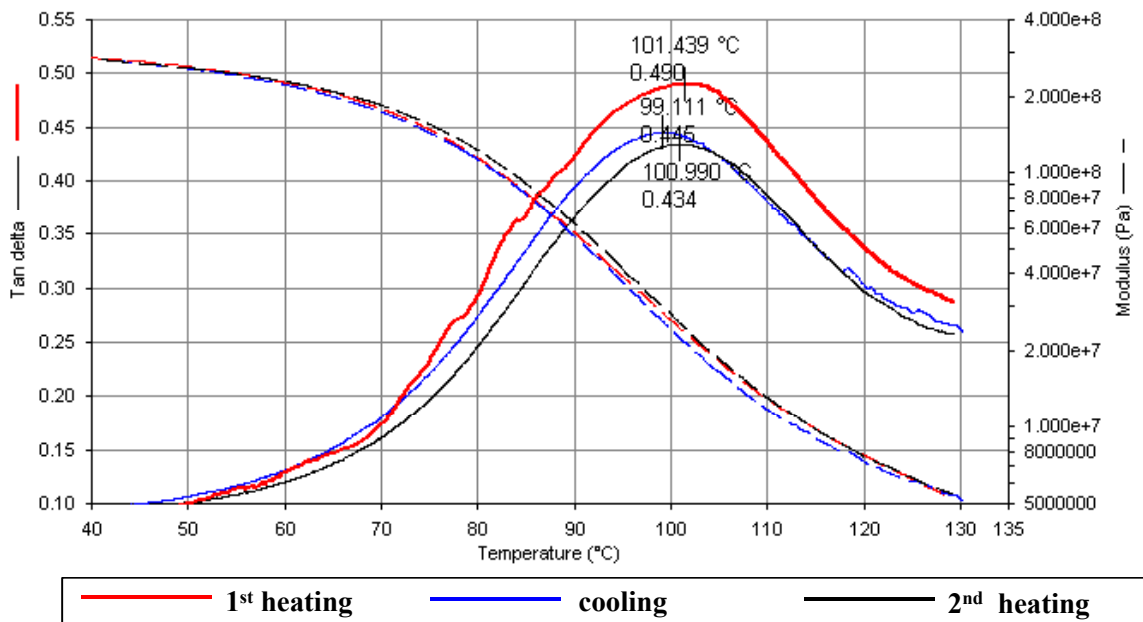


Figure 4.1.14 DMA Scan of the Nafion® Membrane Heat, Hold at 130°C, Cool, Heat Cycle

The results of the studies of Nafion® aged in DI water at 65°C are shown in Figure 4.1.15. The  $T_g$  of the membranes increases as a function of aging time.

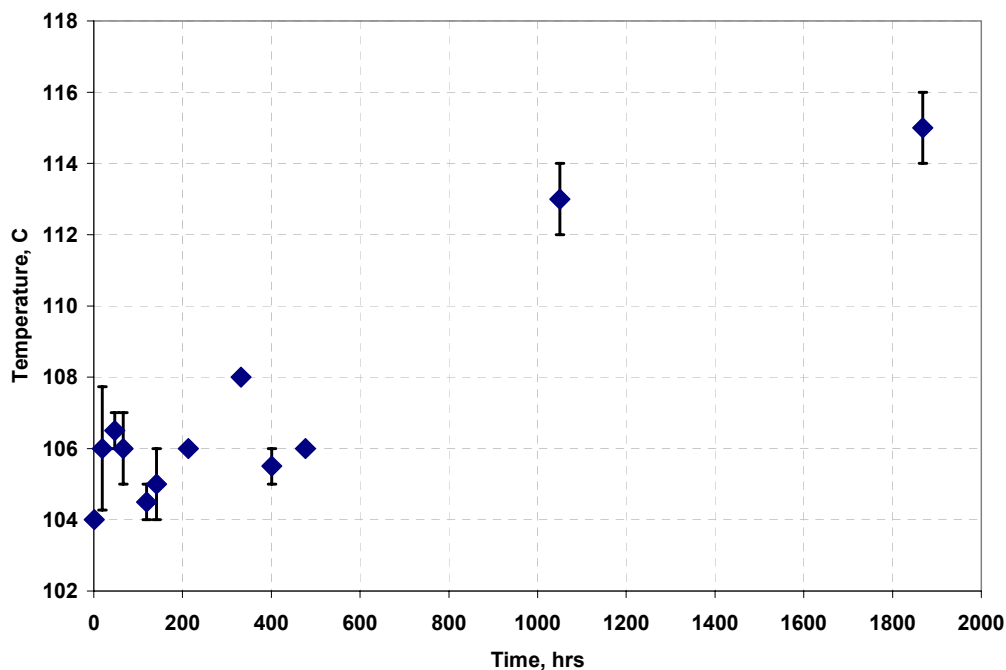


Figure 4.1.15 Tan  $\delta$  Peak Positions of Nafion® Samples Aged in DI Water at 65°C

## 4.2 DMA: Dais<sup>®</sup> Membranes

The DMA spectra of Dais<sup>®</sup> membranes for 30% and 60% sulfonation are shown in Figure 4.2.1 and Figure 4.2.2 respectively. The spectrum of Dais<sup>®</sup> 30% sulfonation shows two  $\tan \delta$  peaks at  $-54^\circ\text{C}$  and at  $145^\circ\text{C}$ . The storage modulus curve has two major drops, one from  $6.8 \times 10^8 \text{ Pa}$  to  $1.1 \times 10^8 \text{ Pa}$  in the temperature range between  $-80^\circ\text{C}$  and  $0^\circ\text{C}$  and a second one from  $1.0 \times 10^8 \text{ Pa}$  to  $3.3 \times 10^6 \text{ Pa}$  in the temperature range between  $80^\circ\text{C}$  and  $170^\circ\text{C}$ . 60% sulfonated Dais<sup>®</sup> demonstrates behavior similar to that of Dais<sup>®</sup> with 30% sulfonation: it has two  $\tan \delta$  peaks and two major drops in storage modulus; however, the upper transition occurs at a higher temperature than in the 30% sulfonated membrane.  $\tan \delta$  peaks for 60% sulfonation membrane are at  $-53^\circ\text{C}$  and  $220^\circ\text{C}$  and they are accompanied by the storage modulus drops from  $4.2 \times 10^8 \text{ Pa}$  to  $9.3 \times 10^7 \text{ Pa}$  in the temperature range between  $-85^\circ\text{C}$  and  $-7^\circ\text{C}$  and from  $1.4 \times 10^8 \text{ Pa}$  to  $3.3 \times 10^6 \text{ Pa}$  in the temperature range between  $128^\circ\text{C}$  and  $250^\circ\text{C}$ .

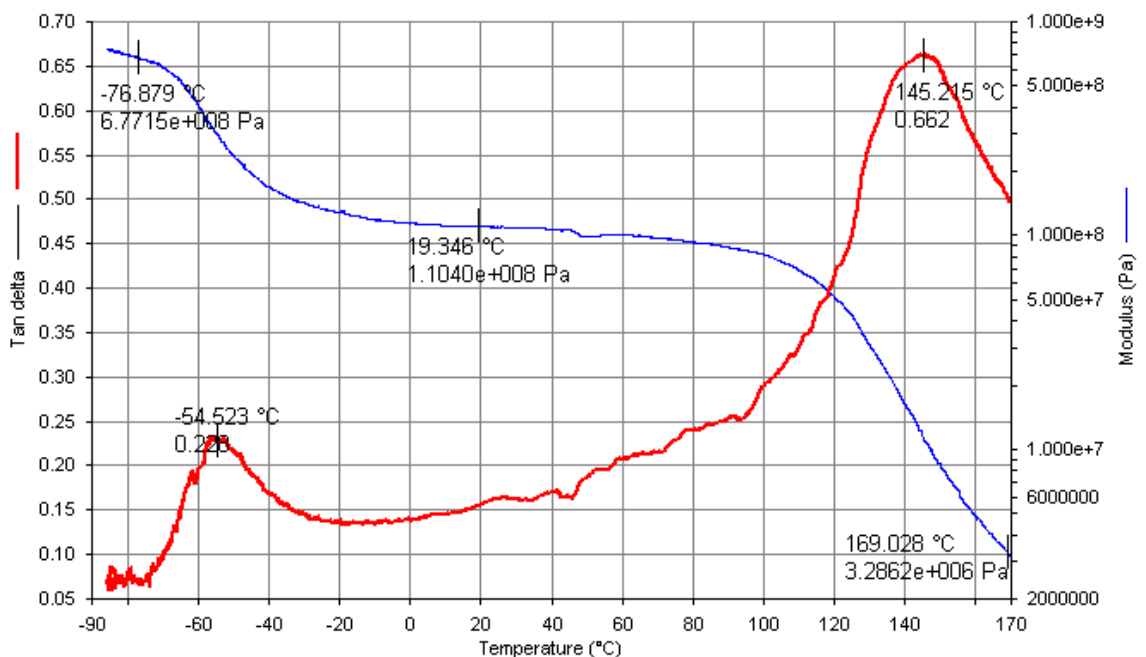
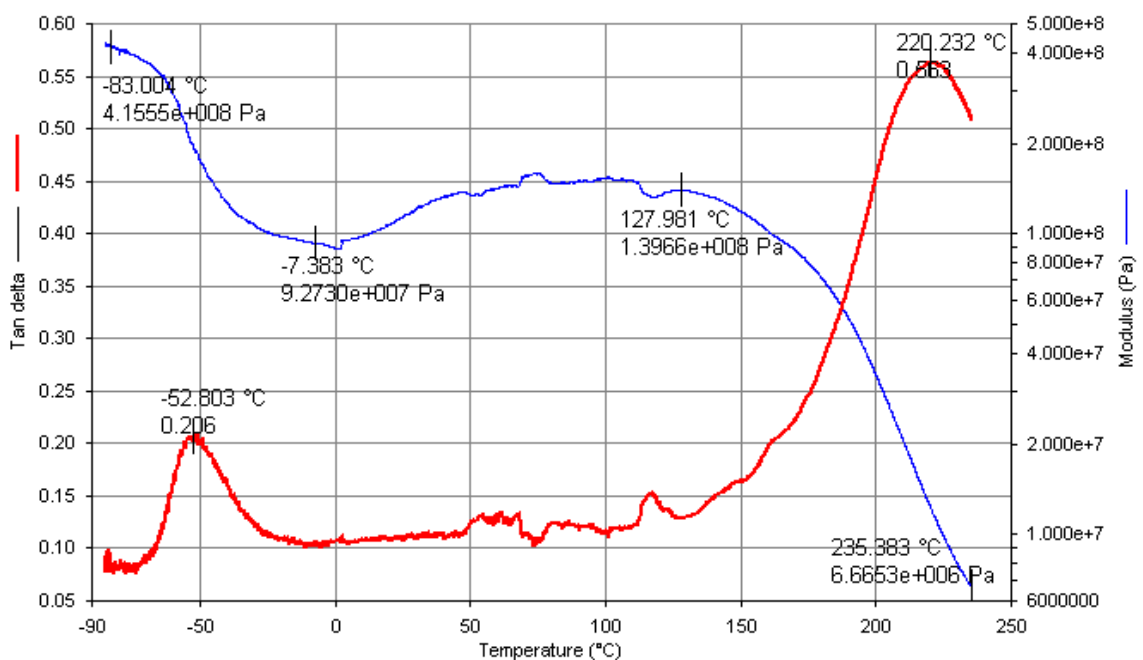


Figure 4.2.1 Dais<sup>®</sup> 30% Sulfonation DMA Spectrum



**Figure 4.2.2 Dais® 60% Sulfonation DMA Spectrum**

Results of the ambient DMA scan of the dry 30% sulfonation membrane are shown in Figure 4.2.3 and results of the ambient DMA scan of the saturated 30% sulfonation membrane are shown in Figure 4.2.4. In order to compare the two, the scans are combined in Figure 4.2.5. The  $\tan \delta$  curve of the dry sample has an apparent peak at 140°C and the storage modulus of the sample drops from  $1.4 \times 10^8$  Pa to  $2.3 \times 10^6$  Pa in the temperature range between 60°C and 205°C. The saturated Dais® 30% sulfonation sample has a drop of modulus from  $3.0 \times 10^7$  Pa to  $1.4 \times 10^6$  Pa in the temperature range between 25°C and 85°C.

The effect of the scanning rate on the position of the inflection point in storage modulus of the saturated Dais® 30% sulfonation membrane is demonstrated in Figure 4.2.6. The inflection point of the sample scanned at 1°C/min is at 51.5°C and of the sample scanned at 2°C/min is at 57.8°C.

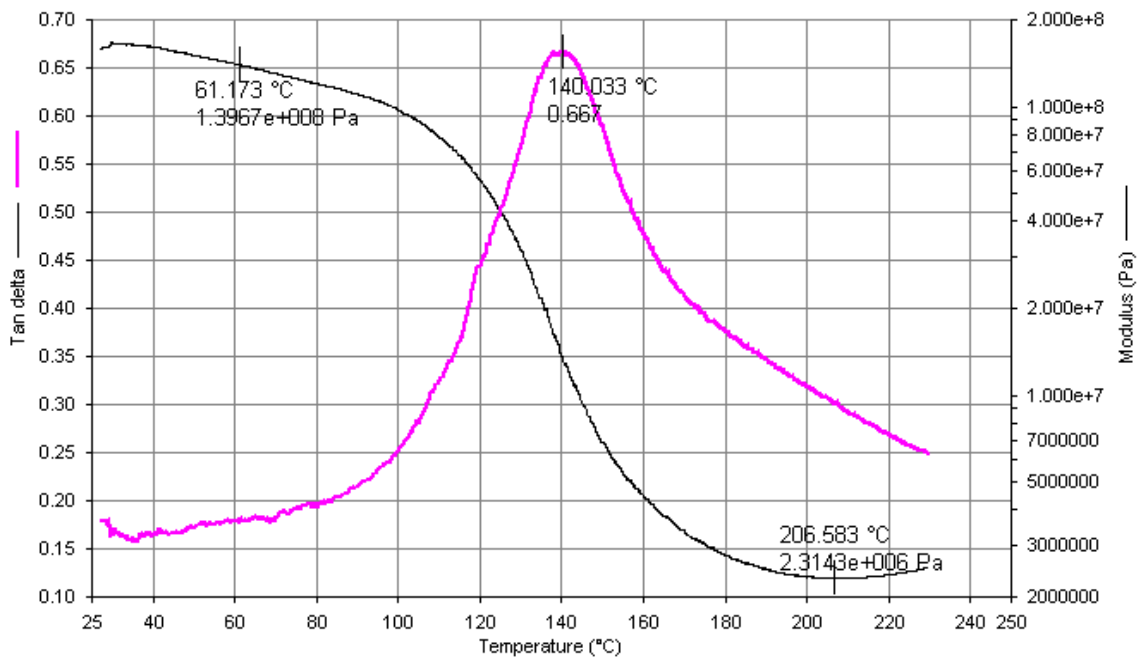


Figure 4.2.3 Ambient DMA Scan of Dry Dais® 30% Sulfonation Membrane

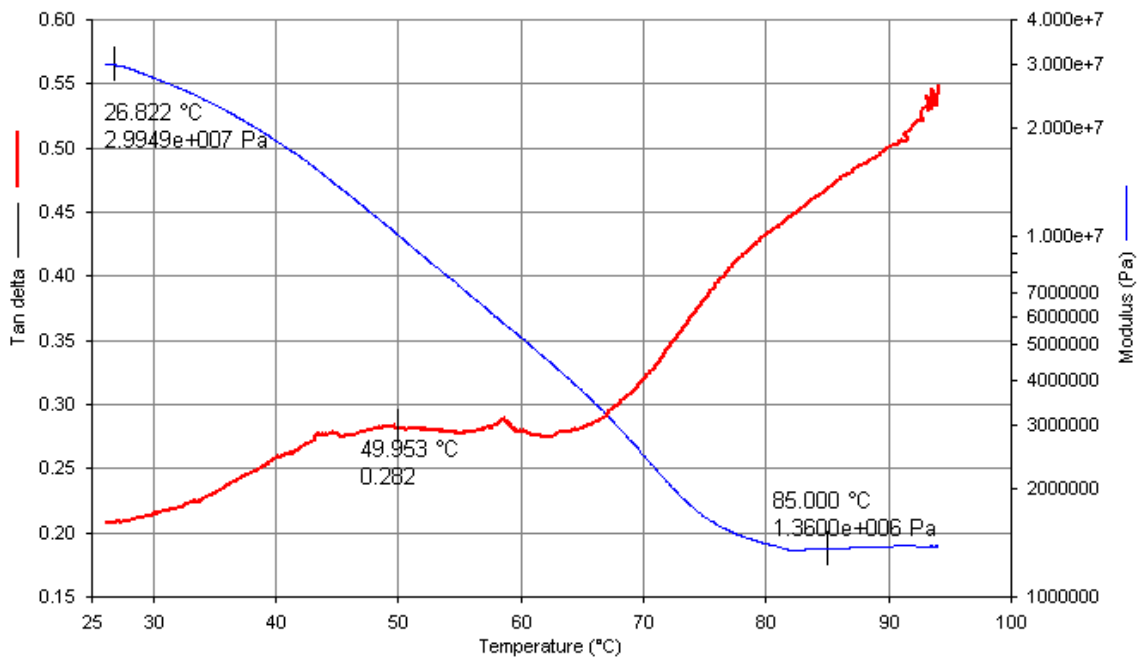


Figure 4.2.4 Ambient DMA Scan of Saturated Dais® 30% Sulfonation Membrane

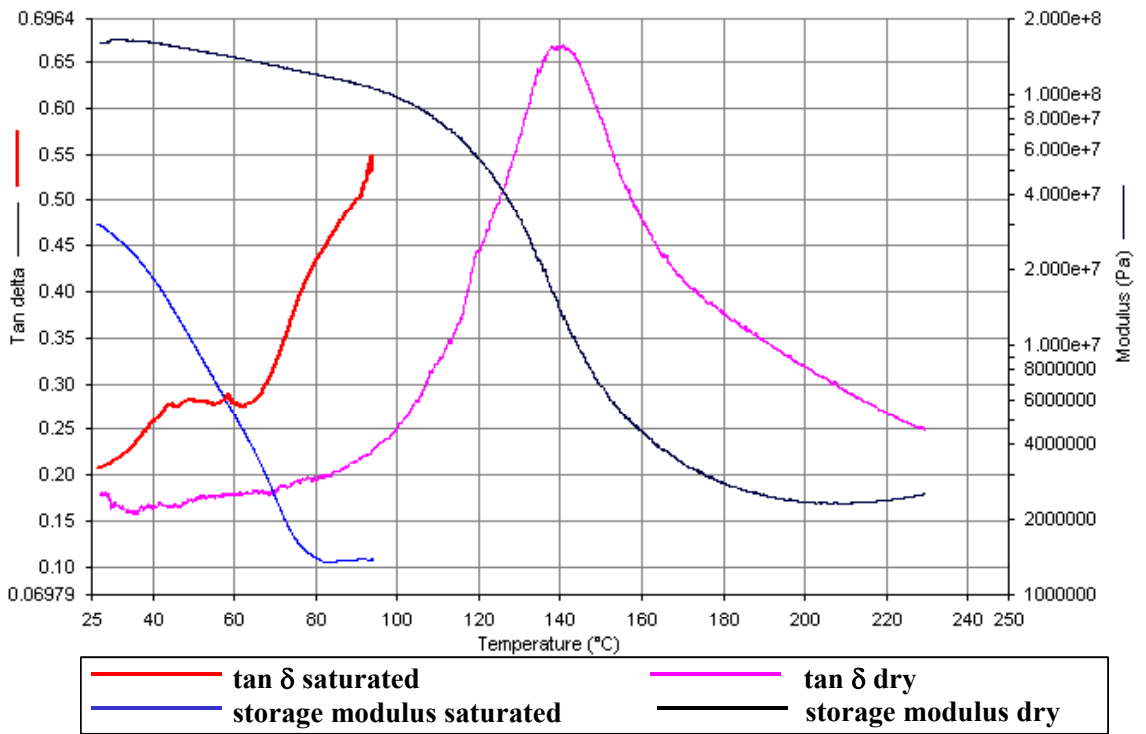


Figure 4.2.5 Comparison of Dry and Saturated Dais® 30% Sulfonation Membrane

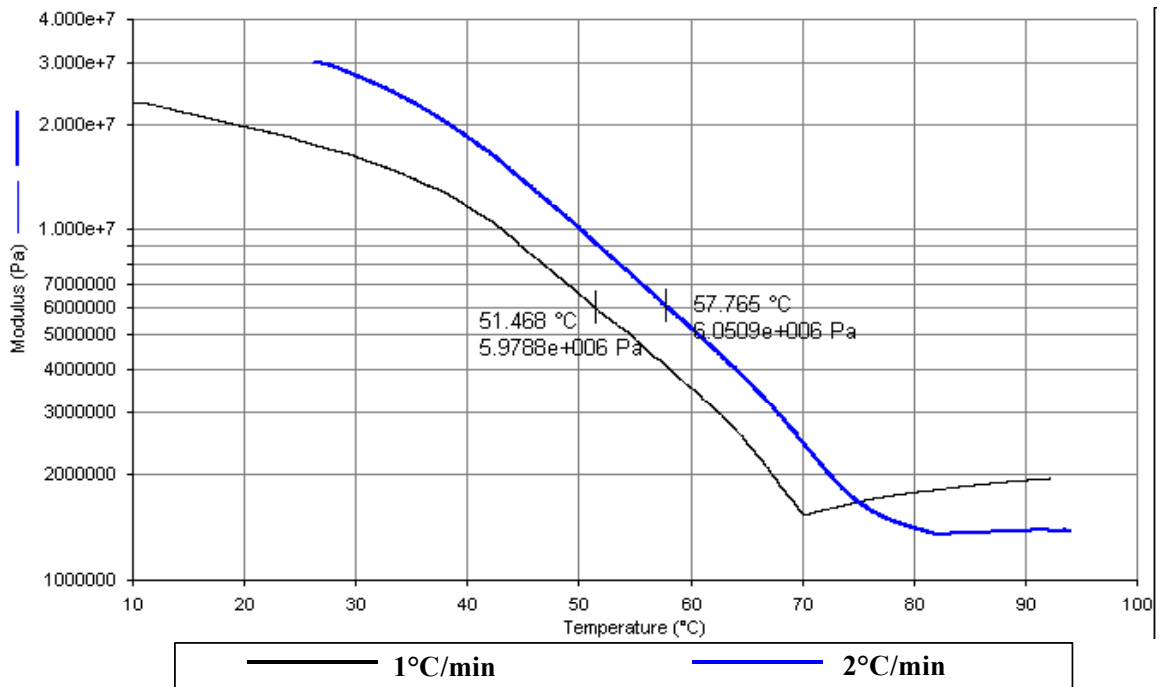
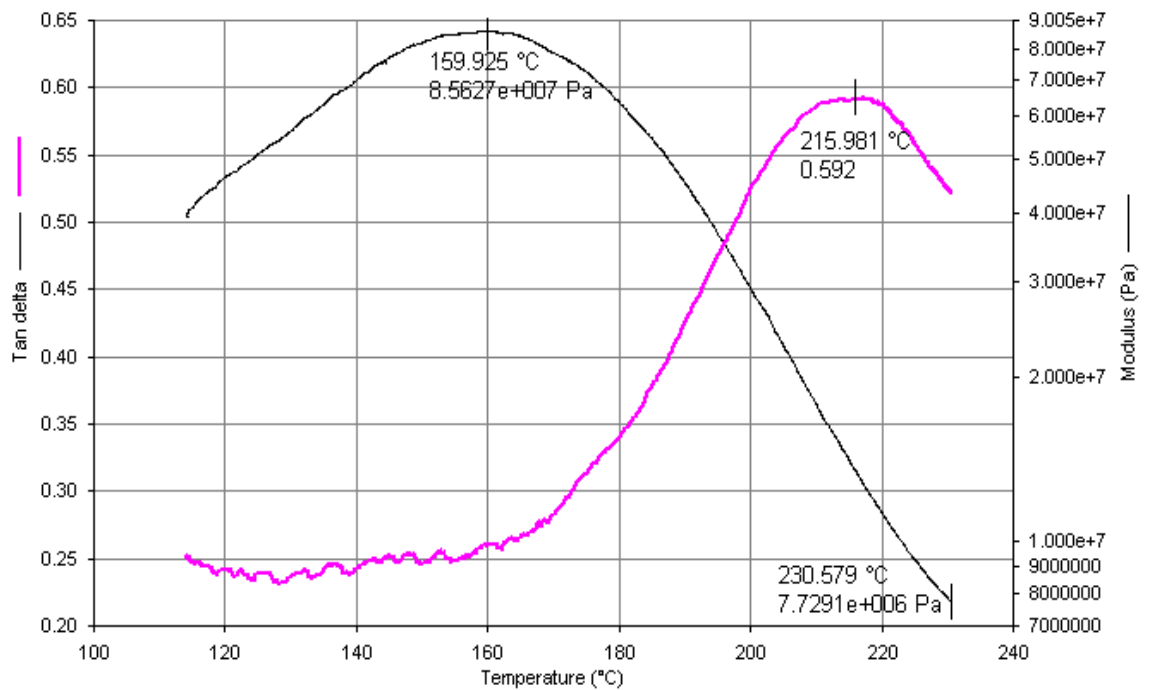
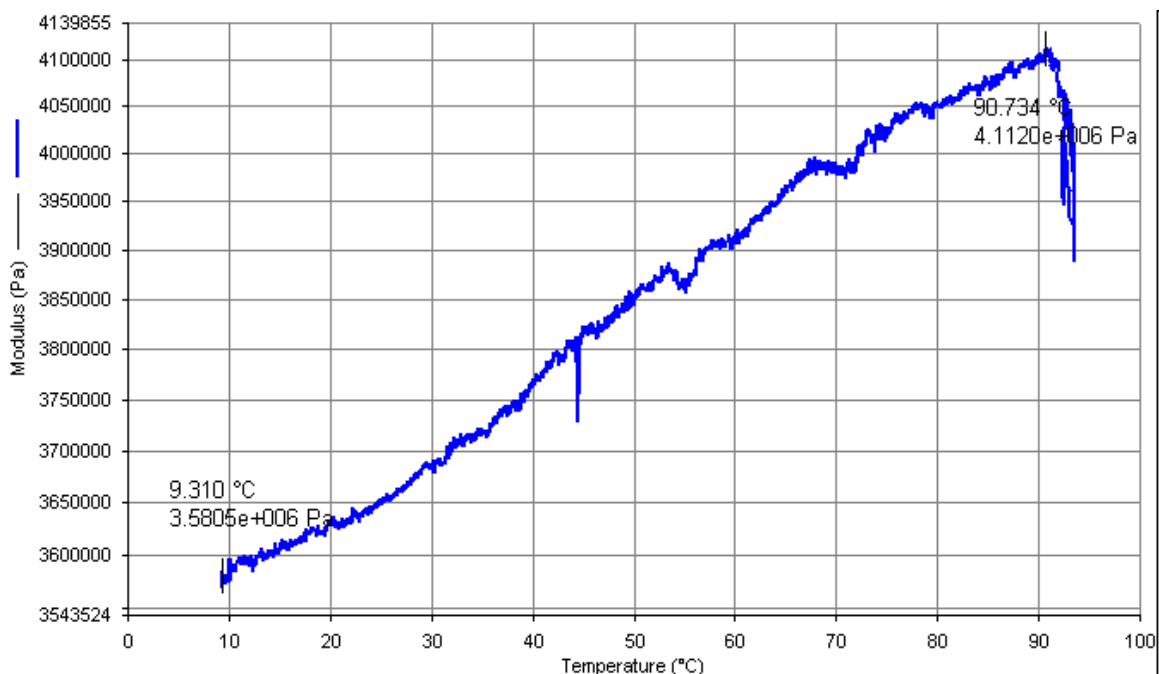


Figure 4.2.6 The Effect of the Scanning Rate on Storage Moduli of the Saturated Dais® 30% Sulfonation Membranes

The results of the ambient DMA scan of dry 60% sulfonation membrane are shown in Figure 4.2.7 and the results of the ambient DMA scan at 10Hz of the saturated 60% sulfonation membrane are shown in Figure 4.2.8. The  $\tan \delta$  curve of the dry sample has an apparent peak at 216°C and the storage modulus of the sample drops from  $8.6 \times 10^8$  Pa to  $7.7 \times 10^6$  Pa in the temperature range between 160°C and 231°C. The scan of the saturated 60% sulfonation membrane at 10Hz does not demonstrate any transition characteristics in the temperature range between 9°C and 92°C. The scan of the saturated membrane at 1Hz was not obtained because the material became extremely soft and prone to tear upon immersion into the solvent sleeve and the subsequent application of the initial forces.



**Figure 4.2.7 Ambient DMA Scan of Dry Dais® 60% Sulfonation Membrane**



**Figure 4.2.8 Ambient DMA Scan of Saturated Dais® 60% Sulfonation Membrane, 10Hz**

An interesting behavior for both 30% and 60% sulfonated membranes was observed during DMA scans involving cycling the membranes up and down in temperature. The 30% sulfonated Dais® was heated at 2°C/min to 165°C, cooled at 2°C/min to 92°C and heated again at 2°C/min (Figure 4.2.9). The tan  $\delta$  peak moved from 140°C for the first heating to 148°C for the second heating. A different sample of 30% sulfonated Dais® membrane was subjected to a similar cycling but was annealed for 1hr at 165°C before the cooling step was initiated (Figure 4.2.10). The tan  $\delta$  peak moved from 142°C to 154°C. The 60% sulfonated Dais® was heated at 2°C/min to 170°C, annealed for 1 hr, cooled at 2°C/min to 120°C and heated again at 2°C/min to 240°C (Figure 4.2.11). There was no change in the position of the tan  $\delta$  peak. However, when one sample of 60% sulfonated Dais® membrane was heated to 235°C (Figure 4.2.12), cooled down at 2°C/min to 120°C and heated back up and the second one was annealed at 235°C for 1hr (Figure 4.2.13), then cooled at 2°C/min to 120°C and heated again, the tan  $\delta$  peak moved from 216°C to 234° in the first case and from 217°C to 260°C in the second case.

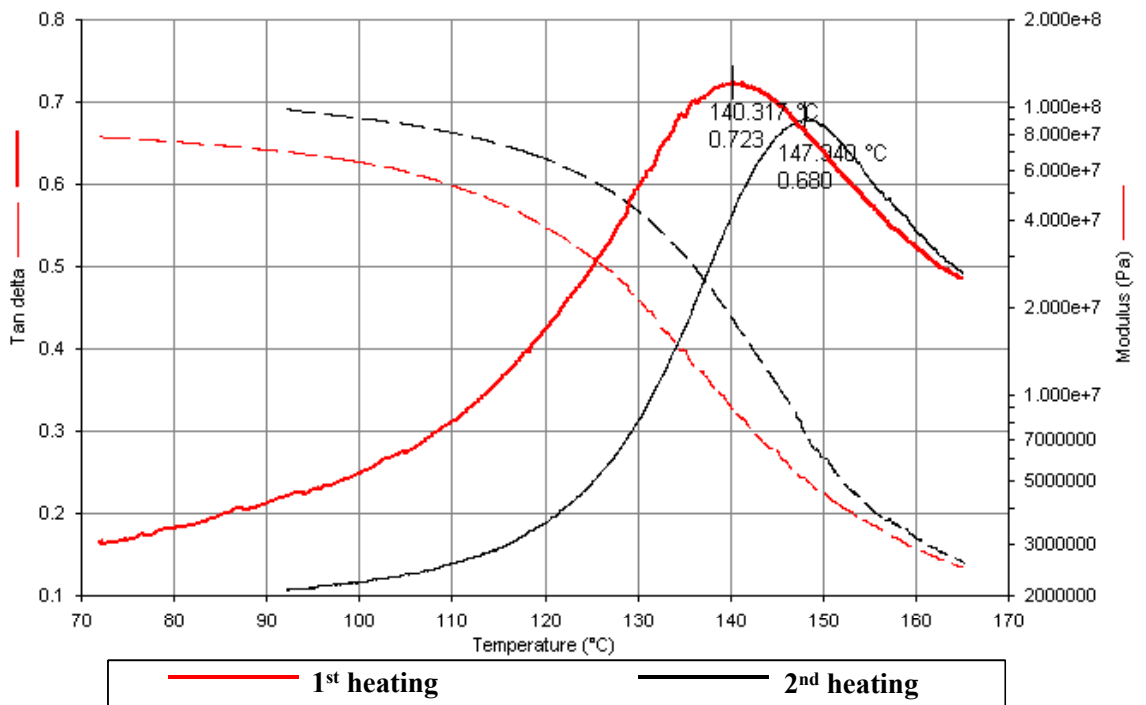


Figure 4.2.9 DMA Scan of Dais® 30% Sulfonation Membrane: Heat, Cool, Heat Cycle

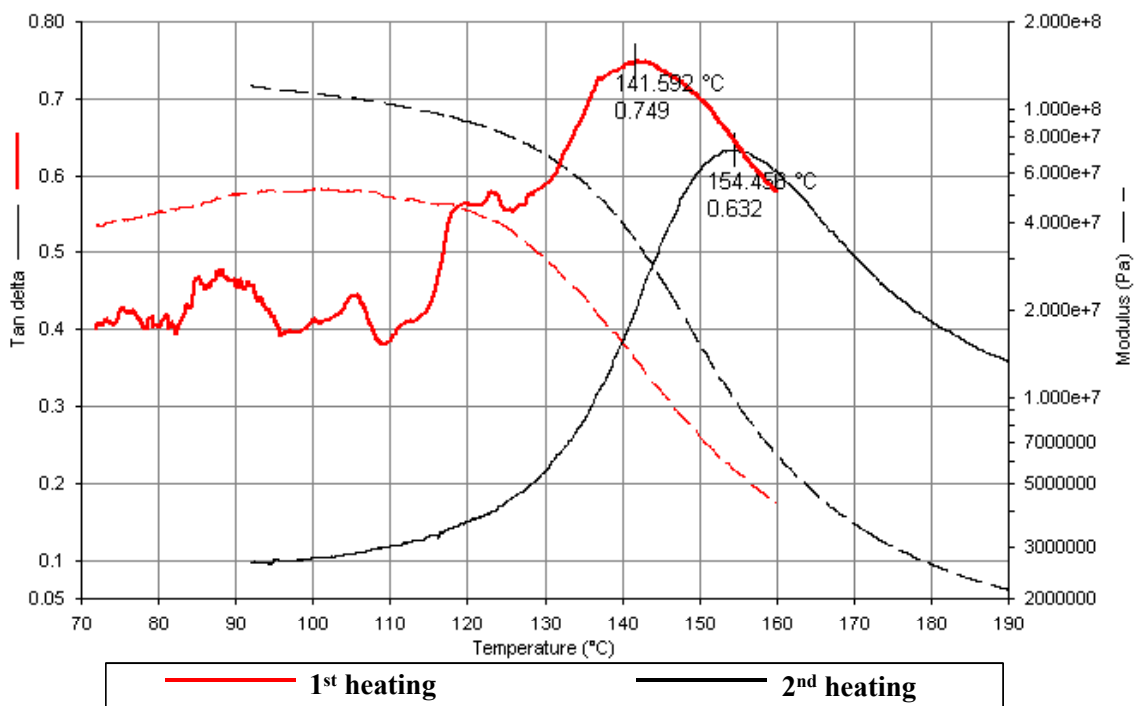


Figure 4.2.10 DMA Scan of Dais® 30% Sulfonation Membrane: Heat, Hold at 160°C, Cool, Heat Cycle

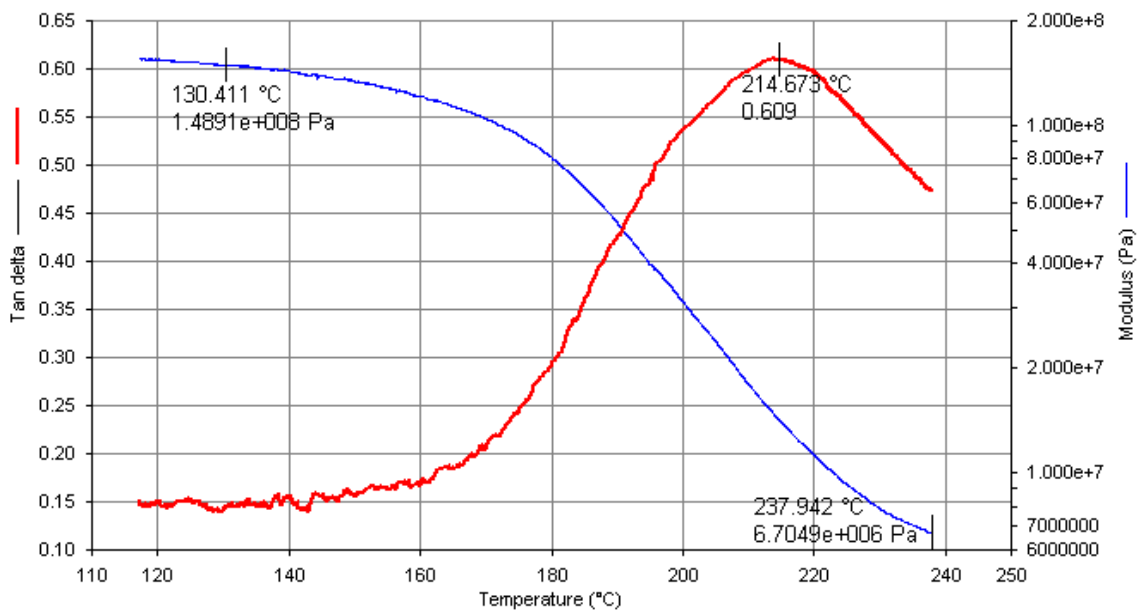


Figure 4.2.11 Second Heating of Dais® 60% Sulfonation Membrane: Heat, Hold at 170°C, Heat Cycle

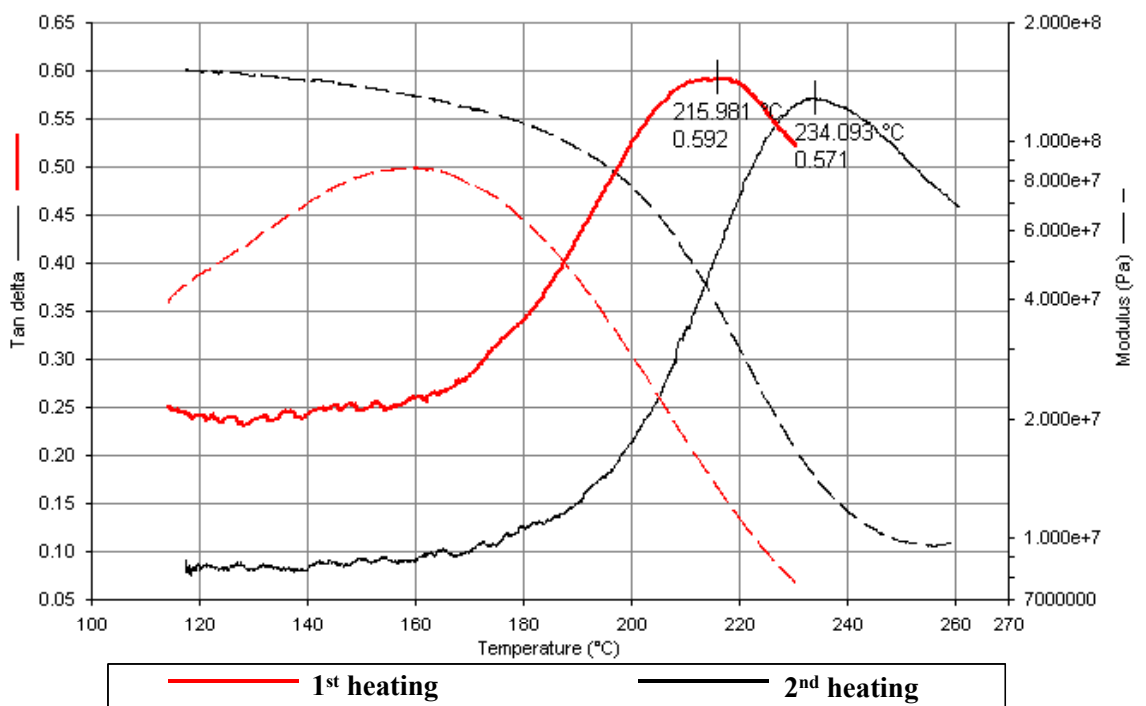


Figure 4.2.12 DMA Scan of Dais® 60% Sulfonation Membrane: Heat to 235°C, Cool, Heat Cycle

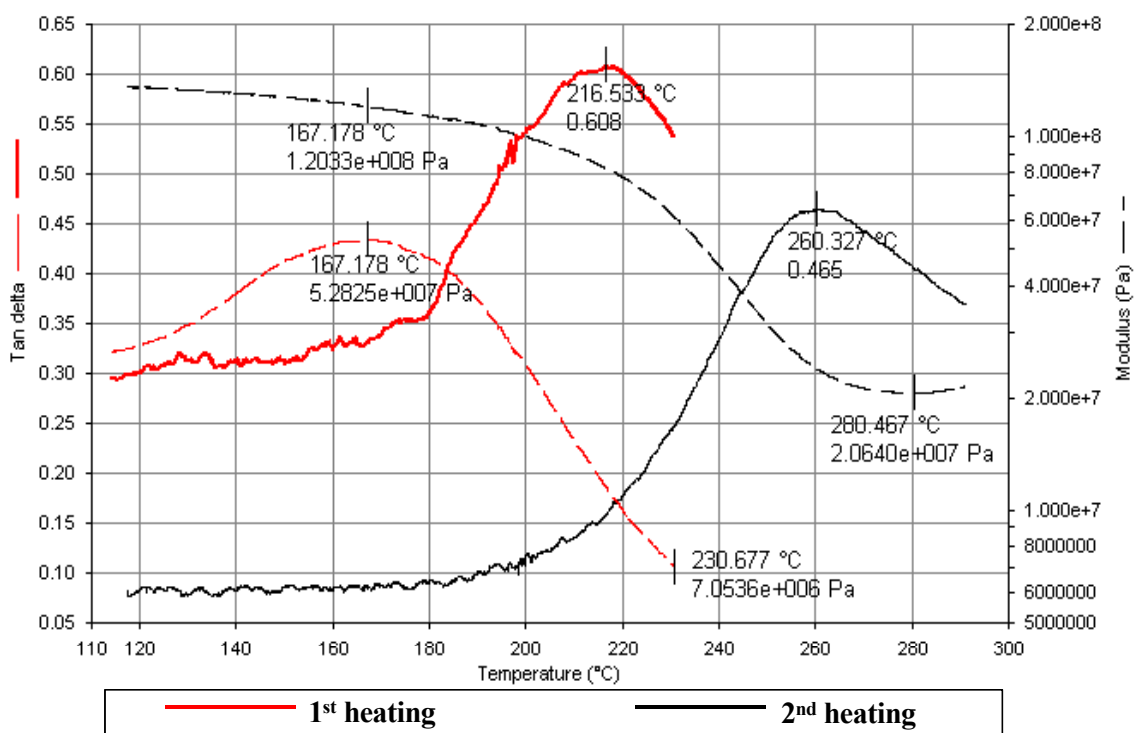


Figure 4.2.13 DMA Scan of Dais® 60% Sulfonation Membrane: Heat, Hold at 235°C, Cool, Heat Cycle

The DMA scans of 60% sulfonated Dais® membrane as a function of temperature for the range of frequencies between 0.05Hz and 10Hz are shown in Figure 4.2.14 (the data are subsequently used to construct a mastercurve). There is an apparent shift in the  $\tan \delta$  peak and in the storage modulus toward the higher temperature with the increase in the frequency of the scan.

The results of the aging studies of 30% sulfonated Dais® membranes in DI water at 90°C are shown in Figure 4.2.15 and Figure 4.2.16. The  $T_g$  in these experiments is defined as an inflection point in the storage modulus because the  $\tan \delta$  of the aged samples never reaches a peak (Figure 4.2.17). The  $T_g$  of 30% sulfonated Dais® membranes increases as a function of aging time.

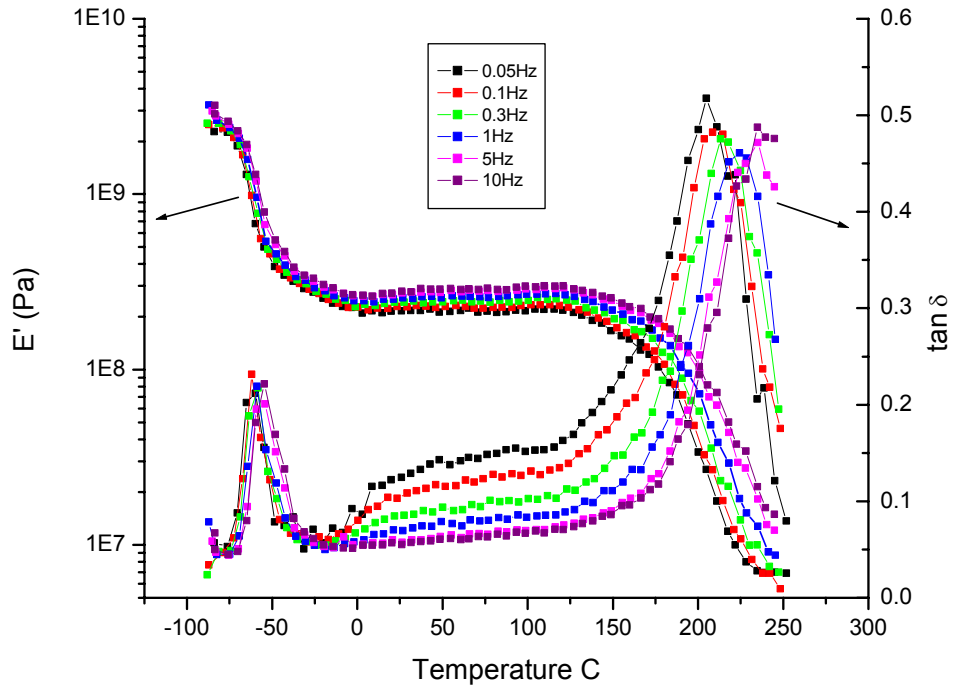


Figure 4.2.14 Frequency Shifts DMA Data for Dais® 60% Sulfonation Membrane

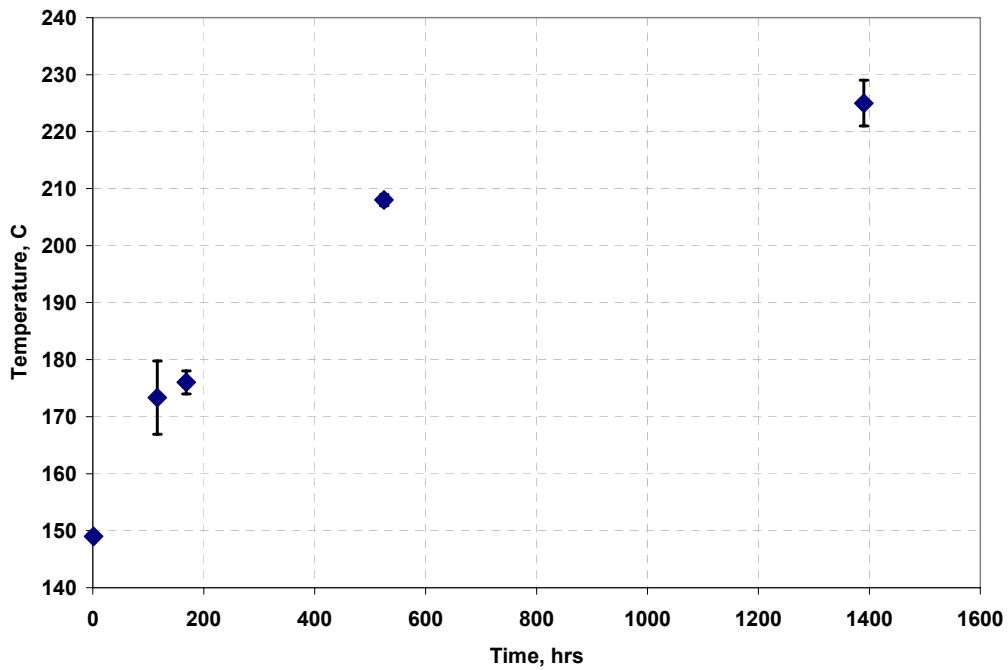


Figure 4.2.15 Tan  $\delta$  Peak Positions of Dais® 30% Sulfonation Membrane Aged in DI Water at 90°C (Experiment 1)

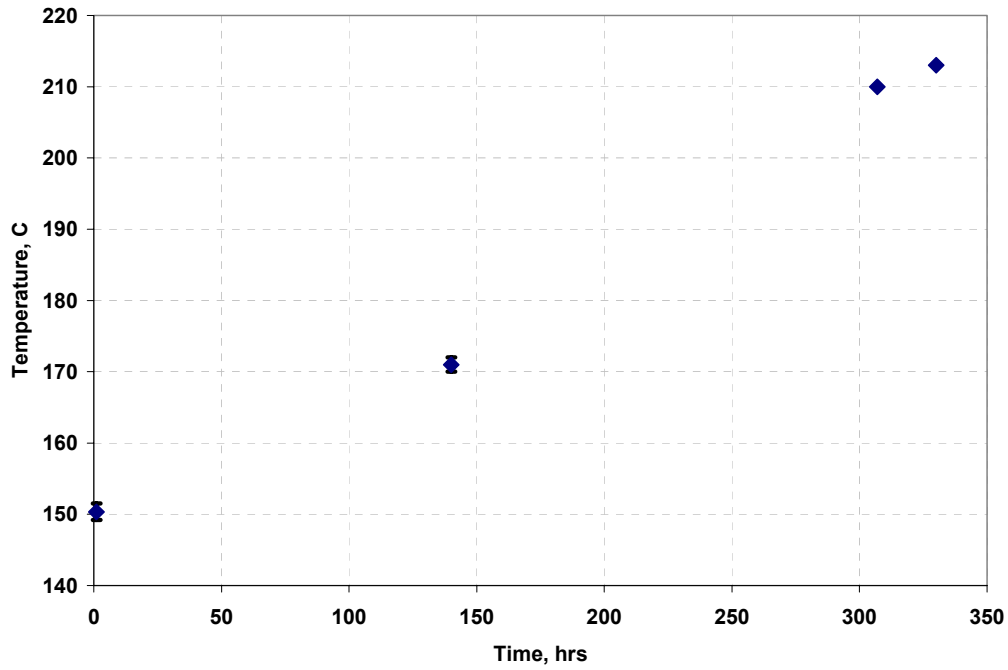


Figure 4.2.16 Tan  $\delta$  Peak Positions of Dais<sup>®</sup> 30% Sulfonation Membrane Aged in DI Water at 90°C (Experiment 2)

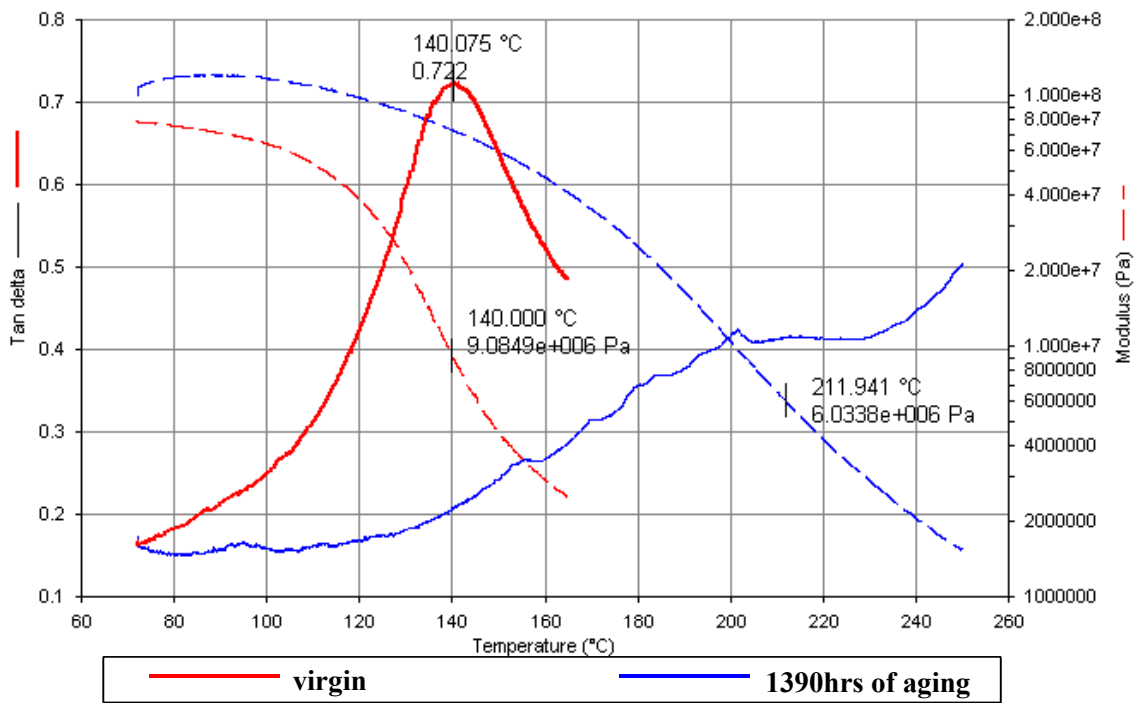


Figure 4.2.17 DMA Scans of the virgin and 1390hrs Aged Dais<sup>®</sup> 30% Sulfonation Membrane

### 4.3 TGA: Nafion<sup>®</sup> Membranes

The results of TGA scans of Nafion<sup>®</sup> membranes under air and N<sub>2</sub> atmosphere are shown in Figure 4.3.1 and Figure 4.3.2 respectively. Both traces show a small peak in the weight derivative curve in the temperature range between 300°C and 325°C, and two shoulders at 425°C and 523°C for the sample tested in air and at 415°C and 505°C for the sample tested in N<sub>2</sub> atmosphere. The major weight derivative peak is observed at 506°C for the air sample and at 488°C for the N<sub>2</sub> sample.

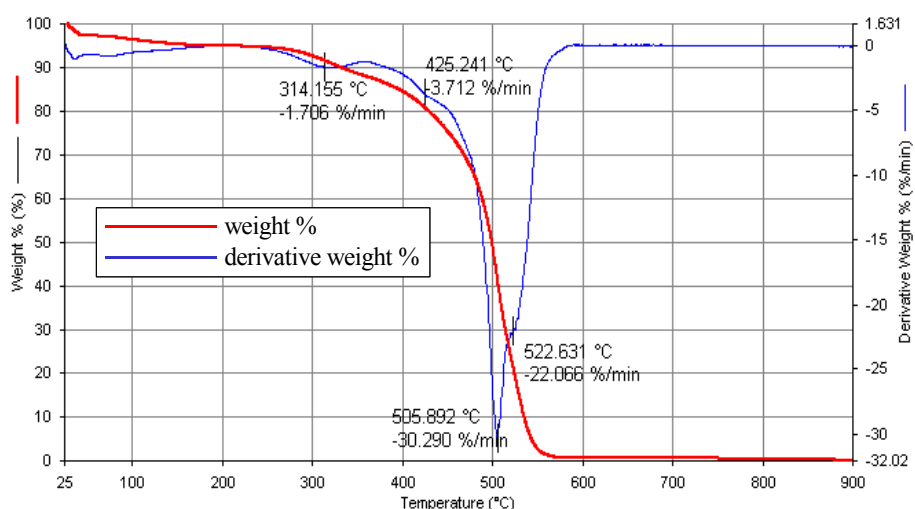


Figure 4.3.1 TGA of Nafion<sup>®</sup> Membrane in Air

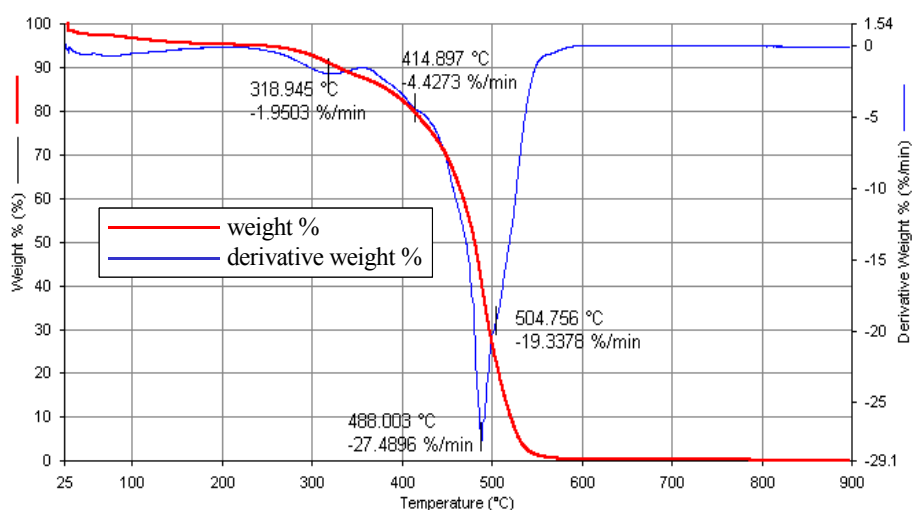


Figure 4.3.2 TGA of Nafion<sup>®</sup> Membrane in N<sub>2</sub>

The effect of the pre-treatment on the degradation behavior of Nafion<sup>®</sup> membranes is shown in Figure 4.3.3. There is no significant difference between the positions of the peaks in the derivative weight % curves of the untreated and treated Nafion<sup>®</sup> membranes.

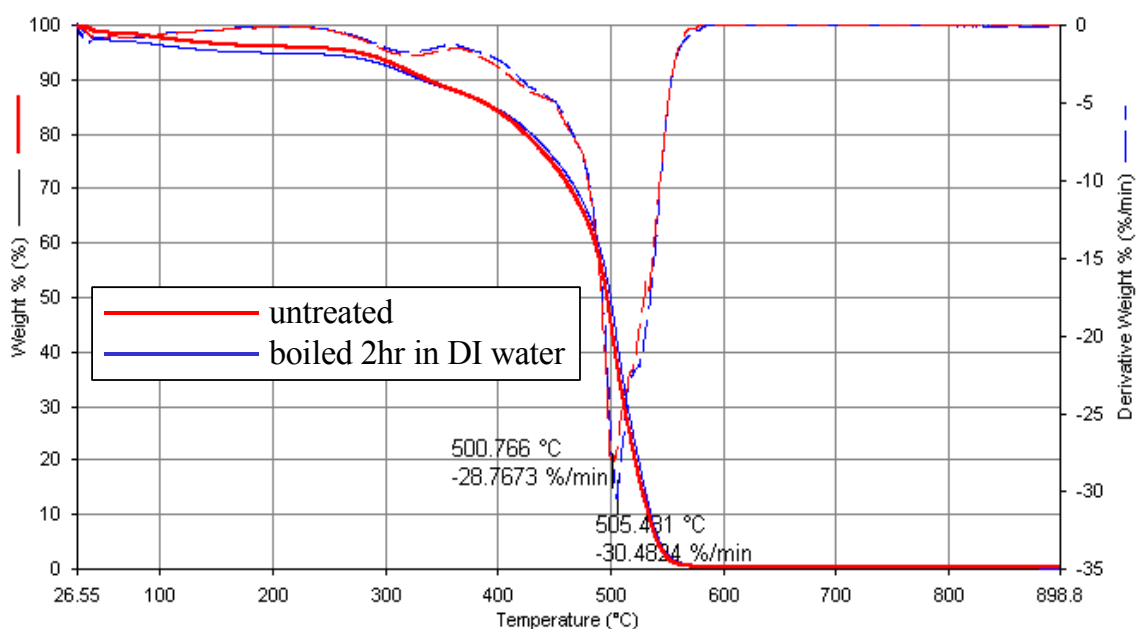


Figure 4.3.3 The Effect of Pre-Treatment on TGA of Nafion<sup>®</sup> Membranes

#### 4.4 TGA: Dais<sup>®</sup> Membranes

The results of the TGA scans for 30% sulfonated Dais<sup>®</sup> membranes under air and N<sub>2</sub> atmosphere are demonstrated in Figure 4.4.1 and Figure 4.4.2 and for 60% sulfonated Dais<sup>®</sup> membranes in Figure 4.4.3 and Figure 4.4.4, respectively. All four scans possess much of the same characteristic peaks in the derivative weight % curve (Table 4.4.1).

The effect of drying 60% sulfonated Dais<sup>®</sup> membrane in the vacuum oven at RT overnight is demonstrated in Figure 4.4.5. The TGA traces of the dry membrane and the one equilibrated at ambient conditions are very similar.

**Table 4.4.1 The Temperature Positions of the Characteristic Features of Dais<sup>®</sup> TGA Scans**

	Dais <sup>®</sup> 30% Sulfonation		Dais <sup>®</sup> 60% Sulfonation	
	Air	N <sub>2</sub>	Air	N <sub>2</sub>
<b>First Shoulder</b>	302°C	307°C	300°C	296°C
Second Shoulder	403°C	414°C	absent	439°C
Major Peak	469°C	476°C	451°C	468°C
Small Peak	588°C	absent	594°C	absent

The effects of drying 30% sulfonated Dais<sup>®</sup> membrane in a vacuum oven at RT overnight and of aging the membrane in DI water at 90°C for 168 hrs on the TGA scans are shown in Figure 4.4.6 and Figure 4.4.7, respectively. The differences between the scans are as follows: the shoulder on the derivative weight % curve at 403°C present in the virgin Dais<sup>®</sup> membrane is absent in both dried and aged membranes, the peak at 588°C present in virgin and dried membranes is absent in aged membranes and the position of the large loss peak has moved from 469°C for virgin and dried membranes to 457°C for the aged 30% sulfonated Dais<sup>®</sup> membranes.

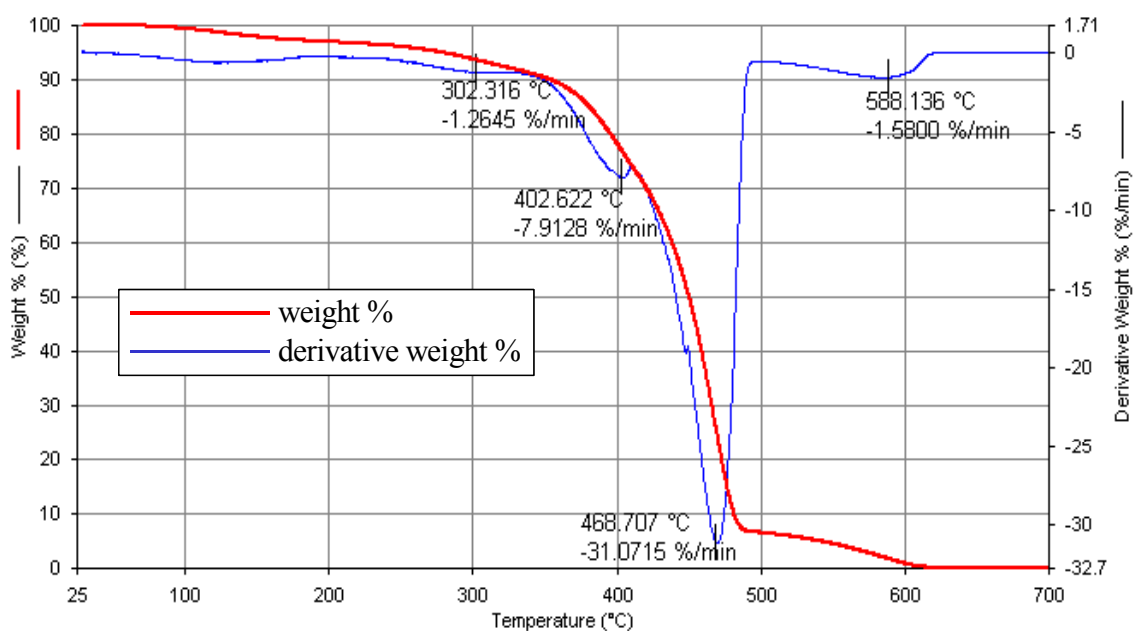


**Figure 4.4.1 TGA Scan of Dais<sup>®</sup> 30% Sulfonation Membrane in Air**

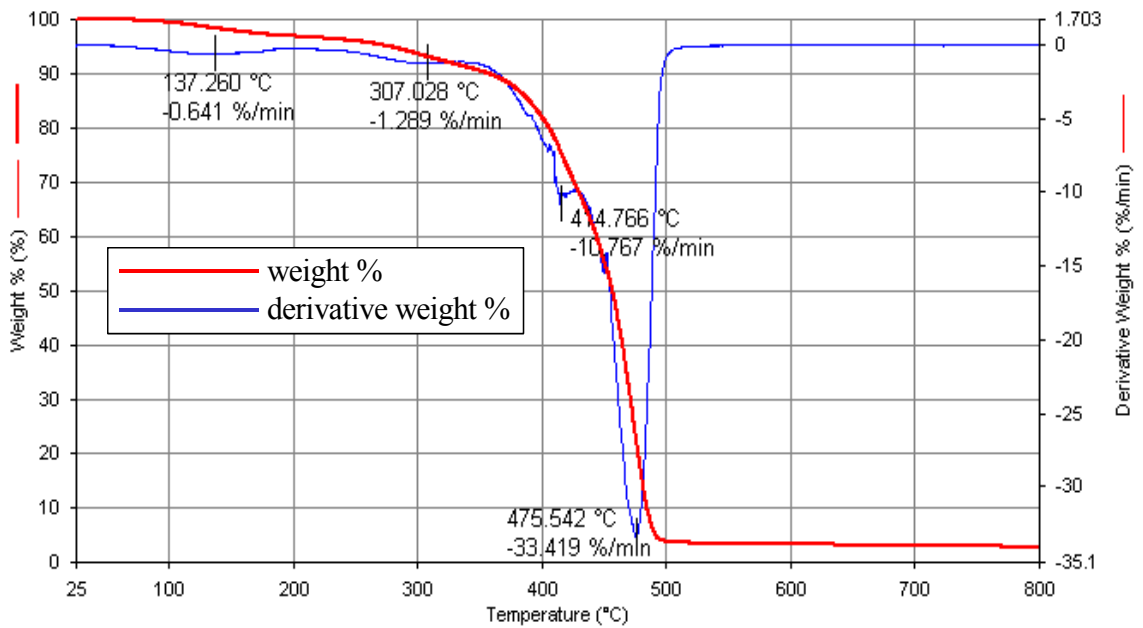


Figure 4.4.2 TGA Scan of Dais<sup>®</sup> 30% Sulfonation Membrane in N<sub>2</sub>

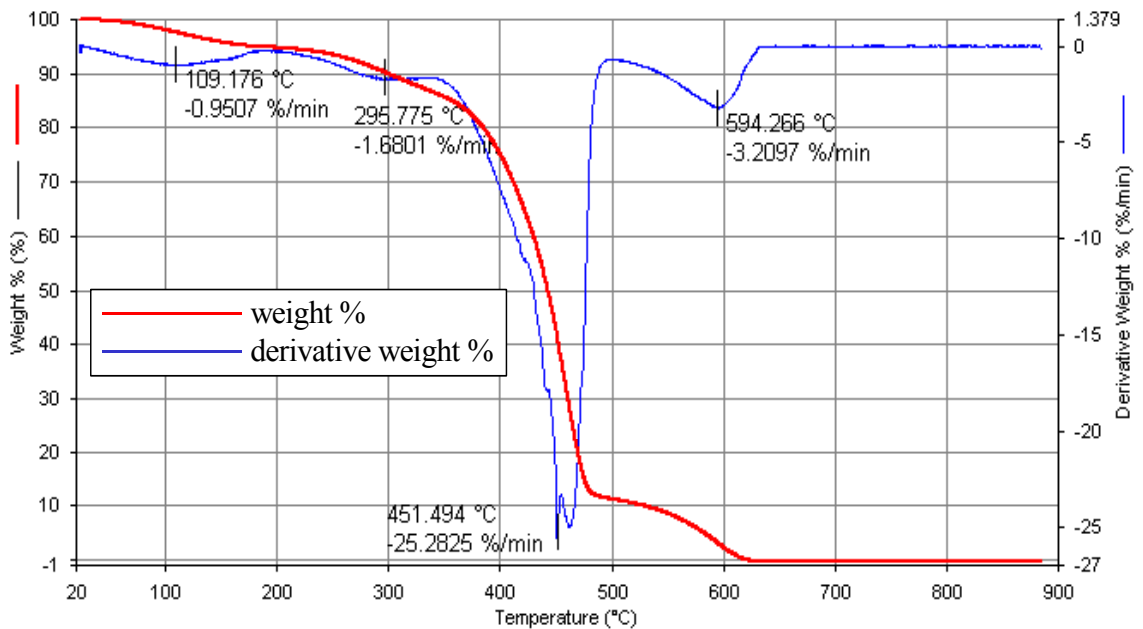


Figure 4.4.3 TGA Scan of Dais<sup>®</sup> 60% Sulfonation Membrane in Air

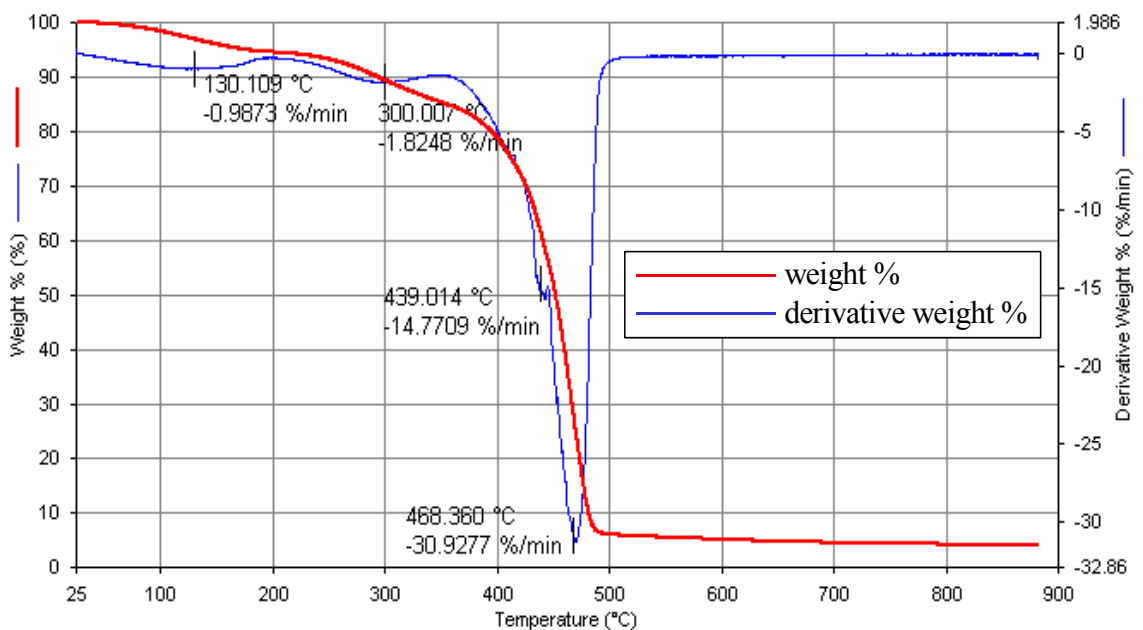


Figure 4.4.4 TGA Scan of Dais<sup>®</sup> 60% Sulfonation Membrane in N<sub>2</sub>

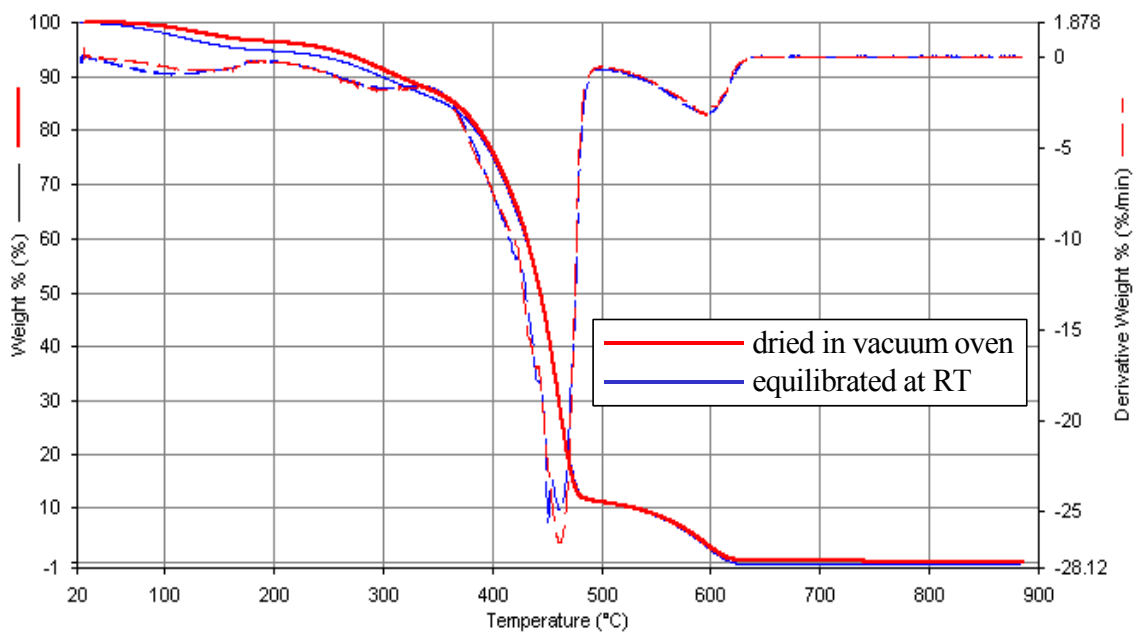
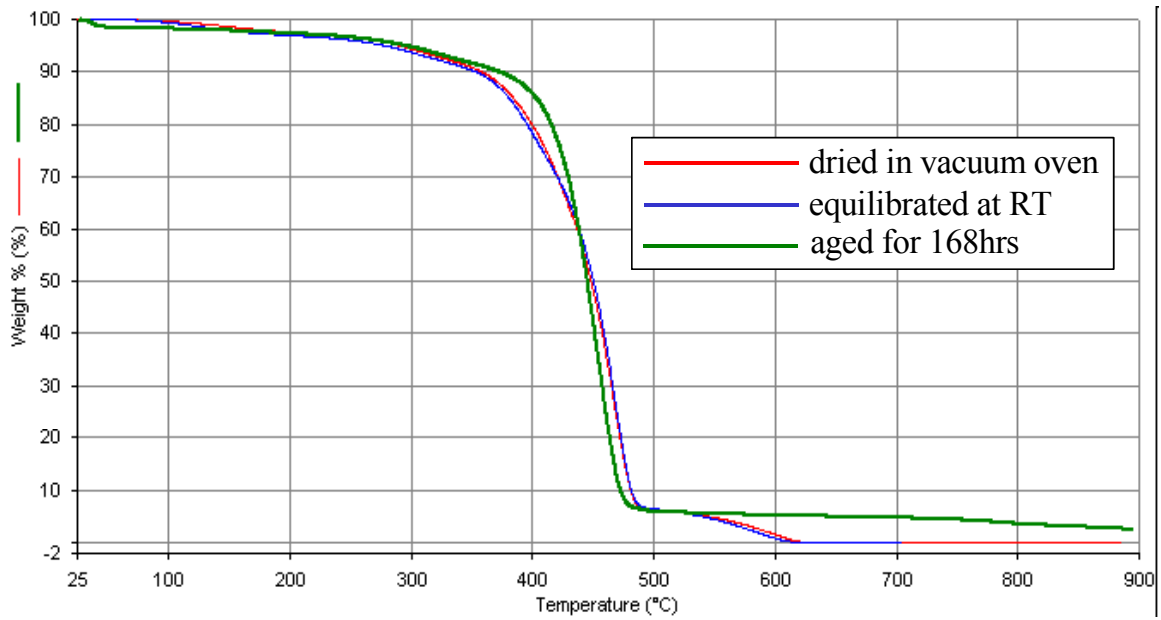
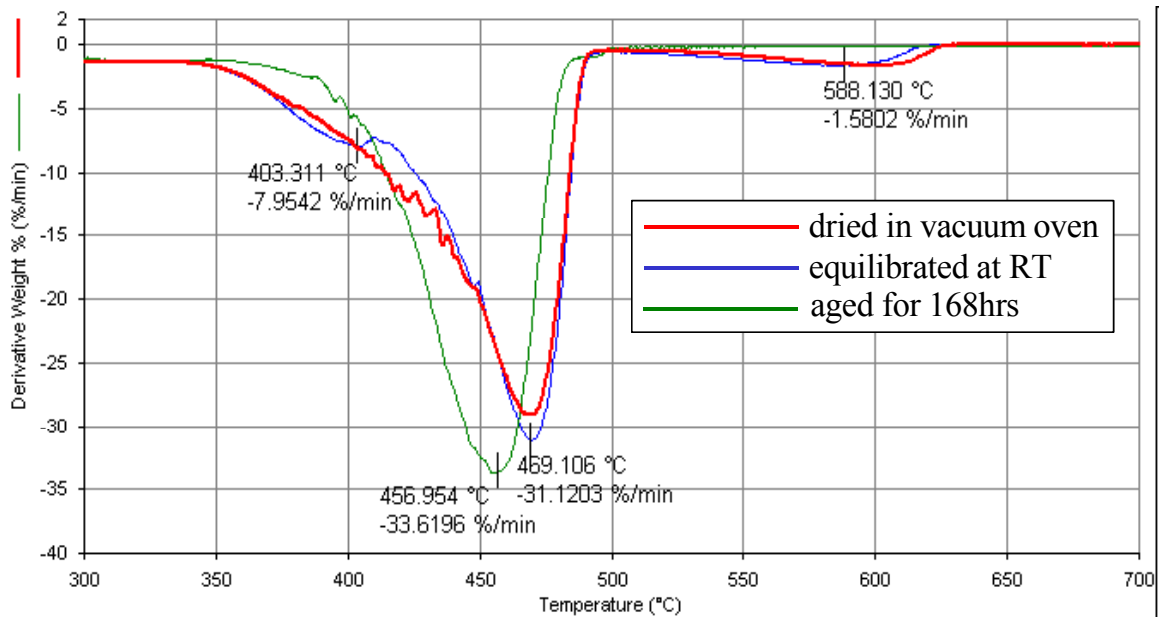


Figure 4.4.5 The Effect of Drying Dais<sup>®</sup> 60% Sulfonation Membrane in the Vacuum Oven Overnight (TGA in Air)



**Figure 4.4.6 TGA Scan in Air of 30% Sulfonated Dais® Membrane: equilibrated at RT Conditions, Dried in Vacuum Oven and Aged for 168hrs in DI Water at 90°C (Weight %)**



**Figure 4.4.7 TGA Scan in Air of 30% Sulfonated Dais® Membrane: equilibrated at RT Conditions, Dried in Vacuum Oven and Aged for 168hrs in DI Water at 90°C (Derivative Weight %)**

The effect of the heating rate on the TGA scans of 30% sulfonated Dais® membranes is shown in Figure 4.4.8 and Figure 4.4.9. The first sample was heated at 20°C/min up to 700°C and the second sample was heated at 2°C/min up to 250°C and at

20°C/min from 250°C to 800°C. With the decrease in the heating rate, the position of the shoulder of the derivative weight % curve had moved from 403°C to 437°C, the main loss peak from 469°C to 496°C and the peak at 588°C had disappeared.

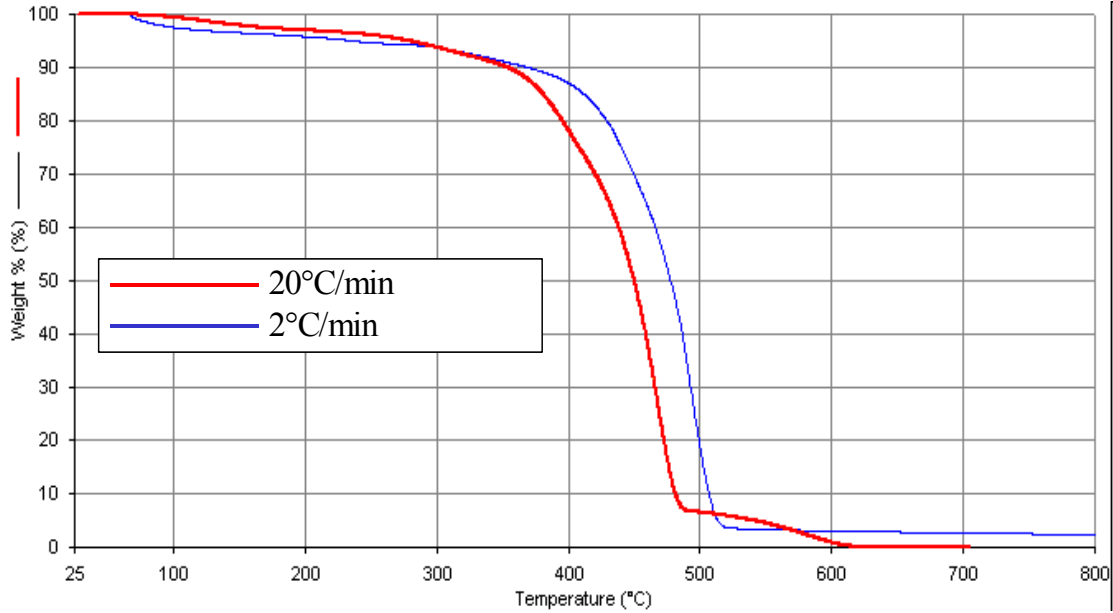


Figure 4.4.8 The Effect of the TGA Heating Rate in Air on 30% Sulfonated Dais® Membrane (Weight %)

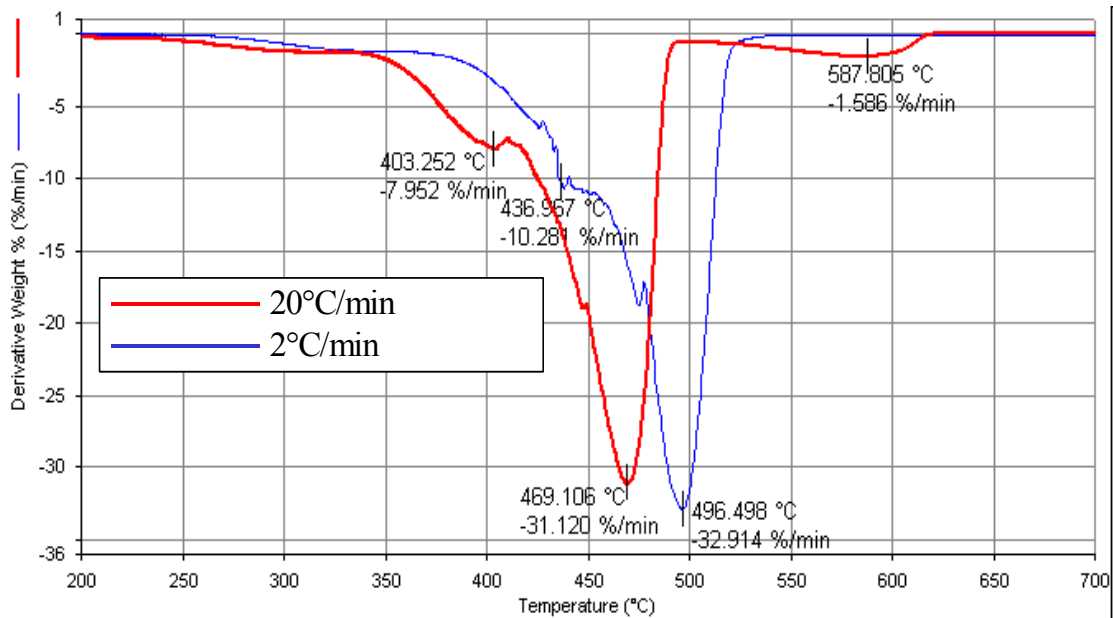


Figure 4.4.9 The Effect of the TGA Heating Rate in Air on 30% Sulfonated Dais® Membrane (Derivative Weight %)

## 4.5 FTIR: Dais<sup>®</sup> Membranes

The FTIR spectra of 30% and 60% sulfonated Dais<sup>®</sup> membranes are shown in Figure 4.5.1. Both possess similar characteristic peaks; however 60% sulfonated samples have higher peak intensity in the 800-1400cm<sup>-1</sup> region. Figure 4.5.2 and Figure 4.5.3 show the results of FTIR scans of five random samples of 30% sulfonated Dais<sup>®</sup> membranes. The major differences between the scans are in the 2800-3000cm<sup>-1</sup> region.

The effect of the heating on FTIR spectra of 30% sulfonated Dais<sup>®</sup> membranes is shown in Figure 4.5.4 and Figure 4.5.5. There are no significant differences between the scans of the fresh and heated membranes. The effect of the heating on FTIR spectra of 60% sulfonated Dais<sup>®</sup> is shown in Figure 4.5.6 and Figure 4.5.7. The peak intensity of the fresh sample is higher than that of the samples that were heated in the oven at 225°C.

The effect of aging for 150hrs in DI water at 90°C on FTIR spectrum of 30% sulfonated Dais<sup>®</sup> membranes is shown in Figure 4.5.8 and Figure 4.5.9. The intensity of the peaks of the aged sample is higher than that of a virgin sample throughout the whole wavelength region.

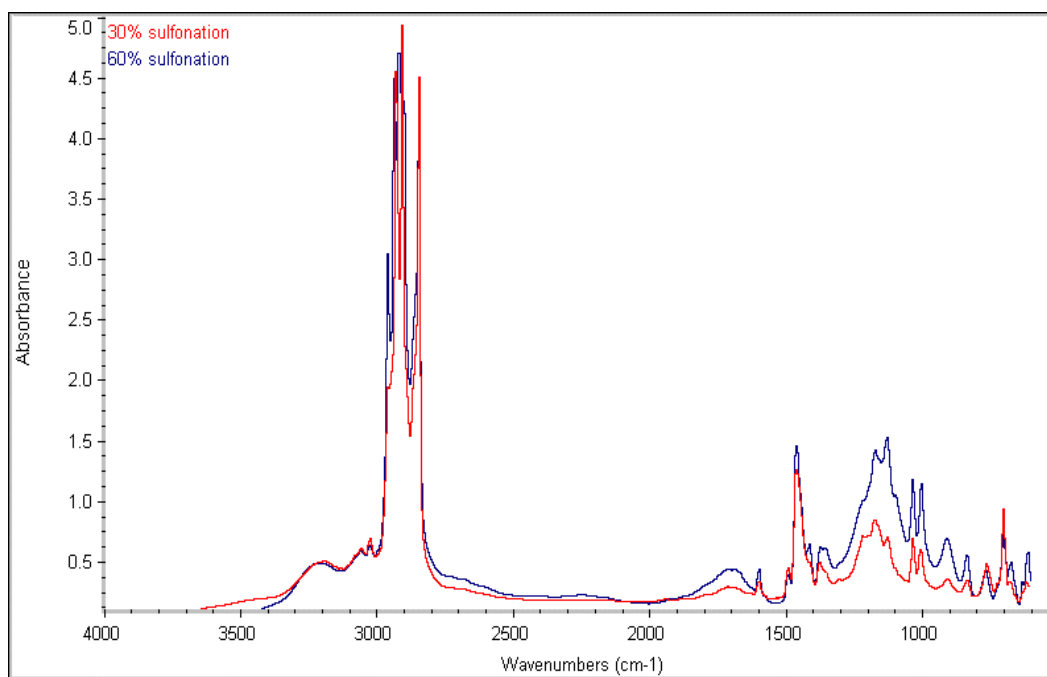
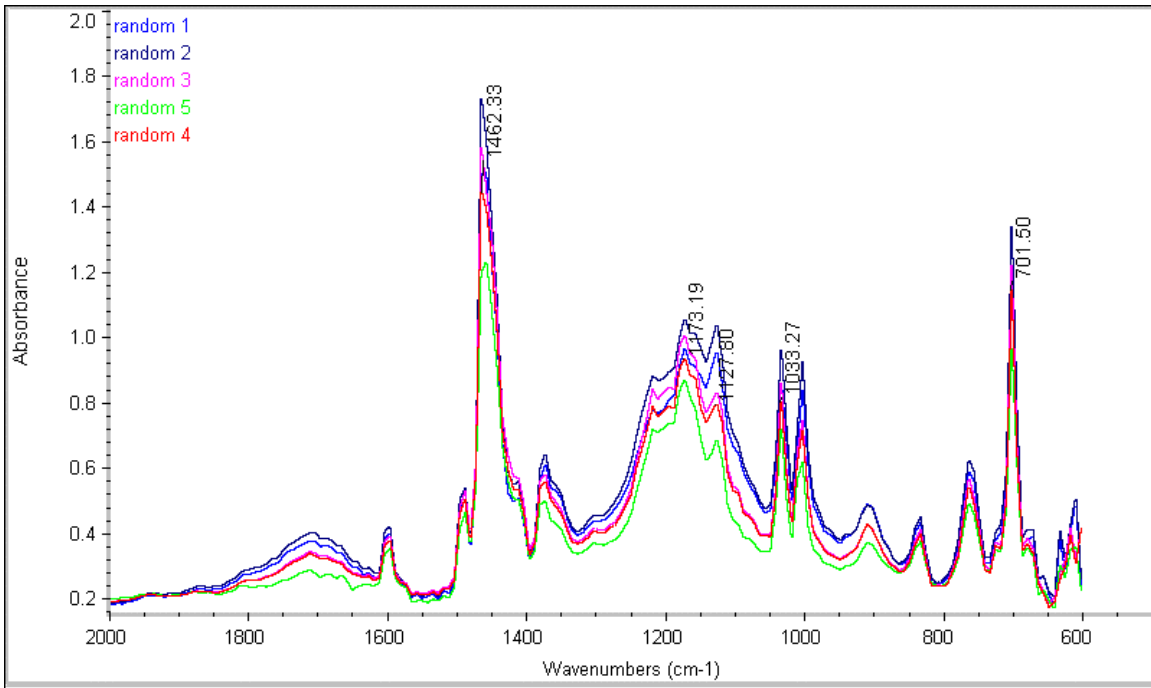
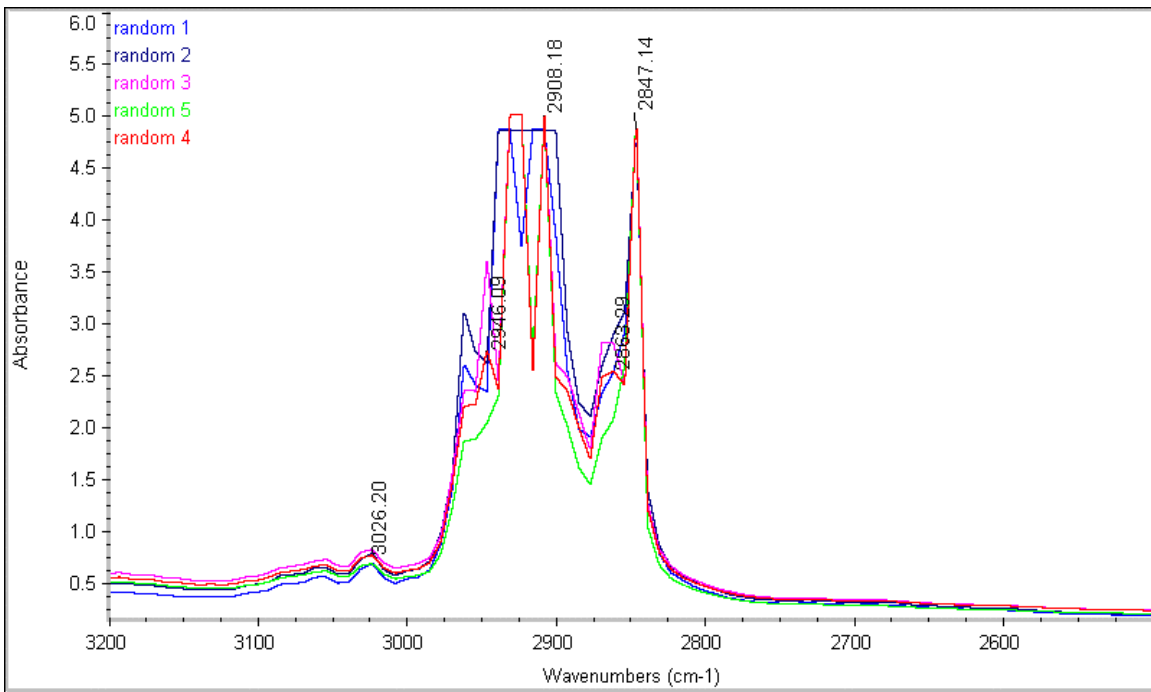


Figure 4.5.1 FTIR of 30% vs. 60% Sulfonated Dais<sup>®</sup> Membranes



**Figure 4.5.2 FTIR of Random Samples of 30% Sulfonated Dais<sup>®</sup> Membranes (Low Wavelengths)**



**Figure 4.5.3 FTIR of Random Samples of 30% Sulfonated Dais<sup>®</sup> Membranes (High Wavelengths)**

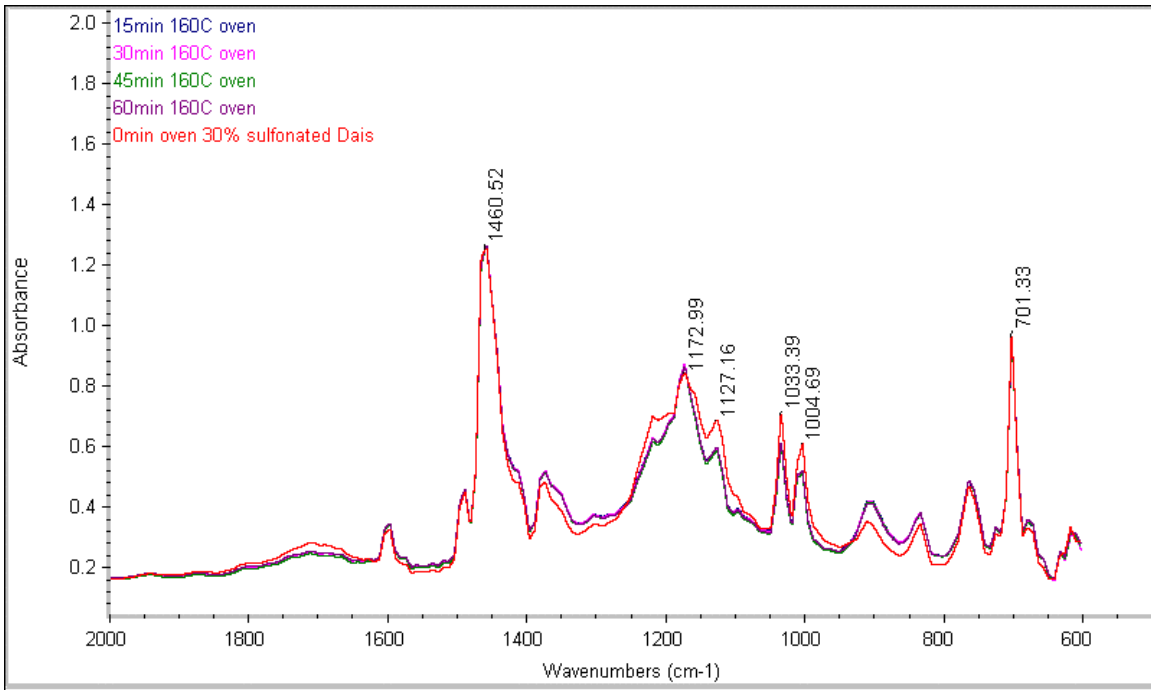


**Figure 4.5.4 FTIR of 30% Sulfonated Dais<sup>®</sup> Membrane: the Effect of Heating (Low Wavelengths)**

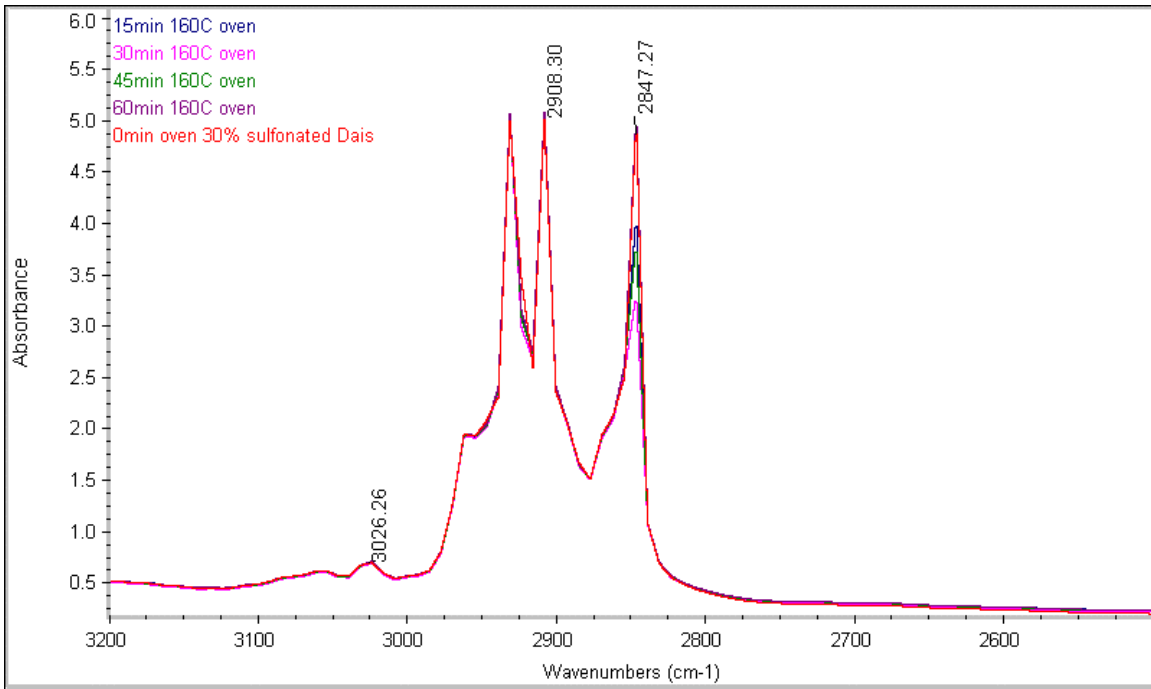


**Figure 4.5.5 FTIR of 30% Sulfonated Dais<sup>®</sup> Membrane: the Effect of Heating (High Wavelengths)**

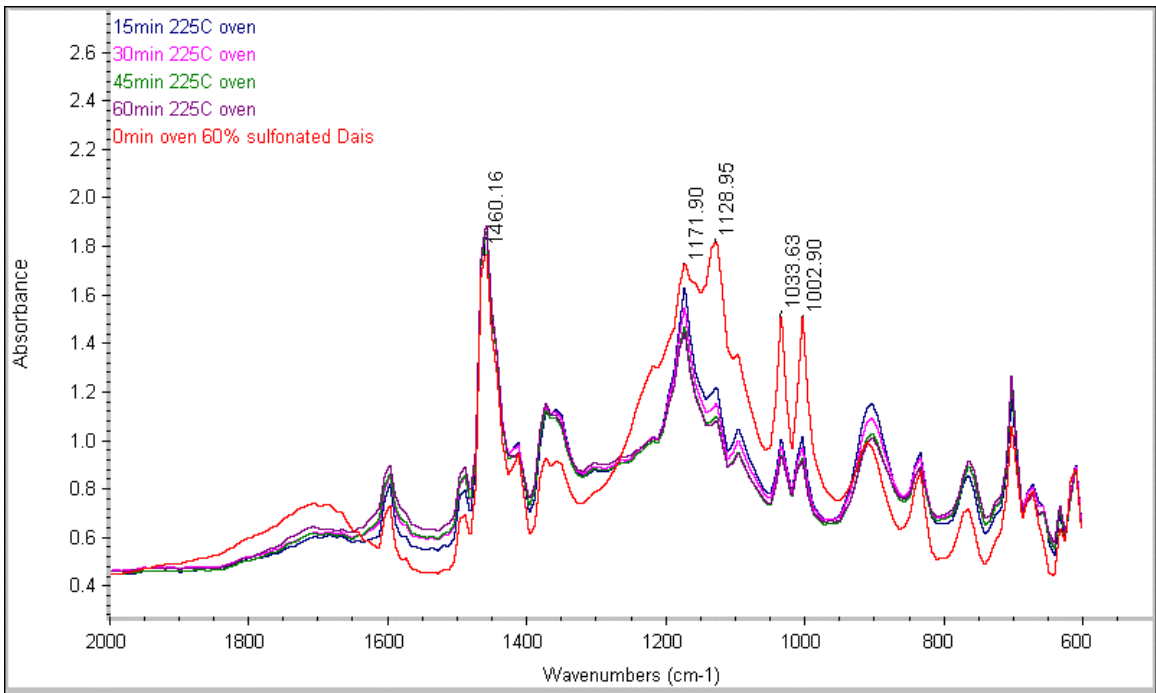


Figure 4.5.6 FTIR of 60% Sulfonated Dais<sup>®</sup> Membrane: the Effect of Heating (Low Wavelengths)

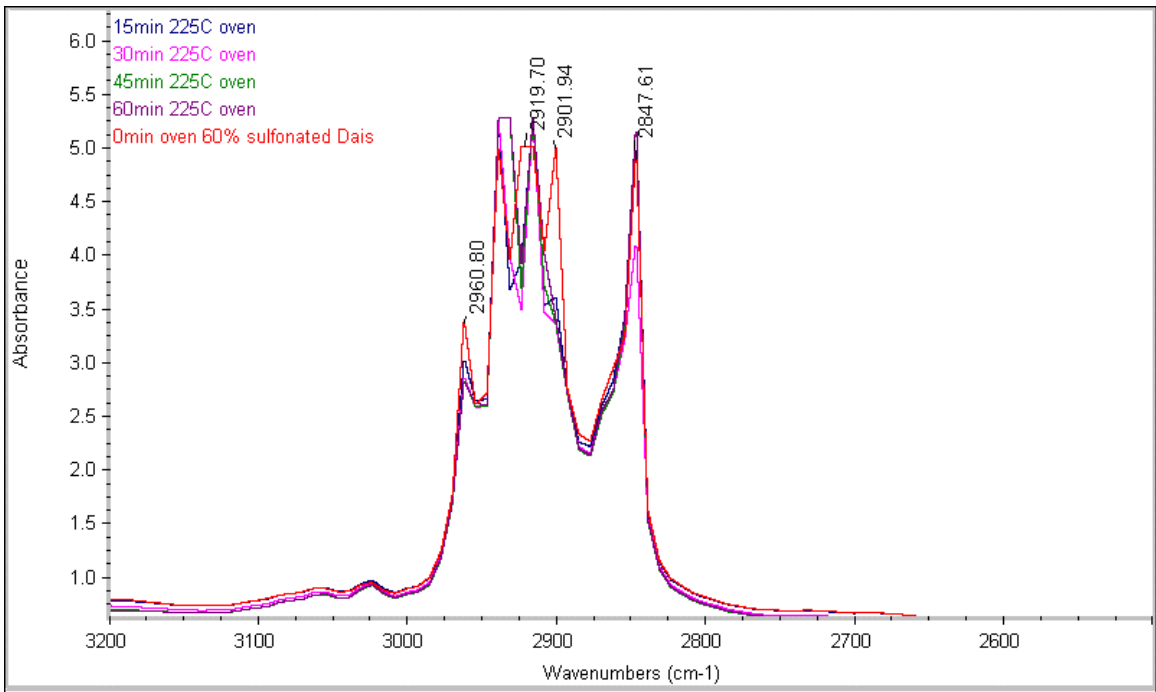


Figure 4.5.7 FTIR of 60% Sulfonated Dais<sup>®</sup> Membrane: the Effect of Heating (High Wavelengths)

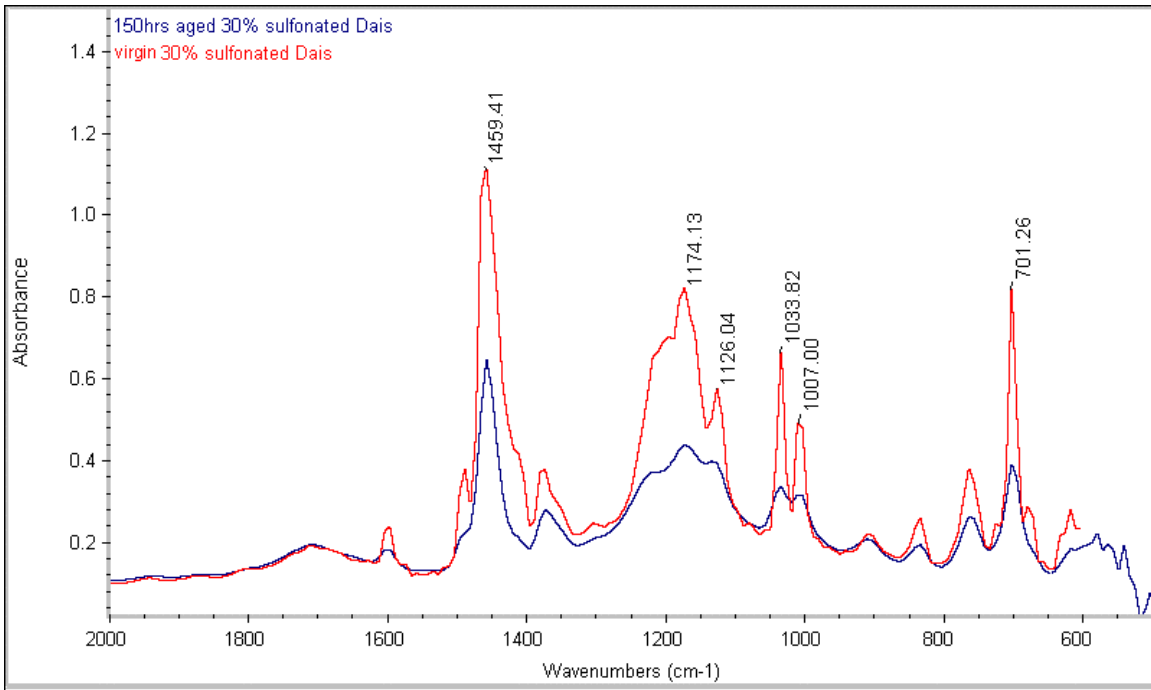


Figure 4.5.8 FTIR of 30% Sulfonated Dais<sup>®</sup> Membrane: the Effect of Aging (Low Wavelengths)

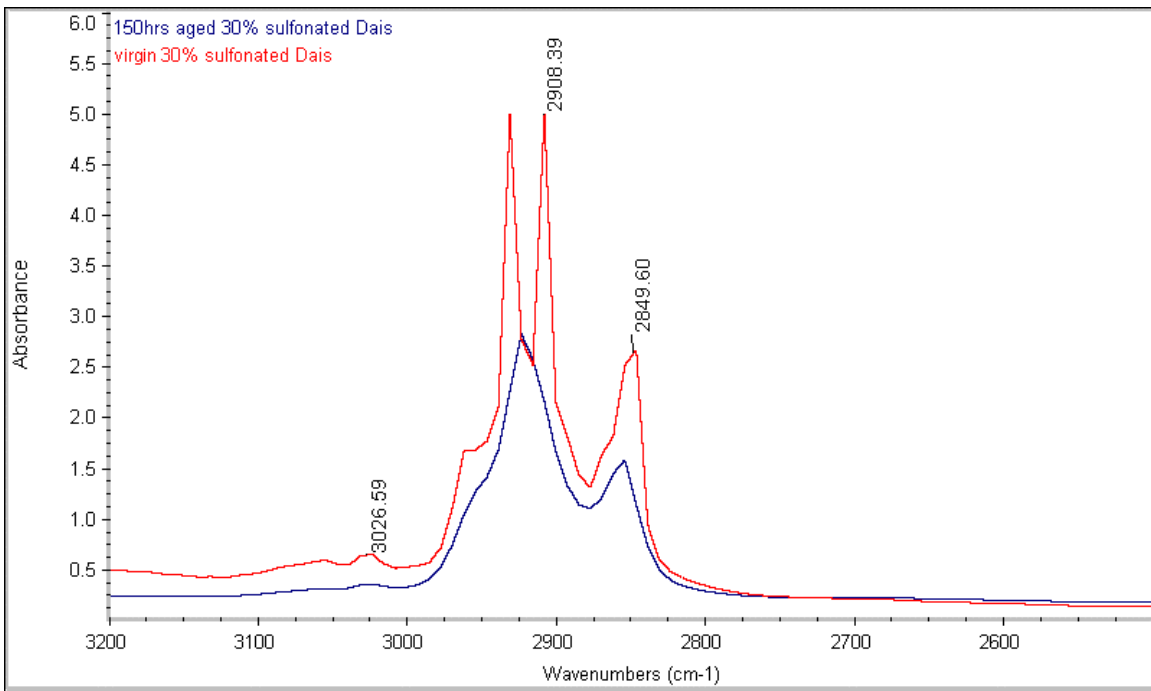


Figure 4.5.9 FTIR of 30% Sulfonated Dais<sup>®</sup> Membrane: the Effect of Aging (High Wavelengths)

## 4.6 Water Uptake: Nafion<sup>®</sup> Membranes

The results of water uptake studies of virgin and aged (for seven months in DI water at 65°C) Nafion<sup>®</sup> membranes are shown in Figure 4.6.1. The maximum water uptake of the aged Nafion<sup>®</sup> membranes is only slightly higher than that for the virgin membranes ( $26.1 \pm 1.0$  wt% for aged vs.  $24.4 \pm 2.1$  wt% for virgin).

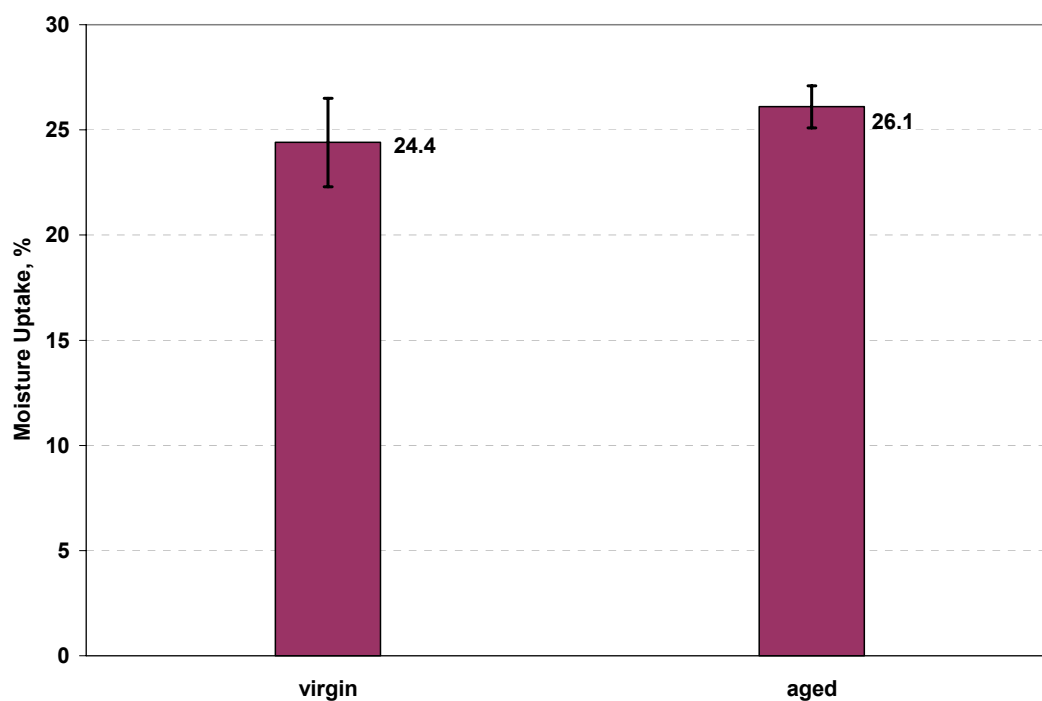


Figure 4.6.1 Maximum Water Uptake of Nafion<sup>®</sup> Membranes

The effect of drying Nafion<sup>®</sup> membranes in the oven at 160°C on the maximum water uptake is shown in Figure 4.6.2. Sample 1 was equilibrated at RT conditions, sample 2 was heated in the oven at 160°C for 1 hour and sample 3 was heated in the oven at 160°C for 2 hours. As the result of heating, sample 2 lost 3.3 wt% and sample 3 lost 3.2 wt% as compared to the original pre-oven weight. Samples 2 and 3 were then equilibrated at RT conditions and their weight was recorded. The unrecovered weight percent, as compared to the original pre-oven weight, was 0.4 wt% for the sample 2 and

0.2 wt% for the sample 3. In order to measure the maximum water uptake, samples 1,2 and 3 were immersed in DI water for 24 hours and weighted. Sample 1 gained 29.8% of water, sample 2 gained 15.8 wt% and sample 3 gained 16.2 wt% (as compared to the original pre-oven weight).

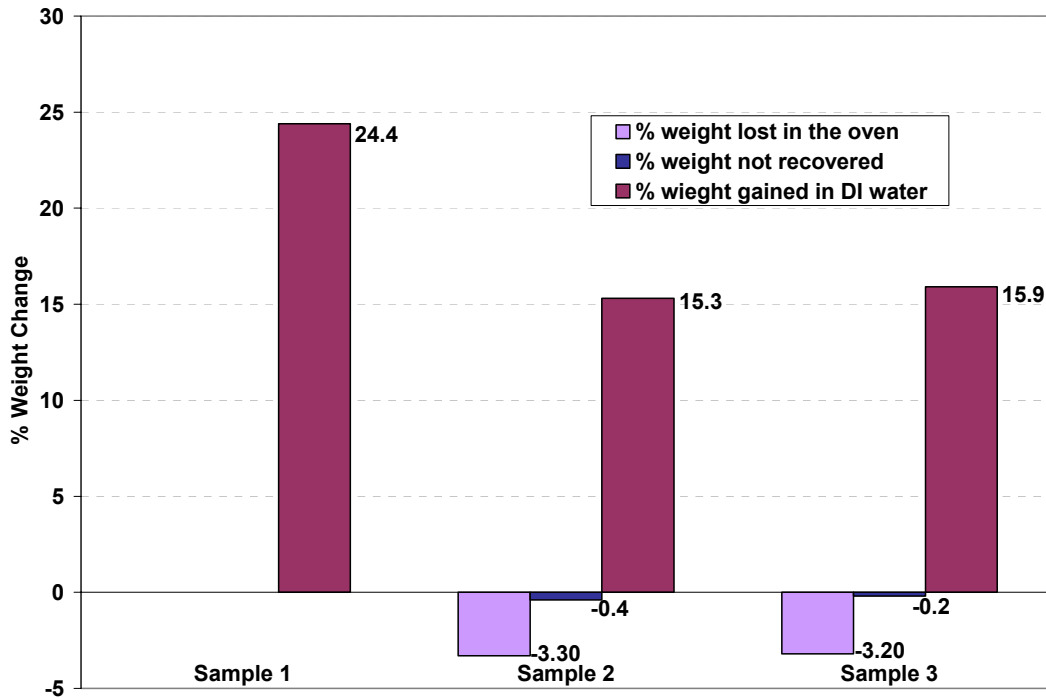


Figure 4.6.2 Effect of Drying Nafion<sup>®</sup> Membranes in the Oven at 160°C

#### 4.7 Water Uptake: Dais<sup>®</sup> Membranes

The results of the water uptake studies of virgin 30% and 60% sulfonated and 30% sulfonated Dais<sup>®</sup> membranes aged for 100 days in DI water at 90°C are shown in Figure 4.7.1. The 30% sulfonated Dais membranes gained 27.2±0.2 wt%, 60% sulfonated membranes gained 190.2±3.2 wt% and 30% aged sulfonated membranes gained 85.8 wt% as compared to initial sample weights. Only one aged sample was measured because of the limited number of aged samples.

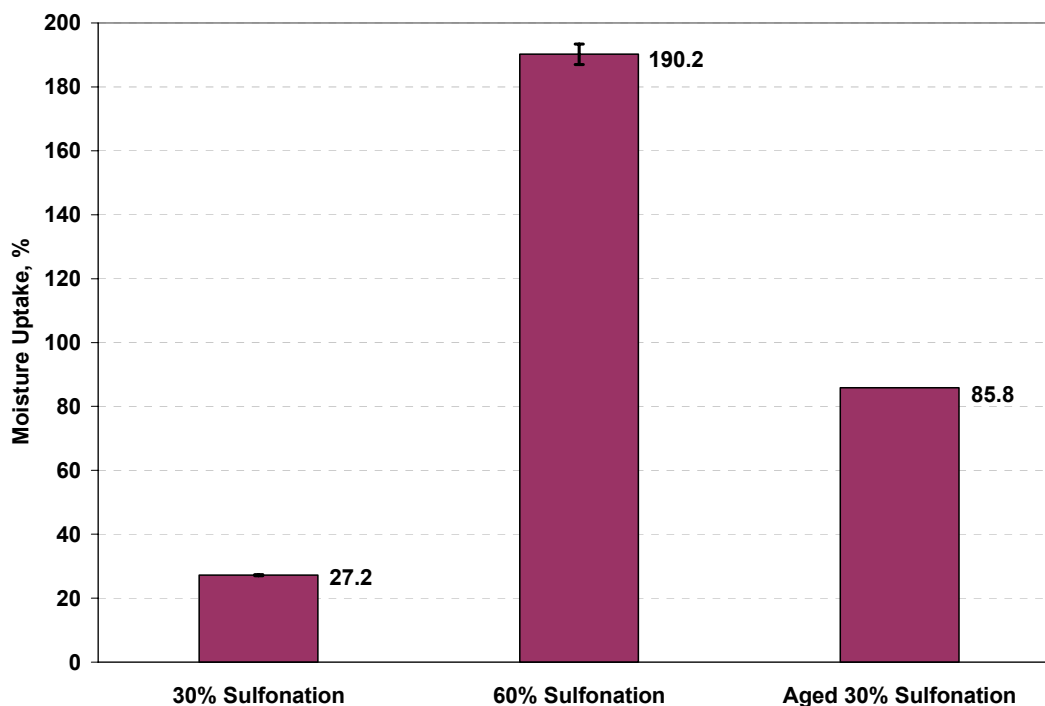


Figure 4.7.1 Maximum Water Uptake of Dais® Membranes

#### 4.8 Water Sorption Kinetics: Nafion® Membranes

The results of the water sorption kinetics studies of virgin Nafion® membranes and membranes aged for seven months in DI water at 65°C are shown in Figure 4.8.1 and Figure 4.8.2, respectively. The aged membranes, on average, equilibrated at higher moisture content (12%) than did virgin samples (10%).

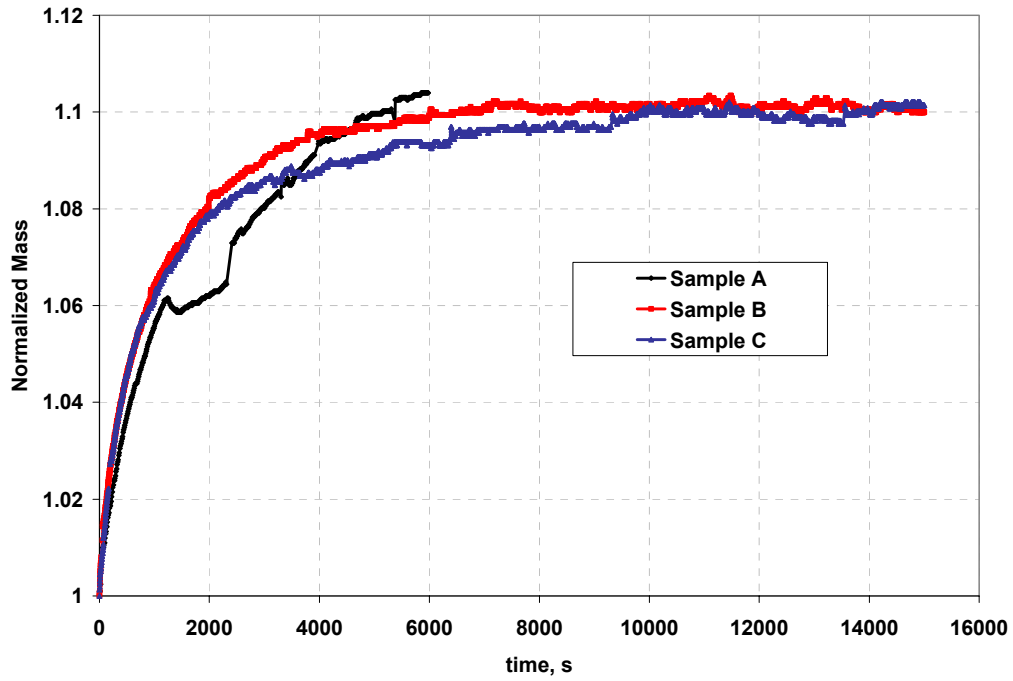


Figure 4.8.1 Vapor Phase Water Sorption Studies of Virgin Nafion® Membranes

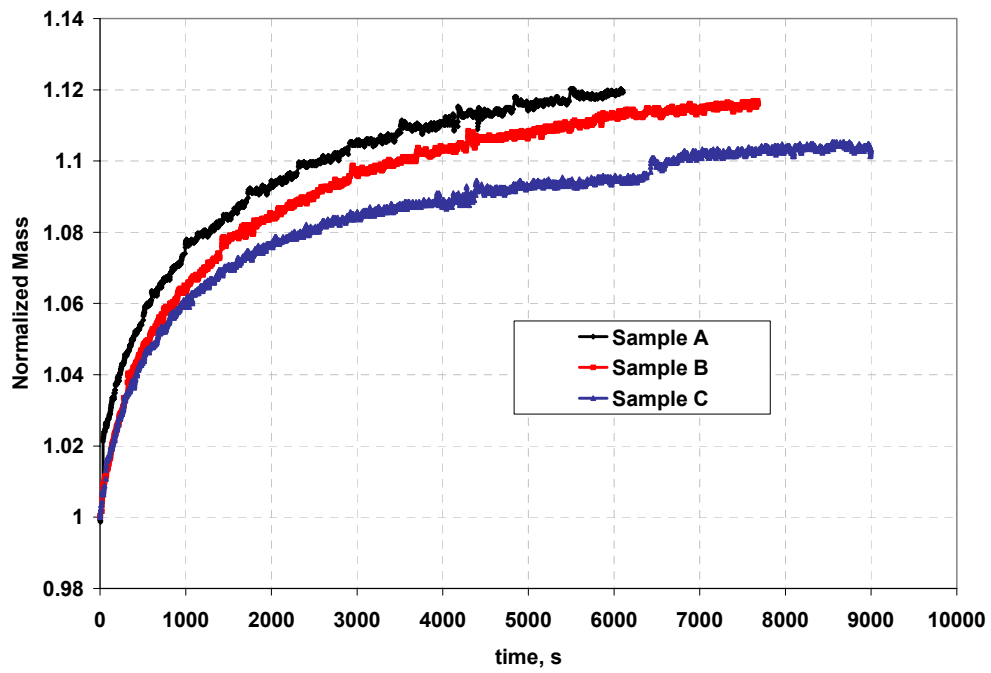


Figure 4.8.2 Vapor Phase Water Sorption Studies of Aged Nafion® Membranes

#### 4.9 Water Sorption Kinetics: Dais<sup>®</sup> Membranes

The results of the water sorption kinetics studies of 30% and 60% sulfonated Dais<sup>®</sup> membranes are shown in Figure 4.9.1 and Figure 4.9.2. 30% sulfonated Dais<sup>®</sup> gained  $9.3 \pm 0.6$  wt% of moisture from air and 60% sulfonated membranes gained  $25.0 \pm 1.0$  wt%. The results of the kinetics study of 30% sulfonated Dais<sup>®</sup> membranes aged for 100 days in DI water at 90°C are shown in Figure 4.9.3. The aged membrane gained 6.5 wt% of moisture but this value is based only on one measurement because of the limited number of aged samples.

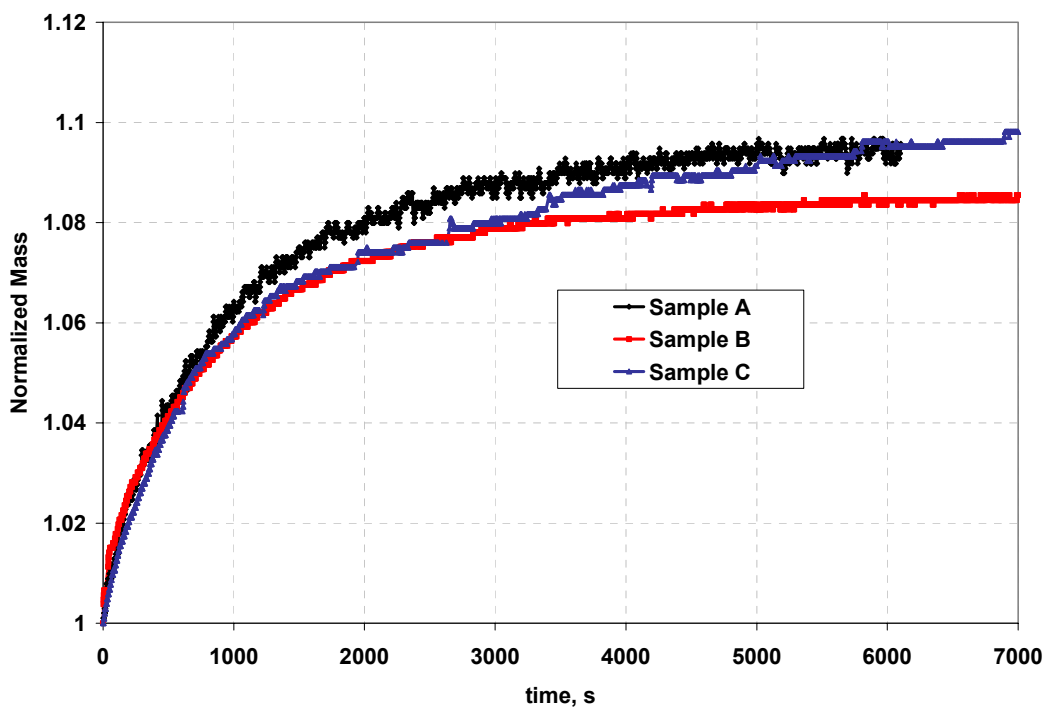


Figure 4.9.1 Vapor Phase Water Sorption Studies of 30% Dais<sup>®</sup> Membranes

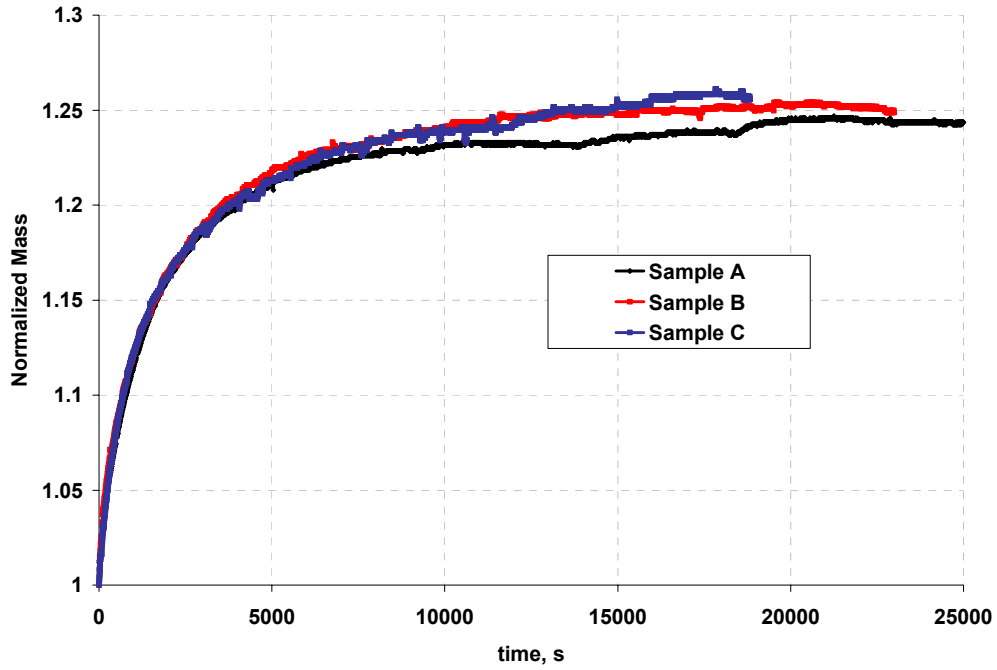


Figure 4.9.2 Vapor Phase Water Sorption Studies of 60% Dais<sup>®</sup> Membranes

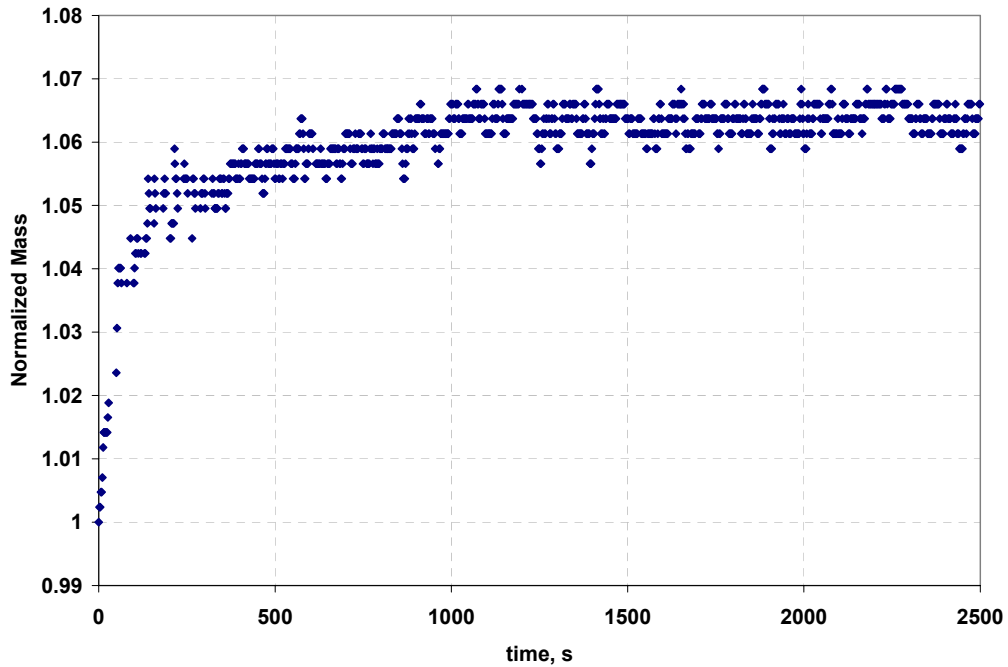


Figure 4.9.3 Vapor Phase Water Sorption Studies of Aged 30% Dais<sup>®</sup> Membranes

#### 4.10 Water Desorption Kinetics: Nafion<sup>®</sup> Membranes

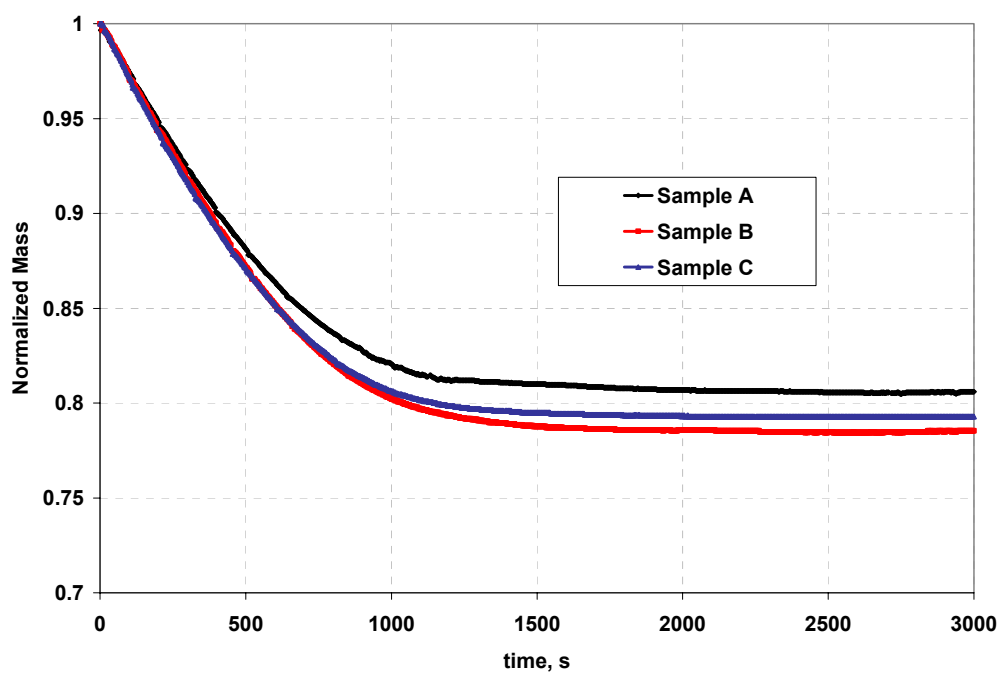


Figure 4.10.1 Water Desorption Studies of Nafion<sup>®</sup> Membranes

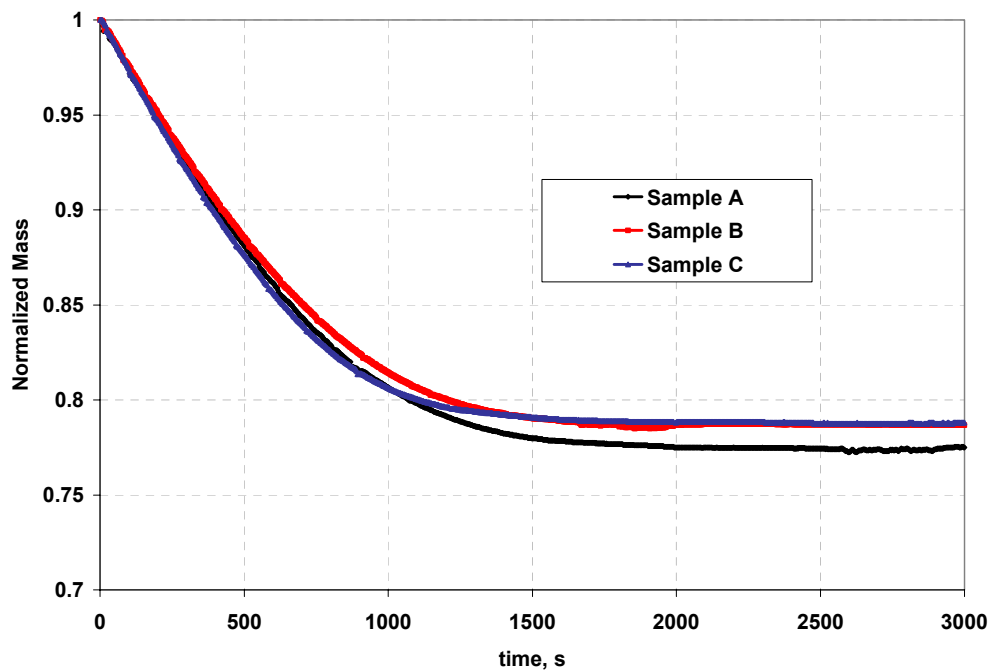
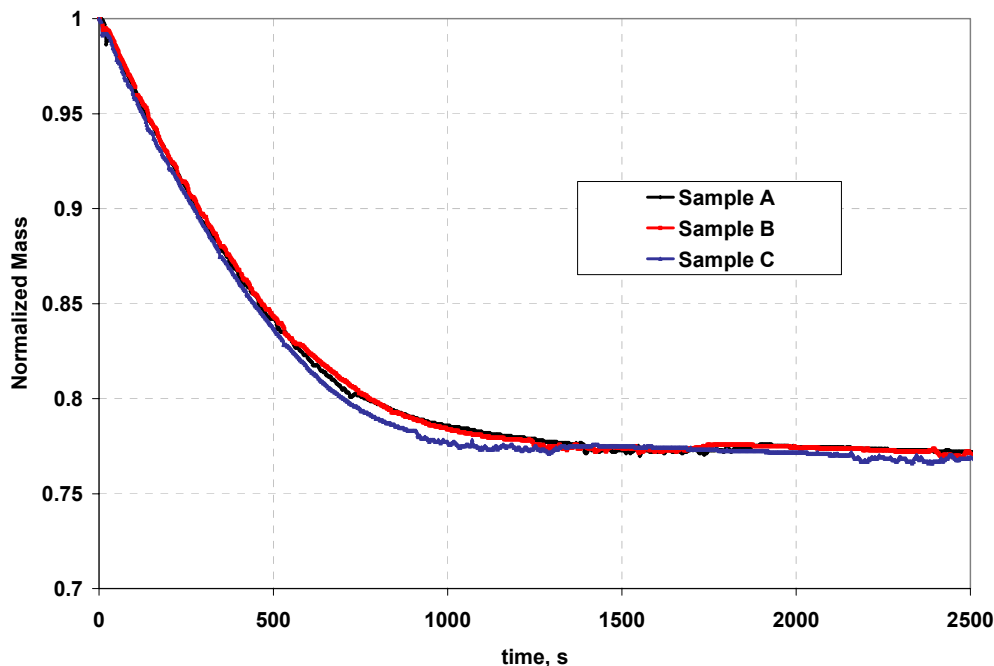


Figure 4.10.2 Water Desorption Studies of Aged Nafion<sup>®</sup> Membranes

The results of the water desorption studies of virgin Nafion<sup>®</sup> membranes and membranes aged in DI water at 65°C for seven months are shown in Figure 4.10.1 and Figure 4.10.2, respectively. Both membranes achieved equilibrium after about 1700-2000s. The virgin Nafion<sup>®</sup> membranes retained 79.5±0.7 wt% of their original (membranes plus water) weight and aged membranes retained 78.3±1.0 wt% of their original (membranes plus water) weight.

#### ***4.11 Water Desorption Kinetics: Dais<sup>®</sup> Membranes***

The results of water desorption studies of 30% and 60% sulfonated Dais<sup>®</sup> membranes are shown in Figure 4.11.1 and Figure 4.11.2 respectively. The 30% sulfonated Dais<sup>®</sup> membranes reached equilibrium in about 1,500s while retaining 77.1±0.2 wt% of their original (membrane plus water) weight, where as 60% sulfonated membranes reached an equilibrium in 3,000s while retaining 32.7±0.6 wt% of their original (membrane plus water) weight.



**Figure 4.11.1 Water Desorption Studies of 30% Sulfonated Dais<sup>®</sup> Membranes**

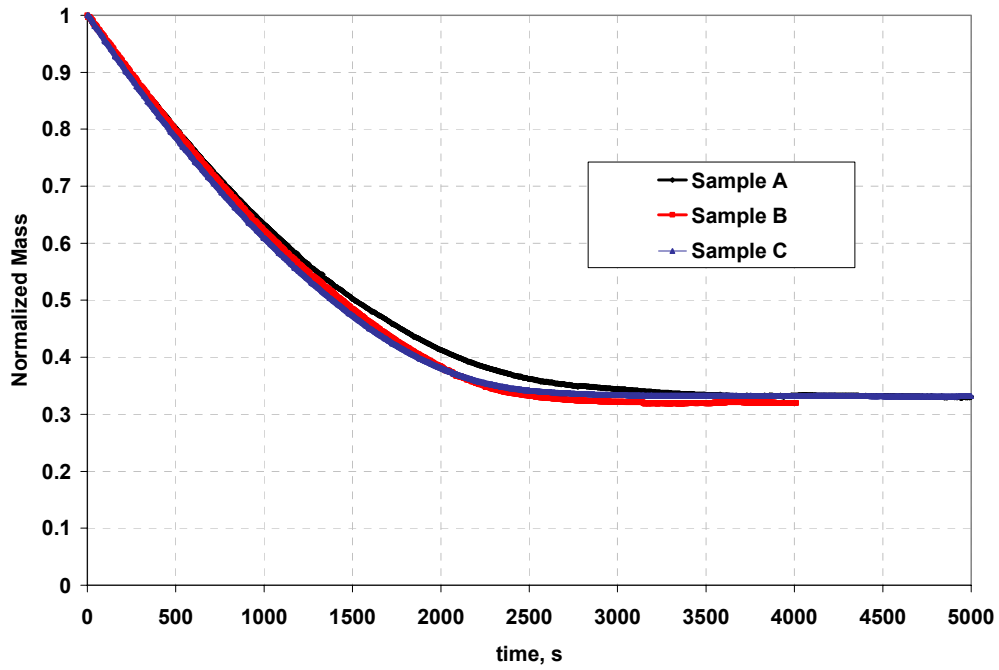


Figure 4.11.2 Water Desorption Studies of 60% Sulfonated Dais® Membranes

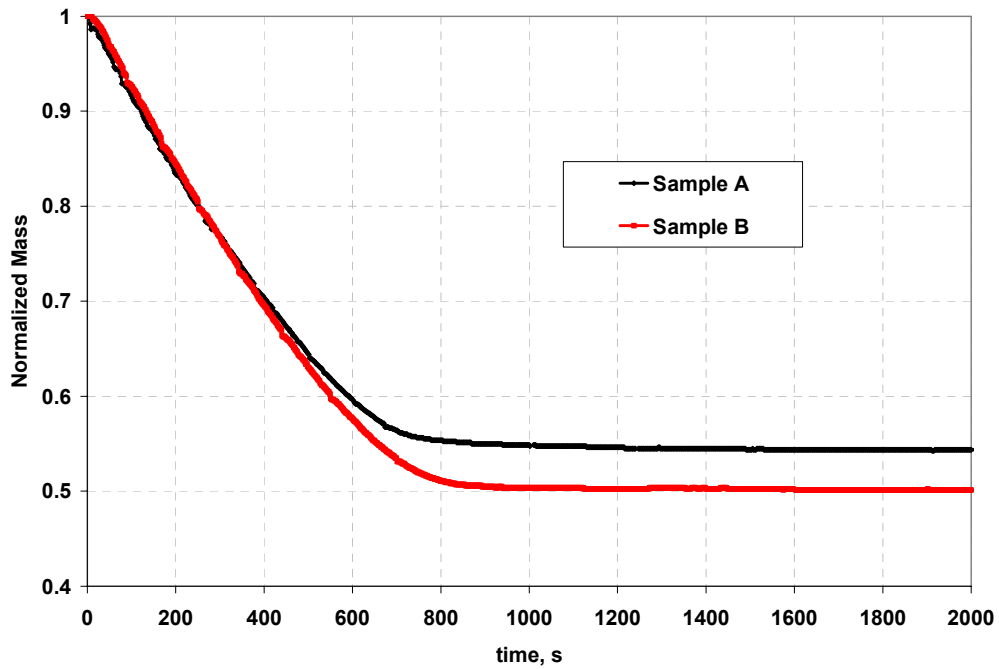


Figure 4.11.3 Water Desorption Studies of Aged 30% Sulfonated Dais® Membranes

The results of the water desorption studies of 30% sulfonated Dais® membranes aged for 100 days in DI water at 90°C are shown in Figure 4.11.3. Only two sets of

measurements were taken because of the limited number of aged samples. The samples reached an equilibrium weight in about 1,000s while retaining  $52.2 \pm 2.0\%$  of their original (membrane plus water) weight.

#### 4.12 SEM: Nafion<sup>®</sup> Membranes

The results of the SEM analysis of the surface topology of untreated and treated Nafion<sup>®</sup> membranes are shown in Figure 4.12.1 Figure 4.12.2, Figure 4.12.3. No significant differences are observed between the three images

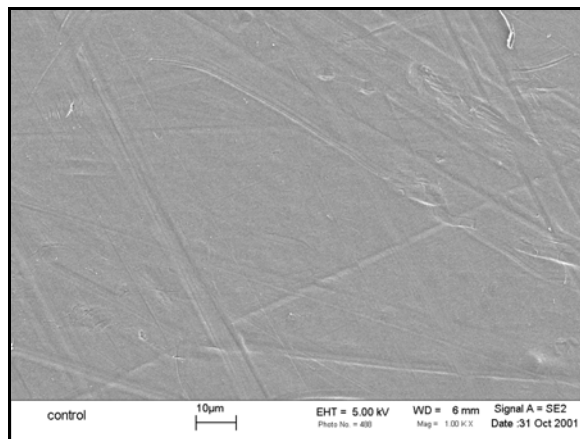


Figure 4.12.1 SEM Image of Untreated Nafion<sup>®</sup> Membrane

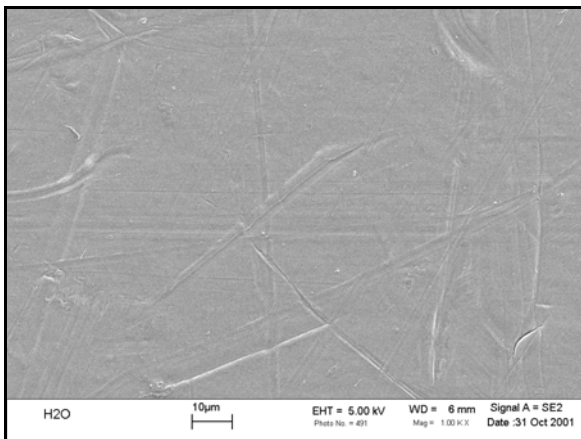


Figure 4.12.2 SEM Image of Nafion<sup>®</sup> Membrane Boiled in DI Water for 1hr

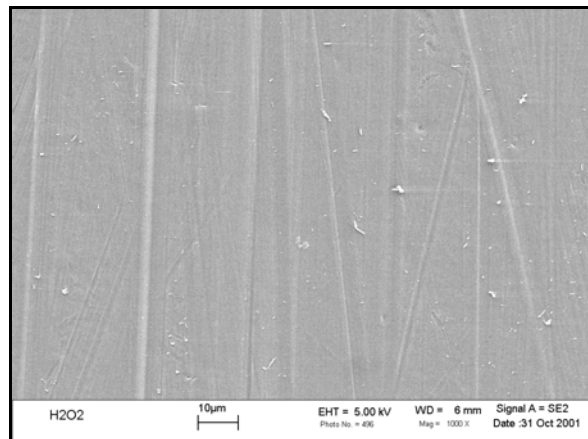


Figure 4.12.3 SEM Image of Nafion<sup>®</sup> Membrane Boiled 1hr in H<sub>2</sub>O and 1hr in H<sub>2</sub>O<sub>2</sub>

## 5 DISCUSSION

This section will focus on the discussion of the results presented in Section 4 and on correlating them with the theoretical concepts introduced in Section 2. First, the structural properties of Nafion<sup>®</sup> membranes will be discussed, followed by the examination of the plasticization effects, thermal degradation behavior and diffusion properties as well as the discussion of the effects of aging and pre-treatment on the properties of this material. Next, the discussion will shift to Dais<sup>®</sup> membranes: their structural properties, effects of sulfonation and plasticization, their diffusion properties and thermal behavior followed by the examination of aging effects on their mechanical and diffusion properties.

### *5.1 Structure, Thermal Degradation and Plasticization of Nafion<sup>®</sup> Membranes*

The DMA spectrum of the Nafion<sup>®</sup> membrane in Figure 4.1.1 clearly possesses two peaks in  $\tan \delta$  curve at  $-74^{\circ}\text{C}$  and at  $109^{\circ}\text{C}$  and two major storage modulus drops: one between  $-104^{\circ}\text{C}$  and  $0^{\circ}\text{C}$  and another between  $50^{\circ}\text{C}$  and  $145^{\circ}\text{C}$ . The upper transition is characterized by a drop of almost two orders of magnitude in storage modulus of the material (from  $3.4 \times 10^8$  Pa to  $4.9 \times 10^6$  Pa) and a large  $\tan \delta$  peak. It corresponds to an  $\alpha$  transition observed by Yeo and Eisenberg<sup>12</sup> at  $111^{\circ}\text{C}$ . The lower transition is characterized by a much smaller drop in storage modulus (from  $1.8 \times 10^9$  Pa to  $3.4 \times 10^8$  Pa) and a small but very broad  $\tan \delta$  peak. From the magnitude of both (the modulus drop and the height of the  $\tan \delta$  peak), it is reasonable to conclude that this transition is not due to large scale molecular motions and corresponds to a  $\gamma$  transition due to the short range motions of the fluorocarbons in the PTFE backbone observed by Yeo and Eisenberg<sup>12</sup> at  $-100^{\circ}\text{C}$ . The  $\beta$  transition observed by Yeo and Eisenberg<sup>12</sup> at  $23^{\circ}\text{C}$  as a

shoulder in the  $\tan \delta$  curve is absent in the DMA spectrum shown here. The height of the shoulder in the data presented in the article is smaller than the height of the peak at  $-100^\circ\text{C}$  and is partly masked by the onset of an  $\alpha$  transition. In the DMA spectrum shown here, the height of the  $\tan \delta$  peak corresponding to a  $\gamma$  transition is very small and if it is assumed that the relative magnitudes of the peaks here and in the article are comparable, it is unlikely that the  $\beta$  peak will be visible in the onset of an  $\alpha$  transition. Yeo and Eisenberg<sup>12</sup> have also presented the results of the dielectric measurements of the Nafion<sup>®</sup> membranes. The  $\beta$  peak is much more pronounced in those experiments, leading to a conclusion that this method is more suitable to use if one wants to investigate the  $\beta$  transition.

The effect of the frequency of the DMA scan on the position of  $\tan \delta$  peak is shown in Figure 4.1.6. There is a shift in the  $\tan \delta$  peak and in the storage modulus curve with the increase in the frequency of the scan. This effect is expected since an increase in frequency implies that the sample is being interrogated at a higher rate and the polymeric chains have less time available for the rearrangement. As a result, the onset of the large scale molecular motions occurs at a higher temperature.

The results of the thermal degradation studies of Nafion<sup>®</sup> membranes in air and  $\text{N}_2$  (Figure 4.3.1 and Figure 4.3.2) agree well with the results reported in the literature (Table 2.8.1). As expected, there is an initial weight loss of 5 wt% below  $200^\circ\text{C}$  due to the loss of the residual water. The loss of 9 wt% in the temperature region between  $200^\circ\text{C}$  and  $370^\circ\text{C}$  correlates to 7.7 wt% loss due to degradation of the sulfonic groups reported by Suroweic and Boroczek<sup>44</sup> and 10 wt% loss reported by Samms *et al*<sup>45</sup>. The losses of 88 wt% in air and 86 wt% in  $\text{N}_2$  between  $370^\circ\text{C}$  and  $600^\circ\text{C}$  are slightly higher than 78 wt% loss reported by Suroweic and Boroczek<sup>44</sup> and 75 wt% loss reported by Samms *et al*<sup>45</sup>; however, both occur in the same temperature region as the ones reported in the literature. The weight loss in this region corresponds to the backbone and side-chain decomposition. The fact that the peak of the derivative weight percent curve for decomposition in air occurs at the temperature higher than that for the decomposition in  $\text{N}_2$  ( $506^\circ\text{C}$  vs.  $488^\circ\text{C}$ ) is slightly unusual. Oxidation is expected to enhance the rate of the thermal degradation. However, the difference between the two cases might not be significant, since the heating

rate of the samples was 20°C/min, so that the discrepancy between the peak positions could be due to the TGA unit resolution and not to the inherent properties of the material.

The effect of water plasticization on the mechanical properties of the Nafion<sup>®</sup> membranes is shown in Figure 4.1.4. There is a clear depression in the values of storage modulus for the saturated membrane as compared to those of the dry sample: dry Nafion<sup>®</sup> has a storage modulus of  $3.4 \times 10^8$  Pa at 25°C and saturated Nafion<sup>®</sup> at the same temperature has a storage modulus of  $8.7 \times 10^7$  Pa. Since the  $\beta$  transition was observed by Yeo and Eisenberg at 23°C, which is lower than the starting temperature of the ambient runs shown in Figure 4.1.4, the differences in the spectra between dry and saturated membranes should be entirely due to the differences between the mechanical properties of the dry and saturated states of the region undergoing an  $\alpha$  transition.

According to Kyu and Eisenberg<sup>13</sup>, the  $\alpha$  transition is due to the relaxation of the ionic regions, although this conclusion might not be evident from the data for the following reasons. The ionic regions should be extremely sensitive to water because of their high polarity. The suppression of the  $\alpha$  transition then should have been predicted by the Fox equation (Equation 2.2.1). It was found that Nafion<sup>®</sup> membranes absorb about 24 wt% of water (Figure 4.6.1); since water has  $T_g$  of -130°C (143°K), then  $T_\alpha$  should be:

$$\frac{1}{\left( \frac{0.24}{143^\circ K} + \frac{0.76}{382^\circ K} \right)} = 273^\circ K = 0^\circ C$$

The actual  $T_\alpha$  should occur at even lower temperature for the following reason. The mass fractions used in the calculation above are for the total polymer weight and water; however, only the weight of the ionic regions should be considered, and, since most of the water is detained inside of the ionic regions, the mass fraction of water used in the calculation should be much higher. This means that  $T_\alpha$ , as predicted by the Fox equation, is much lower than 0°C. As a result, the saturated polymer should be above all three of its transitions in the experimental temperature window shown in Figure 4.1.4. However, although the presence of water has lowered the value of the storage modulus by half an

order of magnitude, it seems that the material is still below the  $\alpha$  transition and it does not seem that the transition had taken place between 20°C and 90°C. If the  $\alpha$  transition is due to the relaxation of the matrix, the  $T_g$  suppression is not expected to be very significant because of the incompatibility of the PTFE backbone and water molecules. Some degree of plasticization would still occur: small suppression of the storage modulus and a small shift in the position of the  $\tan \delta$  to a lower temperature are to be expected, but the transition would not, most likely, be visible between 20°C and 90°C.

The discussion above seems to indicate that the  $\alpha$  relaxation is due to the matrix relaxation; however, one more argument should be taken into the consideration. In the study conducted by Fujimura *et al*<sup>33, 52</sup>, it was found that Nafion<sup>®</sup> membranes contain about 12 wt% of crystallinity. The crystallinity might be able to restrict the suppression of the storage modulus by hindering the movement of the polymeric chains.

Whether the  $\alpha$  transition is due to the matrix relaxation or to the relaxation of the ionic regions might still be arguable; however, there is no doubt that the presence of water has a detrimental effect on the mechanical properties of the  $\alpha$  region. With this in mind, the following conclusion can be drawn from the water plasticization experiments: the water plasticization softens Nafion<sup>®</sup> membranes as evidenced by the suppression of the storage modulus of the material. This is an important point, since it demonstrates that in order to accurately predict the mechanical behavior of the Nafion<sup>®</sup> membranes in the conditions of saturation and high temperature (or in other words in the conditions at which they are actually utilized), the mechanical testing should be performed on the saturated membranes as opposed to the conventional testing of the dry form of Nafion<sup>®</sup>.

## ***5.2 Diffusion Properties of Nafion<sup>®</sup> membranes***

Let us now consider the diffusion properties of Nafion<sup>®</sup> membranes. It was determined that the maximum water uptake of the virgin Nafion<sup>®</sup> membranes is 24.4±1.0 wt% (Figure 4.6.1). It compares well with the values found in the literature: Duplessix *et*

*al*<sup>32</sup> report a value of 20 wt%, Hashimoto *et al*<sup>33</sup> of 32 wt%, and Cappadonia *et al*<sup>35</sup> of 20-25 wt% (Table 2.6.1).

The results of the study examining the effect of drying the membranes in the oven agree with the results of the similar study conducted by Zawodzinski *et al*<sup>26</sup>. In both cases the samples that have been exposed to the elevated temperatures (160°C in this work and 105°C in the article) achieve a much lower maximum water uptake weight than the samples that have never seen the temperature treatment (Figure 4.6.2). In this study the samples lost about 3% of their weight as the result of drying. After the immersion in DI water, the samples that have been dried in the oven gained 15-16 wt% as opposed to 24 wt% gained by the virgin membranes. Zawodzinski *et al*<sup>26</sup> concluded that the exposure to elevated temperatures results in the irreversible destruction of the ionic clusters that play a key role in the process of water diffusion of the ionomers.

The results of the water sorption analysis indicate that the maximum water uptake of Nafion<sup>®</sup> membrane from the vapor phase is about 10 wt% (Figure 4.8.1) and this process follows a Fickian type of behavior for initial 7 wt% water gain as illustrated by the linear region of the plot of normalized mass as a function of time<sup>1/2</sup> in Figure 5.2.1. More precisely, at initial times, the water sorption follows pseudo-Fickian type of behavior, since the log-log plot of  $M_t/M_e$  as a function of time  $t$  (Figure 5.2.2) has a slope of  $n=0.66$ .

Using equation 2.6.3, the diffusion coefficient for vapor-phase water sorption by Nafion<sup>®</sup> membranes was found to be  $(2.8 \pm 0.4) \times 10^{-8}$  cm<sup>2</sup>/s. The value is consistent with the diffusion coefficient value of  $2 \times 10^{-8}$  cm<sup>2</sup>/s observed for the water sorption from vapor phase by Takamatsu<sup>37</sup> and is two orders of magnitude smaller than the value for the liquid phase diffusion coefficient of  $2.6 \times 10^{-6}$  cm<sup>2</sup>/s reported by Yeo and Eisenberg<sup>12</sup> (Table 2.6.1). According to Morris and Sun<sup>36</sup>, the disparity between the diffusion coefficients for sorption from liquid and vapor phase is due to a two-phase structure of Nafion<sup>®</sup> membranes (hydrophilic ionic clusters and hydrophobic matrix). Immersion in water induces swelling and, as result, enhances the diffusion. Of course, this also means that the diffusion coefficients discussed above are approximated values, since the assumption made in the derivation of equation 2.6.3 is that the diffusion coefficients are independent of the concentration. If swelling of the membrane is taken into account,

several issues should be addressed. First, the change in the membrane thickness and the overall volume should be taken into account; and second, the rates of water diffusion through a swelled membrane are higher than those of water diffusion through a dry membrane and hence, are dependent on the water concentration. With this in mind, the diffusion coefficients calculated above should be treated not as absolute but rather as relative values used for the comparison of diffusion between different types of membranes.

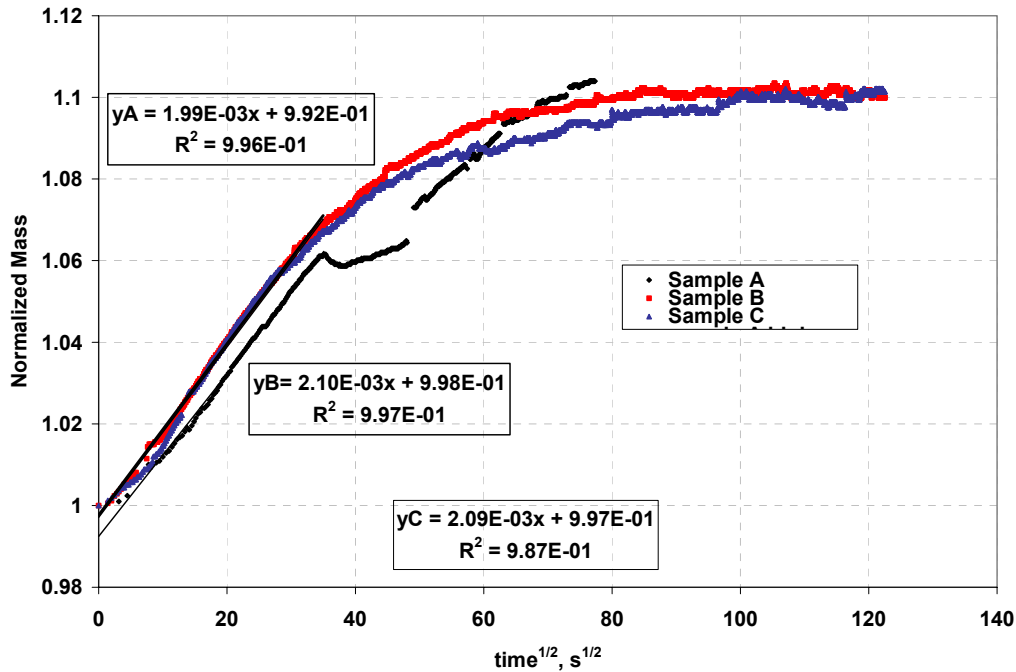
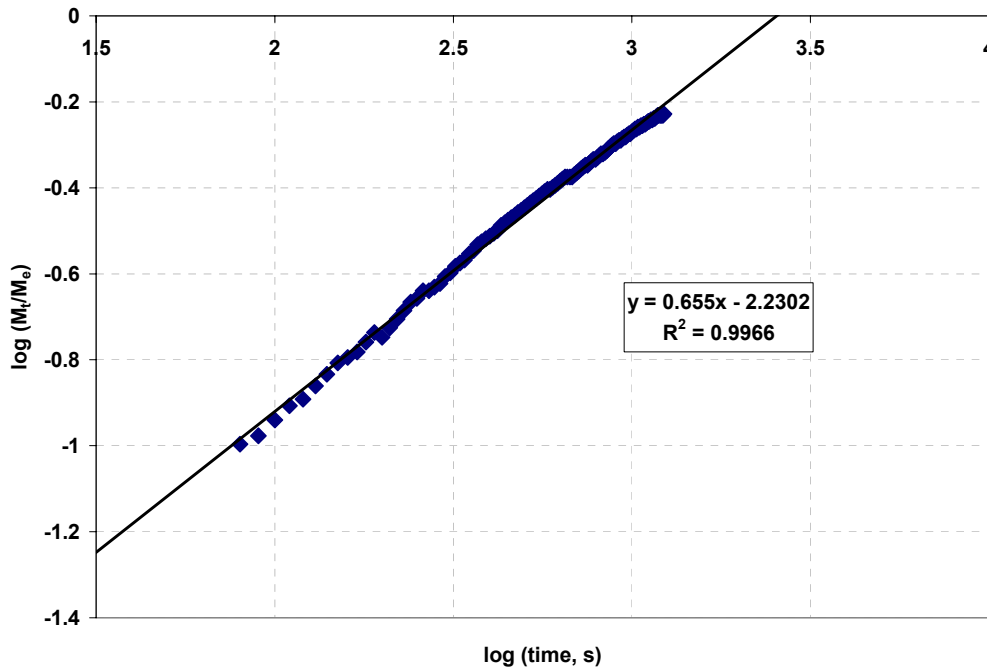


Figure 5.2.1 Vapor Phase Sorption Behavior of Nafion® Membranes

The results of the water desorption analysis indicate that Nafion® membranes retain  $79.5 \pm 0.7$  % of the original (membrane plus water) weight when they are dried from the saturated state at  $10 \pm 2$  %RH (Figure 4.10.1). The plots of the normalized mass as a function of the drying time of Nafion® membranes are linear up to 500s and have an average slope of  $(-3.4 \pm 0.2) \times 10^{-4} \text{ s}^{-1}$  (Figure 5.2.3). The membranes reach an equilibrium moisture content in a much shorter time during the desorption process than they do during sorption (1700s vs. 8000s), which indicates that the effective rate of

drying is much faster than that of the vapor phase sorption. According to Krtil *et al*<sup>53</sup>, the differences in sorption and desorption rates arise from the initial swollen state of the membrane during desorption process. If the size of the ionic clusters increases with an increase in a degree of swelling, the saturated membranes will have higher rates of water diffusion in and out of the material than the dry samples. This will result in higher diffusion coefficients for water desorption compared to the ones for water sorption.



**Figure 5.2.2 Log-Log Plot of Initial 1,225 s of Nafion<sup>®</sup> Sorption Data (Sample A)**

The desorption process does not follow the Fickian type of diffusion. The shape of the desorption curve seems to imply that drying is not limited by diffusion and is controlled by other mechanisms. The matters are highly complicated by the fact that, as the material loses water, it might be changing from the rubbery to a glassy state. As a result, diffusion coefficients for the drying process were not calculated; however, the values of the slopes of desorption curves can be successfully used to compare the relative rates of desorption for different types of membranes.

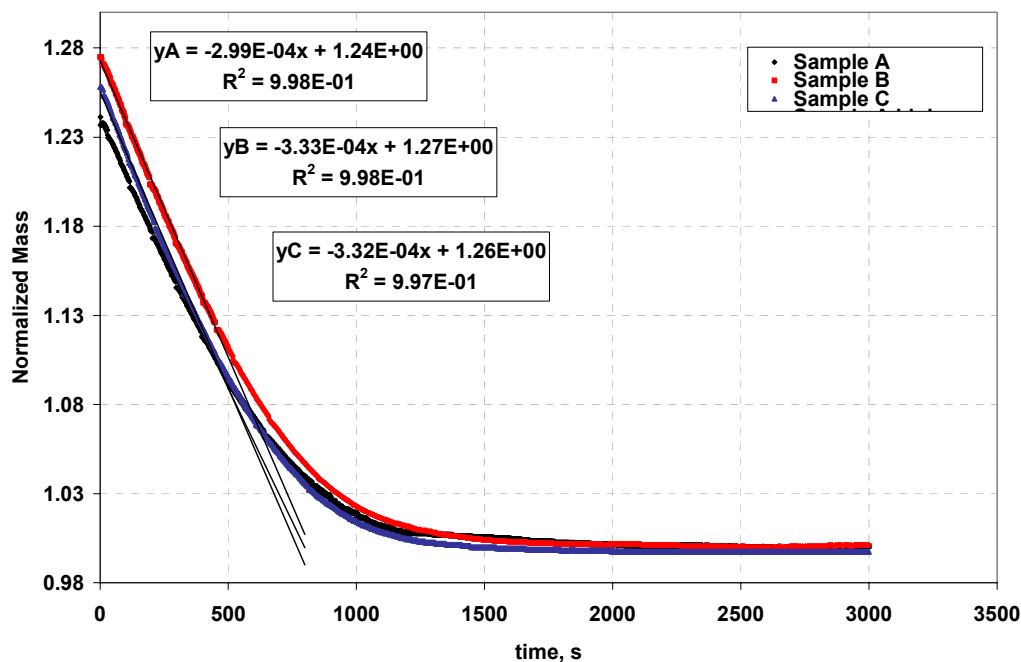


Figure 5.2.3 Water Desorption Behavior of Nafion<sup>®</sup> Membranes

### 5.3 Pre-treatment of Nafion<sup>®</sup> Membranes

The effect of the pre-treatment of Nafion<sup>®</sup> membranes was investigated by measuring the mechanical properties of the films pre-treated by four methods listed in Table 3.1.2 and comparing them to those of the untreated samples. As evidenced by the results presented in Table 4.1.1 and Figure 4.1.7, the position of the  $\tan \delta$  peak shifted significantly to higher temperatures with increase in severity of the treatment procedure, indicating a drastic increase in the glass transition temperatures of the membranes. It is clear that the treatment procedures instigate the changes in the morphology of the membranes that, as will be shown, are not the result of aging as was assumed previously (Section 2.5). If aging was responsible for the shift of the  $\tan \delta$  peak to a higher temperature, this process would be reversible: the  $T_g$  of the material would shift to that of

the untreated samples if the system was given the amount of kinetic energy sufficient for chain rearrangement. As demonstrated in Figure 4.1.8, this is not the case here: the  $T_g$  of the treated system seems to be independent of the thermal history of the polymer and, hence, the increase in  $T_g$  is not due to the process of physical aging.

It was observed by Zawodzinski *et al.*,<sup>27</sup> that treatment of the membranes improves their diffusion properties by facilitating growth of the ionic clusters which, in turn, leads to the increase in the water content of Nafion<sup>®</sup> materials. The results of the current study support these findings: the ionic clusters can be viewed as kinds of physical crosslinks that restrict the movement of the polymeric chains. An increase in the amount and/or the dimensions of the clusters will result in the observed shift of the glass transition to a higher temperature.

In order to rule out some of the other variables that could be responsible for enhanced diffusion as a result of the Nafion<sup>®</sup> pre-treatment, two additional experiments were performed. First, the thermal degradation behavior of the treated and untreated samples were compared (Figure 4.3.3) and found to be independent of the material treatment. Second, the surfaces of the treated membranes were examined for signs of possible oxidative cracking due to boiling the materials in DI water and H<sub>2</sub>O<sub>2</sub>. In theory, the cracking could have increased the surface area of the membrane and decreased the water molecule diffusion path resulting in the increase in the values of the effective water diffusion coefficients reported by Zawodzinski *et al.*<sup>27</sup> However, no cracking was observed and the surfaces of untreated and treated samples possessed identical topology (Figure 4.12.1, Figure 4.12.2 and Figure 4.12.3).

Based on the literature review and discussion presented above, it was concluded that the growth of ionic clusters provides an equitable explanation of the effects of pre-treatment of the Nafion<sup>®</sup> membranes that have been observed in this work as well as reported by other investigators<sup>27</sup>.

## 5.4 Aging of Nafion<sup>®</sup> Membranes

It was hypothesized in the background section that aging of Nafion<sup>®</sup> membranes will decrease the free volume of the material system leading to increase in the glass transition temperature and decrease in the values of the water diffusion coefficients. It was expected that the dependence between aging time and the change in the glass transition temperature would be of Arrhenius type (linear plots of  $\ln(\text{time})$  as a function of  $1/T_g$ ) and, as result, it would be possible to calculate the activation energies for aging.

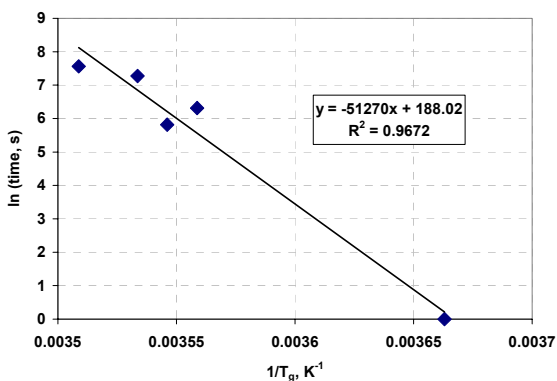


Figure 5.4.1 90°C Aging Data for Nafion<sup>®</sup> Membranes (Experiment 1)

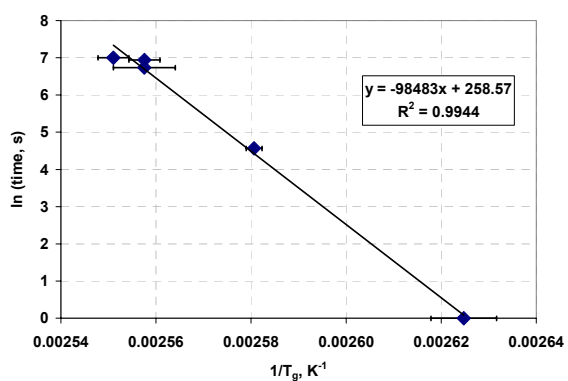


Figure 5.4.2 90°C Aging Data for Nafion<sup>®</sup> Membranes (Experiment 3)

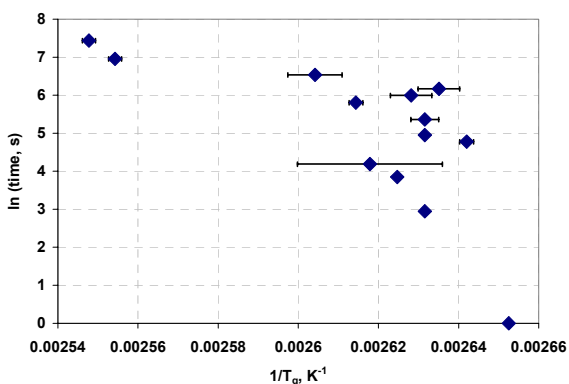


Figure 5.4.3 90°C Aging Data for Nafion<sup>®</sup> Membranes (Experiment 2)

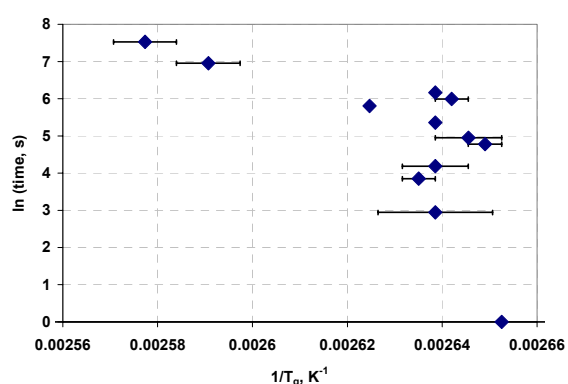


Figure 5.4.4 65°C Aging Data for Nafion<sup>®</sup> Membranes

The aging of Nafion<sup>®</sup> membranes was carried out in DI water at 90°C and 65°C and, in fact, an increase in the glass transition temperature with aging time was generally

detected. However, when the data were plotted in the form of  $\ln(\text{time})$  vs.  $1/T_g$ , several surprising trends were observed. While the data for aging of Nafion<sup>®</sup> membranes at 90°C for experiments 1 and 3 seem to point to an Arrhenius type of dependence between the aging time and the  $T_g$  of the material (Figure 5.4.1 and Figure 5.4.2), the data for experiment 2 and that for aging of Nafion<sup>®</sup> at 65°C at first glance exhibit an unusual behavior (Figure 5.4.3 and Figure 5.4.4).

The results of the DMA scans, in which the membranes aged for 60 and 80 days (experiment 1) were annealed for 1 hr at the temperatures above their respective  $T_g$ s, are also puzzling (Figure 4.1.12 and Figure 4.1.13). The glass transition temperature of the virgin membrane in the experiment 1 was measured at 119°C. It was expected that on the second heat the  $T_g$ s of the aged samples would be measured at 119°C as well, since the annealing at the temperatures 30°C above the glass transition should have been sufficient to erase all thermal history of these polymers. Although the movement of  $\tan \delta$  peaks down in temperature was observed in both cases, the new  $T_g$ s were still 5°C higher than the  $T_g$  of the virgin membrane. This suggests that the changes in the material structure, that took place as a result of “aging”, are irreversible. The assumption in the last argument is that during the cooling step the sample reached the conformational configuration equivalent to that of the virgin material. The validity of this assumption was verified by annealing the virgin Nafion<sup>®</sup> sample 30°C above its transition temperature for 1hr, cooling it at 2°C/min and then heating it back up at 2°C/min (Figure 4.1.14). Since the  $T_g$  of the membrane on the second heating was the same as on the first one, it was concluded that the described cycling results in the return of the membrane to the original conformation of the virgin material.

The plots of water vapor phase sorption and water desorption data of aged Nafion<sup>®</sup> membranes showed the same characteristic features as those of the virgin membranes (Figure 5.4.5 and Figure 5.4.6); however, the detailed examination of both sets of sorption and desorption data did not yield the anticipated results. Although the sorption diffusion coefficient and the slope of desorption curve for initial time period for the aged Nafion<sup>®</sup> membrane were, as expected, lower than the ones determined for the virgin membrane, the maximum moisture uptake was slightly higher for the aged membrane than for the virgin Nafion<sup>®</sup> (Table 5.4.1).

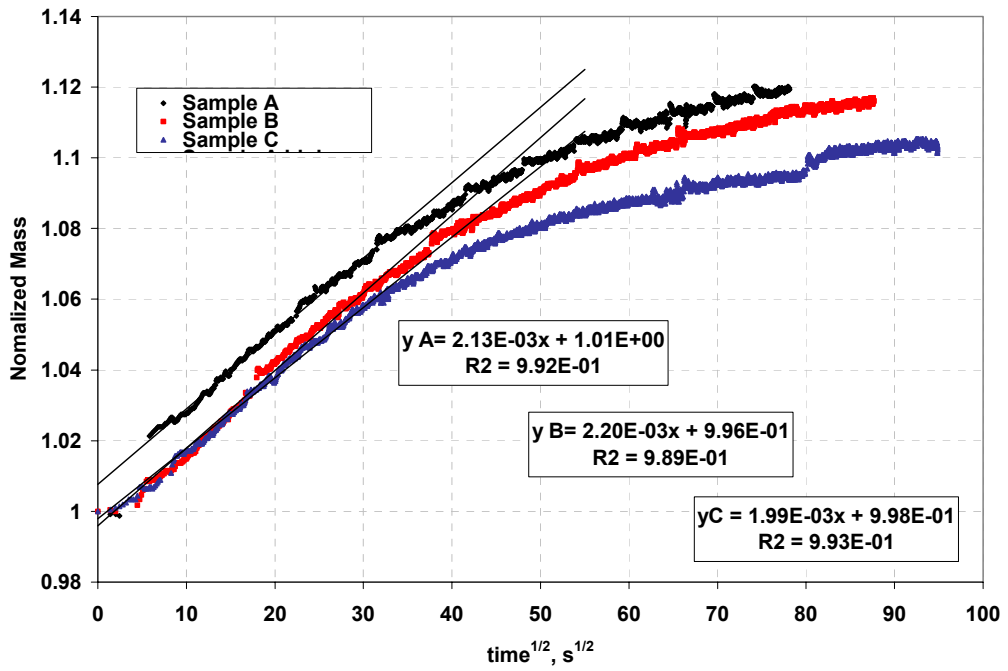


Figure 5.4.5 Vapor Phase Sorption Behavior of Nafion® Membranes Aged at 65°C

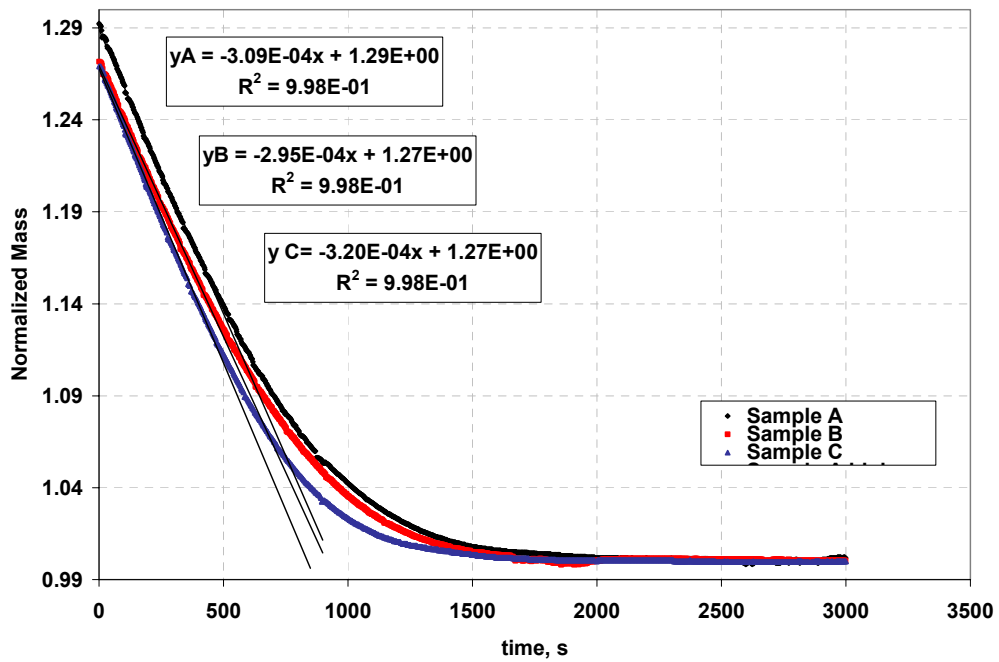


Figure 5.4.6 Water Desorption Behavior of Nafion® Membranes Aged at 65°C

**Table 5.4.1 Diffusion Properties of Virgin and Aged Nafion<sup>®</sup> Membranes**

	<b>Virgin</b>	<b>Aged at 65°C</b>
Sorption	$(2.8 \pm 0.4) \times 10^{-8} \text{ cm}^2/\text{s}$	$(2.5 \pm 0.2) \times 10^{-8} \text{ cm}^2/\text{s}$
Desorption	$(-3.4 \pm 0.2) \times 10^{-4} \text{ s}^{-1}$	$(-3.1 \pm 0.1) \times 10^{-4} \text{ s}^{-1}$
Maximum Uptake	24.4 ± 2.1 wt%	26.1 ± 1.0 wt%

It was predicted that a decrease in the free volume brought about by aging would significantly hinder the mobility of the water molecules. However, data analysis indicates that the differences in the diffusion between the virgin and aged membranes are not substantial and, that, based on the evidence presented, it is impossible to determine unequivocally the effect of aging on the diffusion properties of Nafion<sup>®</sup>. If the sorption, desorption and moisture uptake of the membranes aged at 90°C were measured, it is conceivable that the diffusion properties of the material would show improvement as a result of “aging”. This is corroborated by the increase in the diffusion coefficients and moisture content of the membranes as a result of the pre-treatment procedures discussed in Section 5.3. Since the boiling temperature of water is just 10°C above the aging temperature of the membranes, it is reasonable to conclude that “aging” could have similar effects on the diffusion properties, as did the process of boiling the materials as a part of the pre-treatment procedure.

In light of the discussion above, it is clear that the changes in the properties of Nafion<sup>®</sup>, instigated by storing the membranes in DI water at elevated temperatures, cannot be explicitly described by the process of physical aging. A closer examination of Figure 5.4.3 and Figure 5.4.4 revealed the possibility of existence of two distinct processes indicated by two linear regions of the  $\ln(\text{time})$  vs.  $1/T_g$  plots with some kind of transition in between. It is also conceivable that an apparent linearity of the plots presented in Figure 5.4.1 and Figure 5.4.2 resulted from the fact that the data sets for the experiments 1 and 3 were incomplete because of the unavailability of the data points at the intermediate time intervals. In order to verify this assumption, the data for all three 90°C aging experiments were plotted on a single graph by normalizing each data point with the respect to the  $T_g$  of the virgin membrane for each set of data (Figure 5.4.7). The resultant plot clearly shows two distinct linear regions with a transition region indicated

by a gray box. The same characteristic plot can also be obtained by replotting the data for Nafion<sup>®</sup> membranes aged at 65°C (Figure 5.4.8).

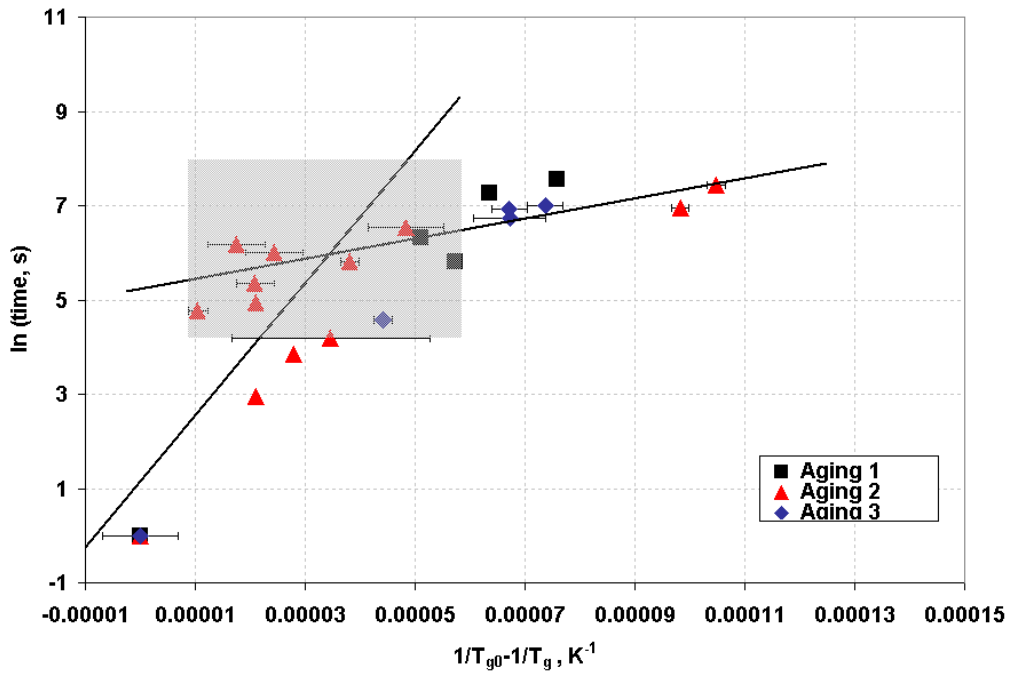


Figure 5.4.7 Results of the Nafion<sup>®</sup> Aging Experiments (90°C)

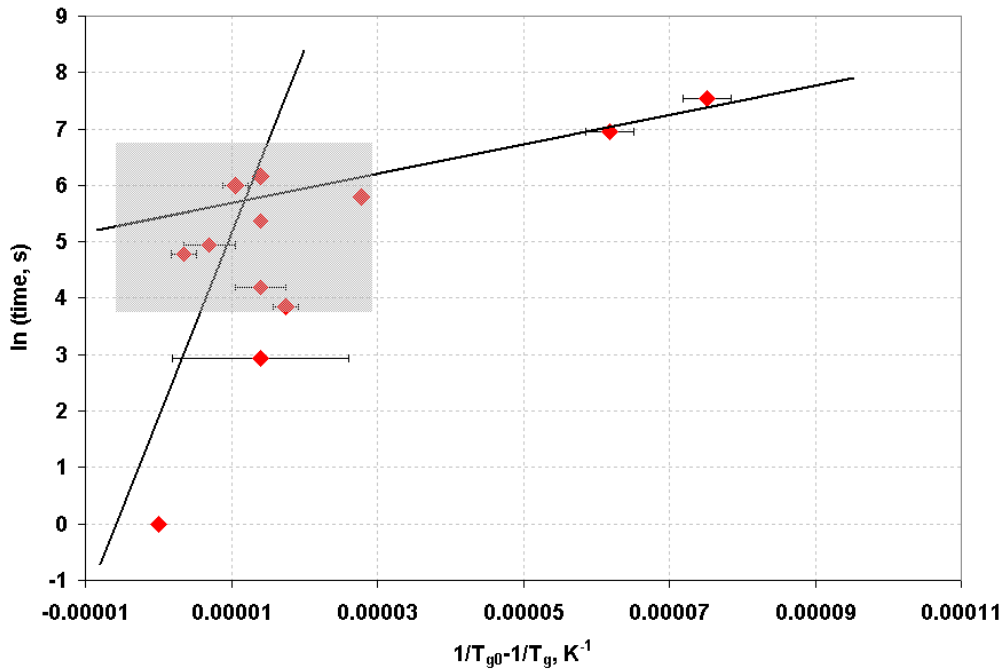


Figure 5.4.8 Results of the Nafion<sup>®</sup> Aging Experiments (65°C)

Two distinct linear regions of the plots in Figure 5.4.7 and Figure 5.4.8 indicate the existence of two competing mechanisms that are responsible for changes in the properties of the membranes as a result of “aging”. One might be classically defined physical aging and the other one might be the growth of the ionic clusters. Both would result in the observed increase in the glass transition temperature; however, only the one due to physical aging is reversible. Aging would diminish the values of the diffusion coefficient, while growth of the ionic clusters would enhance them. If the results presented above are reexamined, it is clear that both mechanisms might in fact be present in this case. The first proof, the shapes of the plots of  $\ln(\text{time})$  as a function of  $1/T_g$ , has been already discussed. The second proof is in a seemingly strange response of the annealed aged samples: the  $T_g$  shifted to a lower temperature due to physical aging, but the process was incomplete because of the irreversibility due to the ionic clusters growth. The third proof is in the analysis of the diffusion properties of the aged specimens: there is no clear decrease in the properties due to aging, but at the same time, there is no clear increase due to the growth of the ionic clusters. It is entirely possible that the effects of the aging and the growth of the clusters on the diffusion properties counteract each other.

It is apparent that further investigation is required in order to make firm conclusions about the exact nature of effects that “aging” of the Nafion<sup>®</sup> in DI water at elevated temperatures has on the properties of the membranes and the proposed experiments will be discussed in Chapter 7. However, the preliminary results strongly suggest that the two competing mechanisms in place are the process of physical aging and the growth of the ionic clusters.

## ***5.5 Structure, Thermal Degradation and Plasticization of Dais<sup>®</sup> Membranes***

The DMA spectrum of 30% sulfonated Dais<sup>®</sup> membrane (Figure 4.2.1) possesses two well-defined transitions characterized by the peaks in  $\tan \delta$  curve at  $-54^\circ\text{C}$  and  $145^\circ\text{C}$  and the modulus drops in the temperature regions between  $-80^\circ\text{C}$  and  $0^\circ\text{C}$  and between

80°C and 170°C. At the first glance, the Dais<sup>®</sup> DMA spectrum looks similar to the one for Nafion<sup>®</sup> membrane discussed in Section 5.1: both have two tan  $\delta$  peaks corresponding to two distinct transitions with a substantial modulus drops associated with each of them. However, the lower tan  $\delta$  peak in Nafion<sup>®</sup> is much smaller in height and is significantly broader than the lower tan  $\delta$  peak in Dais<sup>®</sup>. It is clear that the latter is due to a primary transition and not to a subtransition as it was in the case of Nafion<sup>®</sup>. This observation is consistent with the theoretical concepts presented in Section 2.2, which stated that Dais<sup>®</sup> membranes should have two distinct transitions: one, associated with a sulfonated styrene block and another one associated with ethylene/butylene block.

The position of the ethylene/butylene transition can be predicted by the Fox equation (Equation 2.2.1) by utilizing the  $T_g$ s of the polyethylene and polybutylene. The  $T_g$  of polyethylene is in the range of  $-103^\circ\text{C}$  to  $-133^\circ\text{C}$ <sup>54</sup> and  $T_g$  of polybutylene is in the range of  $-17^\circ\text{C}$  to  $-25^\circ\text{C}$ <sup>55</sup>. Assuming that the number of ethylene and butylene units is the same and the  $T_g$ s of polybutylene and polyethylene are the averages of the reported ranges ( $-21^\circ\text{C}$  and  $-118^\circ\text{C}$  respectively), the  $T_g$  of ethylene/butylene block, taking into consideration the molecular weights of the components, is expected to be around  $-64^\circ\text{C}$ :

$$\frac{1}{T_g} = \frac{28 \text{ g/mol}}{28 \text{ g/mol} + 56 \text{ g/mol}} \left/ 155^\circ\text{K} \right. + \frac{56 \text{ g/mol}}{28 \text{ g/mol} + 56 \text{ g/mol}} \left/ 252^\circ\text{K} \right. = \frac{1}{209^\circ\text{K}} = \frac{1}{-64^\circ\text{C}}$$

The value of  $-54^\circ\text{C}$ , measured for the  $T_g$  of ethylene/butylene block is fairly close to the estimated value of  $-64^\circ\text{C}$ . Several factors could be responsible for the slight discrepancy. First, the calculated  $T_g$  is based on the assumptions stated above which might not be entirely accurate, second, the  $T_g$ s measured by different techniques are not identical and it is unknown how the  $T_g$  values used in the calculations were found, third, the  $T_g$  is not an equilibrium property, and fourth, the Fox equation itself is based on a number of the assumptions and should be used only for obtaining relative values of the glass transition temperatures.

The tan  $\delta$  peak at  $145^\circ\text{C}$  in the spectrum of 30% sulfonated Dais<sup>®</sup> corresponds to the relaxation of the sulfonated styrene block. While the position of the lower tan  $\delta$  peak is the same for 30% and 60% sulfonated Dais<sup>®</sup>, the upper tan  $\delta$  peak is clearly dependent

on the degree of sulfonation, shifting from 145°C for 30% sulfonation to 220°C for 60% sulfonation (Figure 4.2.1 and Figure 4.2.2). The increase in the  $T_g$  of the polymer as a function of sulfonation was also observed by Weiss *et al*<sup>18</sup> for 5.2% and 11.9% sulfonated SEBS and by Hara *et al*<sup>43</sup> for 0% to 8.5% sulfonated polystyrene (Section 2.7). The effect was attributed to the formation of the ionic clusters, which act as physical crosslinks by reducing the mobility of the polymeric chains, thereby increasing the glass transition temperature.

Results from the thermal degradation studies of Dais<sup>®</sup> membranes in air (Figure 4.4.1 and Figure 4.4.3) and N<sub>2</sub> (Figure 4.4.2 and Figure 4.4.4) only partially agree with the results reported by Weiss *et al*<sup>18</sup> (Section 2.8). While the membranes were found to be stable up to 400°C in both studies, the increase in the stability of the membranes with the increase in the sulfonation levels observed by Weiss *et al*<sup>18</sup>, was not seen here. On the contrary, the major peak of the derivative weight % curve measured at 469°C in air and at 476°C in N<sub>2</sub> for 30% sulfonated membrane was observed at the lower temperature (451°C in air and at 468°C in N<sub>2</sub>) for 60% sulfonated membrane. However, these differences might not be that significant due to the problem with the resolution of the TGA unit addressed in Section 5.1.

As was stated in Section 2.4, one of the goals of this thesis was the construction of the mastercurve for Dais<sup>®</sup> material. The mastercurve for 60% sulfonated Dais<sup>®</sup> membrane (Figure 5.5.2) was created using the frequency shifts DMA data (Figure 4.2.14) and following the procedure outlined in Section 3.2. The isothermal frequency data prior to the shifting are shown in Figure 5.5.1. The shift factor plot generated from Figure 5.5.2 is shown in Figure 5.5.3. Both transitions corresponding to the relaxations of ethylene/butylene and sulfonated styrene blocks are clearly seen in both the mastercurve (two drops of storage modulus) and the shift factor plot (regions **A** and **B**). Region **A** in Figure 5.5.3 corresponds to the ethylene/butylene transition, because it was created by using the shift factors obtained by shifting the isothermal frequency data in the temperature range from -80°C to -25°C (the temperature region in which the ethylene/butylene relaxation occurs). Using the same arguments, region **B** is assigned to the relaxation of sulfonated styrene block. Since the two transitions are far from each

other on the temperature scale, region T, an intermediate region, is present between the relaxations of the two types of copolymer blocks.

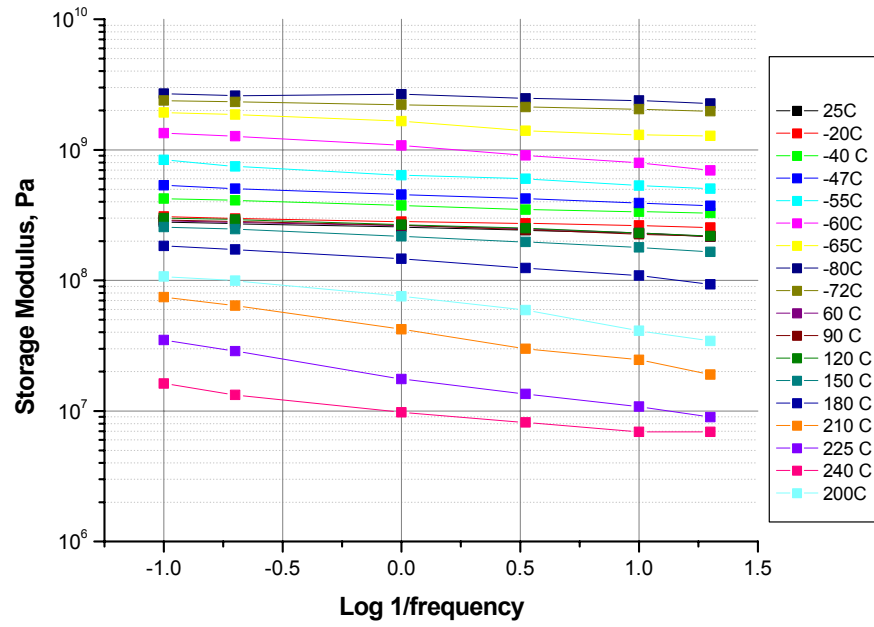


Figure 5.5.1 Isothermal Frequency Data for 60% Sulfonated Dais® Membrane

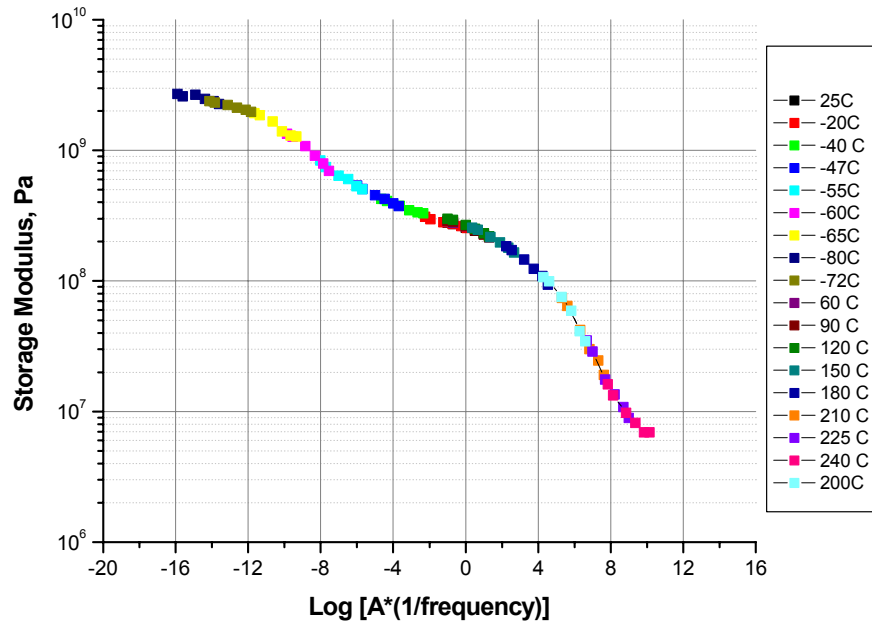
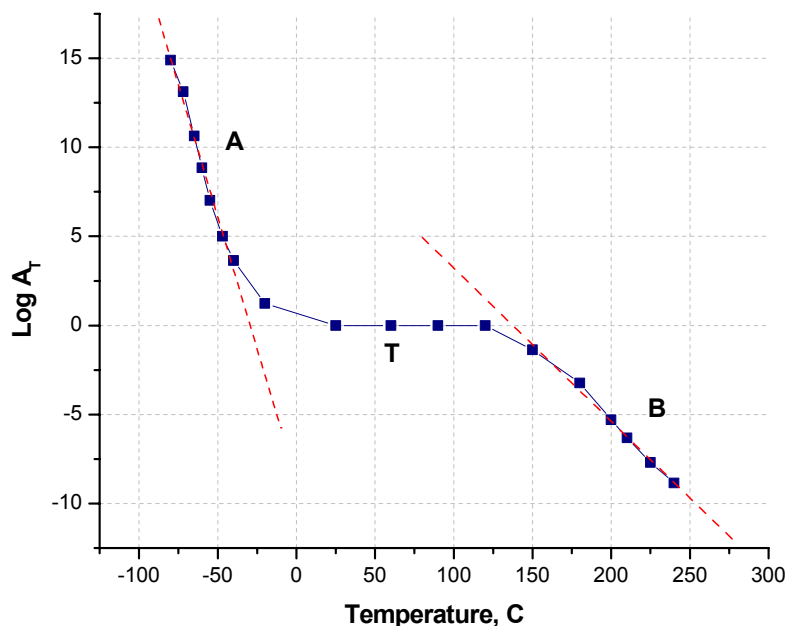


Figure 5.5.2 Mastercurve of 60% Sulfonated Dais® Membrane



**Figure 5.5.3 Shift Factor Plot for 60% Sulfonated Dais<sup>®</sup> Membrane (A: Relaxation of Ethylene/Butylene Block, T: Intermediate Transition Region, B: Relaxation of Styrene Block)**

The effect of water plasticization on the mechanical properties of 30% sulfonated Dais<sup>®</sup> membrane is shown in Figure 4.2.5. The decrease of the storage modulus in the glassy region from  $1.4 \pm 10^8$  Pa for the dry membrane to  $3.0 \pm 10^7$  Pa for the saturated sample is indicative of the softening of the material as result of the water plasticization. The effect can also be observed by comparing the  $\tan \delta$  curves for two samples. While the dry sample has a well-pronounced peak at 140°C, the  $\tan \delta$  peak of the saturated Dais<sup>®</sup> is very broad and small in height due to water dampening. The effect of water plasticization on the 60% sulfonated Dais membranes is even more detrimental, as evidenced by the DMA scan of the saturated membrane at 10Hz shown in Figure 4.2.8. The  $T_g$  of the membrane is suppressed below room temperature and, unless the sample is scanned at higher frequencies (which results in an increase in the material stiffness), the membrane loses its structural integrity and falls apart upon handling. The higher degree of the plasticization, demonstrated by 60% sulfonated membrane, is an expected phenomenon. Since the number of ionic clusters in 60% sulfonated Dais<sup>®</sup> is much higher than that in 30% sulfonated membrane, the material is highly compatible with the water

molecules resulting in the higher degree of interaction between the polymeric material and water.

The effect of the scanning rate on the position of the glass transition of saturated 30% sulfonated Dais<sup>®</sup> membrane is shown in Figure 4.2.6. The results follow the expected trends, since it is anticipated that, as the heating rate is decreased, the polymeric chains will have longer time available for the spatial reconfiguration. As a result, the onset of the large scale motions will take place at a lower temperature compared with that of the sample scanned at a higher rate; therefore, the  $T_g$ , indicated in Figure 4.2.6 by the inflection point in the storage modulus curve, will be lower.

The unusual increase in the  $T_g$  of 30% (Figure 4.2.9 and Figure 4.2.10) and 60% (Figure 4.2.11, Figure 4.2.12 and Figure 4.2.13) sulfonated Dais<sup>®</sup> membranes described in Section 4.2 is puzzling. Several additional experiments were performed in order to understand the nature of the processes underlying this observation. An increase in the  $T_g$  signifies a decrease in the free volume of the system. Under certain conditions, the sample annealed at a temperatures above its  $T_g$  and then cooled, can achieve a lower free volume content than the original material. If the cooling step insures that the chains acquire longer times for rearrangement than was allowed during the manufacturing process, a structure closer to equilibrium than that of the original material would form. Another possible source of free volume reduction can be the removal of bound water present in the ionic clusters. Although the bound water can still be a part of the material system at the temperatures above 100°C, its boiling point, and might be responsible for the changes seen in the 30% sulfonated Dais<sup>®</sup>, it is highly unlikely that it will be a reason for the 30°C difference in the glass transition temperatures between the 60% sulfonated Dais<sup>®</sup> membrane annealed for 1min as opposed to the one annealed for 1hr at 235°C. In order to explore whether the slow scanning rate results in the chemical degradation of the material due to overexposure to elevated temperatures, the TGA traces of the 30% sulfonated Dais<sup>®</sup> membranes heated at 2°C/min (scanning DMA rate) and 20°C/min (Figure 4.4.8 and Figure 4.4.9) were compared. If anything, the results indicate that the decrease in the heating rate improves the thermal stability of the material, giving rise to a 27°C shift of the peak in derivative weight % curve to a higher temperature. The FTIR analysis of the 30% sulfonated Dais<sup>®</sup> membranes annealed at 160°C for up to 1hr and of

the 60% sulfonated membranes annealed at 225°C for up to 1 hr, does not offer any evidence of chemical decomposition. Although the intensity of the peaks in the 800-1300 $\text{cm}^{-1}$  wavelength region decreased, especially in the case of 60% sulfonated membranes, the disappearance of the old peaks or the formation of new peaks, indicative of the rupture or the formation of chemical bonds, were not observed. Based on the arguments presented above, the exact nature of the drastic increase in the  $T_g$ s of the Dais<sup>®</sup> membranes as a result of the annealing is unclear and further experiments, which will be discussed in Chapter 7, are required in order to draw any firm conclusions.

### 5.6 Diffusion Properties of Dais<sup>®</sup> Membranes

The character of the diffusion properties of Nafion<sup>®</sup> and Dais<sup>®</sup> membranes is very similar, since both materials are sulfonated ionomers and their water sorption and desorption processes strongly depend on the amount and size of the ionic clusters formed in the material. This section, therefore, will be frequently referenced to Section 5.2 where the diffusion properties of Nafion<sup>®</sup> membranes were discussed. For comparison, the results of the water sorption and desorption properties of Nafion<sup>®</sup> and Dais<sup>®</sup> membranes are summarized in Table 2.6.1.

**Table 5.6.1 Diffusion Properties of Nafion<sup>®</sup> and Dais<sup>®</sup> Membranes**

	<b>Nafion<sup>®</sup></b>	<b>30% Sulfonated Dais<sup>®</sup></b>	<b>60% Sulfonated Dais<sup>®</sup></b>
Sorption	$(2.8 \pm 0.4) \times 10^{-8} \text{ cm}^2/\text{s}$	$(2.9 \pm 0.4) \times 10^{-8} \text{ cm}^2/\text{s}$	$(8.5 \pm 0.5) \times 10^{-9} \text{ cm}^2/\text{s}$
Desorption	$(-3.4 \pm 0.2) \times 10^{-4} \text{ s}^{-1}$	$(-4.2 \pm 0.04) \times 10^{-4} \text{ s}^{-1}$	$(-1.3 \pm 0.05) \times 10^{-3} \text{ s}^{-1}$
Maximum Uptake	24.4 $\pm$ 2.1 wt%	27.2 $\pm$ 0.2 wt%	190.2 $\pm$ 3.2 wt%

The maximum water uptake of  $27.2 \pm 0.2$  wt% for 30% sulfonated Dais<sup>®</sup> is comparable to  $24.4 \pm 1.0$  wt% determined for Nafion<sup>®</sup> material. A drastic increase with the increase in the sulfonation is observed when the water uptake of 30% ( $27.2 \pm 3.2$  wt%) and 60% ( $190.2 \pm 3.2$  wt%) sulfonated Dais<sup>®</sup> are compared (Figure 4.7.1 and Table 5.6.1). This trend; however, is not surprising, since 60% sulfonated Dais<sup>®</sup> has a higher percentage of the polar ionic clusters that are directly involved in the water absorption and swelling mechanisms.

The results of the vapor phase water sorption analysis indicate that the maximum amounts of moisture absorbed by the Dais<sup>®</sup> membranes are  $9.3 \pm 0.6$  wt% for 30% sulfonated material and  $25.0 \pm 1.0$  wt% for 60% sulfonated membranes. As a comparison, C.Edmondson *et al.*,<sup>38</sup> measured the maximum water uptake from the vapor phase at 100% RH for 60% sulfonated SEBS at 19 wt%.

The sorption processes for 30% and 60% sulfonated Dais<sup>®</sup> membranes follow the pseudo-Fickian type of behavior for initial time period as indicated by a linear log-log plot of  $M_t/M_e$  as a function of time  $t$  (Figure 5.6.1 and Figure 5.6.2) with the slopes of  $n=0.64$  and  $n=0.57$  for 30% and 60% sulfonation respectively.

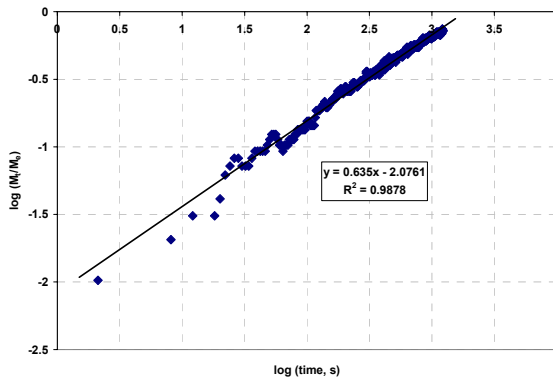


**Figure 5.6.1** Log-Log Plot of Initial 1,225 s of 30% Sulfonated Dais<sup>®</sup> Sorption Data (Sample A)

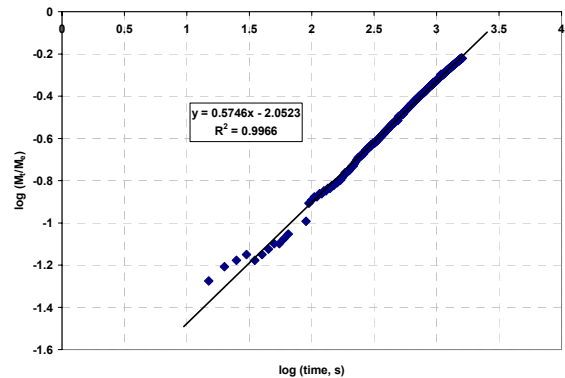


**Figure 5.6.2** Log-Log Plot of Initial 1,225 s of 60% Sulfonated Dais<sup>®</sup> Sorption Data (Sample A)

The diffusion coefficients for vapor phase sorption for Dais<sup>®</sup> membranes were calculated using equation 2.6.3 from the values of the initial slopes of the normalized mass as a function of time<sup>1/2</sup> plots (Figure 5.6.3 and Figure 5.6.4). The values were

found to be  $(2.9 \pm 0.4) \times 10^{-8} \text{ cm}^2/\text{s}$  for 30% sulfonated membranes and  $(8.5 \pm 0.5) \times 10^{-9} \text{ cm}^2/\text{s}$  for 60% sulfonated membranes.

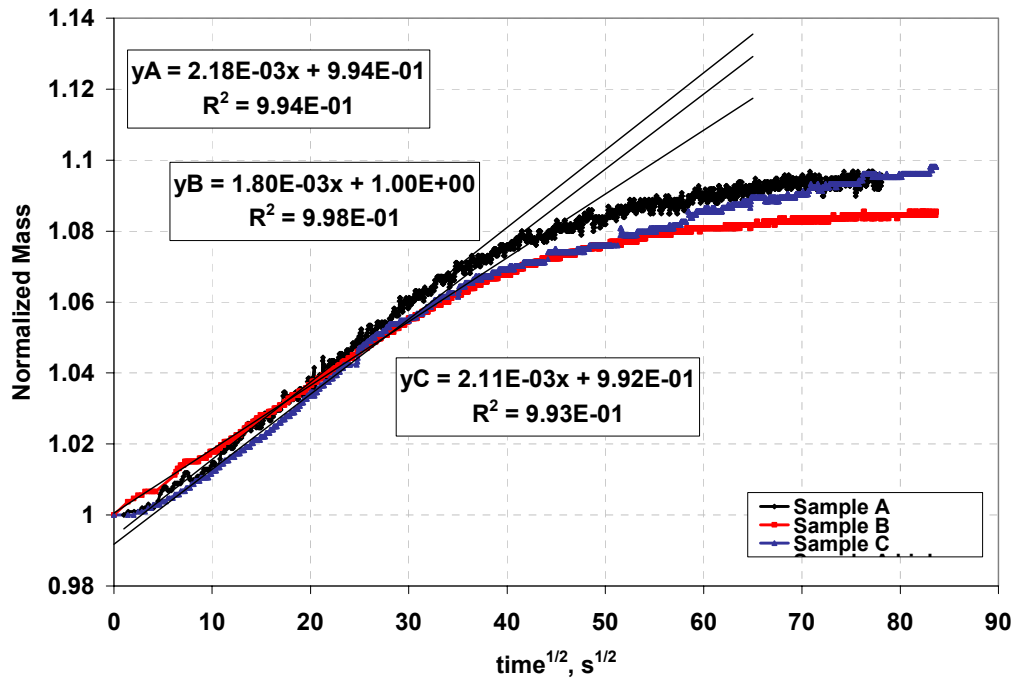


Figure 5.6.3 Vapor Phase Sorption Behavior of 30% Sulfonated Dais® Membrane

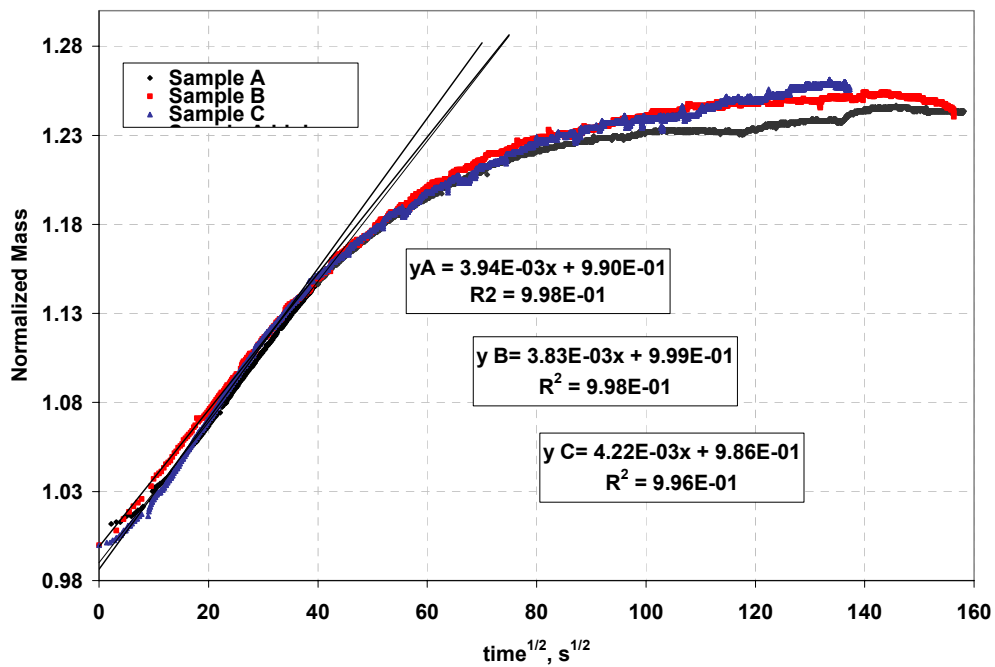


Figure 5.6.4 Vapor Phase Sorption Behavior of 60% Sulfonated Dais® Membrane

The results of the water desorption analysis indicate that 30% sulfonated Dais<sup>®</sup> membranes retain  $77.1 \pm 0.2$  % of the original (membrane plus water) weight and 60% sulfonated Dais<sup>®</sup> membranes retain  $32.7 \pm 0.6$  % of the original (membrane plus water) weight when they are dried from the saturated state at  $10 \pm 2$  %RH (Figure 4.11.1 and Figure 4.11.2). Since the log-log plot of  $M_t/M_e$  as a function of time is not linear, it was concluded that desorption process for Dais<sup>®</sup> membranes does not follow the Fickian type of behavior.

The plots of the normalized mass as a function of the drying time of Dais<sup>®</sup> membranes are linear up to 500 s and have average slopes of  $(-4.2 \pm 0.04) \times 10^{-4} \text{ s}^{-1}$  for 30% sulfonated membranes and  $(-1.3 \pm 0.05) \times 10^{-3} \text{ s}^{-1}$  for 60% sulfonated membranes (Figure 5.6.5 and Figure 5.6.6). The slope for the 60% sulfonated membrane is much higher than the one for 30% sulfonated membrane; however, since the driving forces for desorption and the thickness of the membranes are very different, it is impossible to make conclusions about the dependence of the diffusion coefficients on the sulfonation level of the Dais<sup>®</sup> membranes. As in the case of Nafion<sup>®</sup> membranes, Dais<sup>®</sup> materials reach an equilibrium moisture content in a much shorter time during desorption process than they do during sorption (1,500s vs. 5,000s for 30% Dais<sup>®</sup> and 3,500s vs. 20,000s for 60% Dais<sup>®</sup>), which indicates that the effective rate of drying is much faster than that of the vapor phase sorption (the grounds for this difference and the non-Fickian behavior were discussed in Section 5.2).

The relative magnitudes of the diffusion coefficients for different degrees of sulfonation are surprising. Based on intuition, as well as judging from the values of the initial slopes of the curves in Figure 5.6.3 and Figure 5.6.4, 60% sulfonated samples were expected to have higher diffusion coefficients. However, the values of the slopes in this case are misleading for two reasons. First, they do not take into account the relative thickness of the films (0.018cm for 30% sulfonated membrane and 0.013cm for 60% sulfonated membrane). Second, the surface concentrations of the 30% and 60% samples are not equal due to the difference in the maximum vapor phase water uptake values achieved by the membranes. Since the diffusion coefficients should be independent of the initial concentration, upon normalization, the sample with higher maximum uptake might have a smaller diffusion coefficient, even if it has a larger initial slope of the

normalized mass curve (Equation 2.6.3). The reasons for higher diffusion coefficients calculated for 30% sulfonated membranes are not clear, but they might be attributed to the validity of the assumptions used in the calculations discussed in Section 5.2.

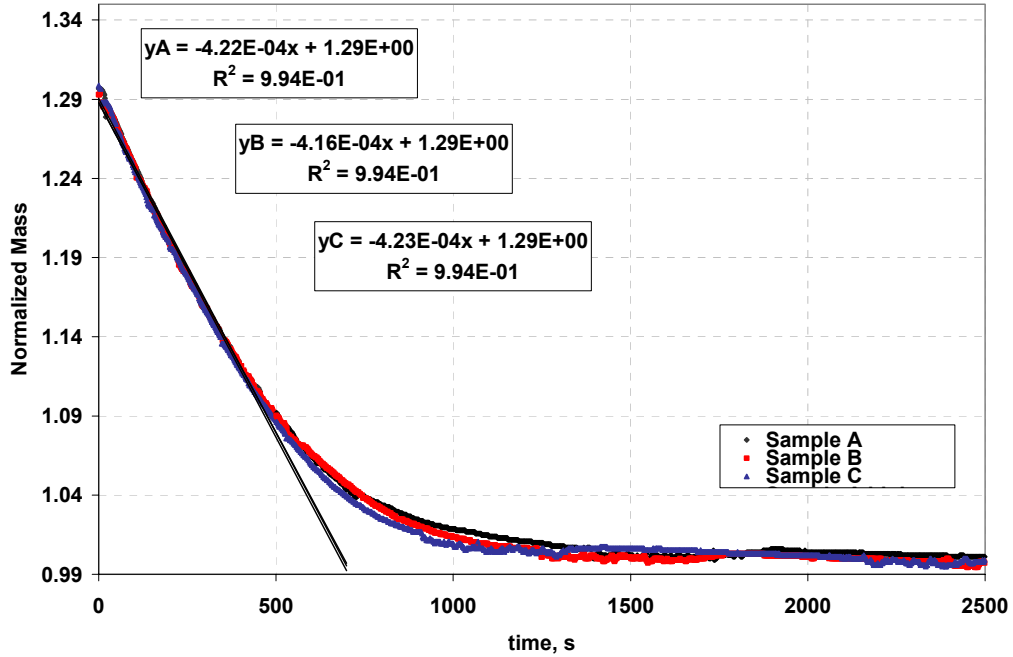


Figure 5.6.5 Water Desorption Behavior of 30% Sulfonated Dais® Membrane

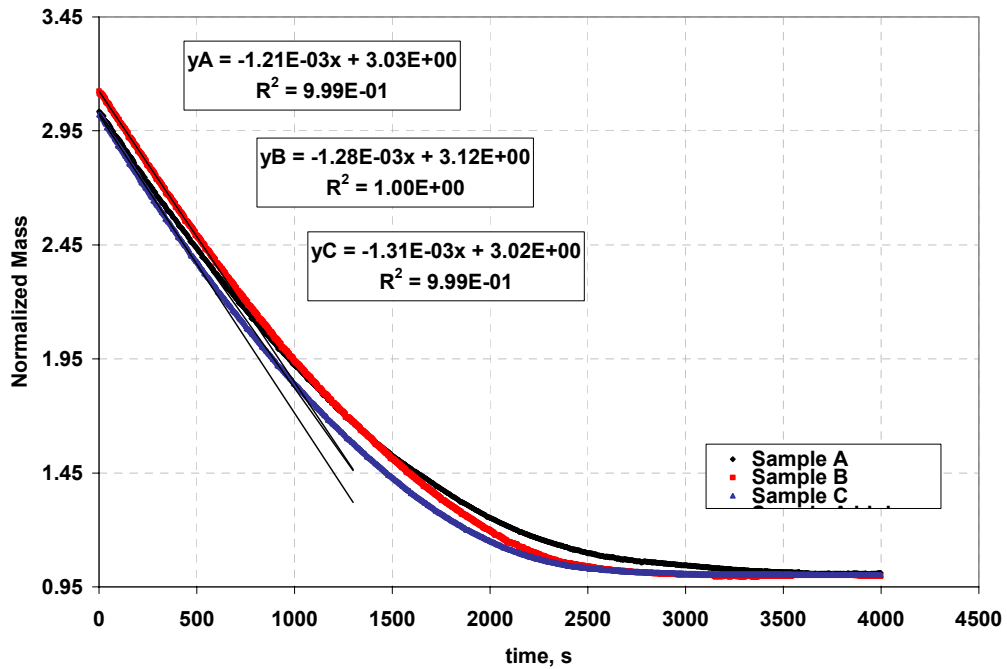


Figure 5.6.6 Water Desorption Behavior of 60% Sulfonated Dais® Membrane

## 5.7 Aging of Dais<sup>®</sup> Membranes

The aging of 30% sulfonated Dais<sup>®</sup> membranes was carried out in DI water at 90°C. As in the case of Nafion<sup>®</sup> membrane, the  $T_g$  of the Dais<sup>®</sup> material was expected to increase as a function of aging time and Arrhenius type of dependence between the  $T_g$  and the time was anticipated. However, the plots of natural log of time vs.  $1/T_g$  of the aging data for Dais<sup>®</sup> for each of the two independently conducted experiments did not demonstrate linearity. Based on the association with Nafion<sup>®</sup>, the data for both Dais<sup>®</sup> aging experiments were combined into one graph by plotting  $\ln(\text{time})$  as a function of the change in the glass transition temperature values,  $\Delta 1/T_g$ , for each data set. The resultant plot, shown in Figure 5.7.1, clearly demonstrates two linear regions with two different slopes. As in the case of Nafion<sup>®</sup>, data analysis indicates, that the changes in the Dais<sup>®</sup> material that take place as the result of “aging” are controlled by two distinct mechanisms.

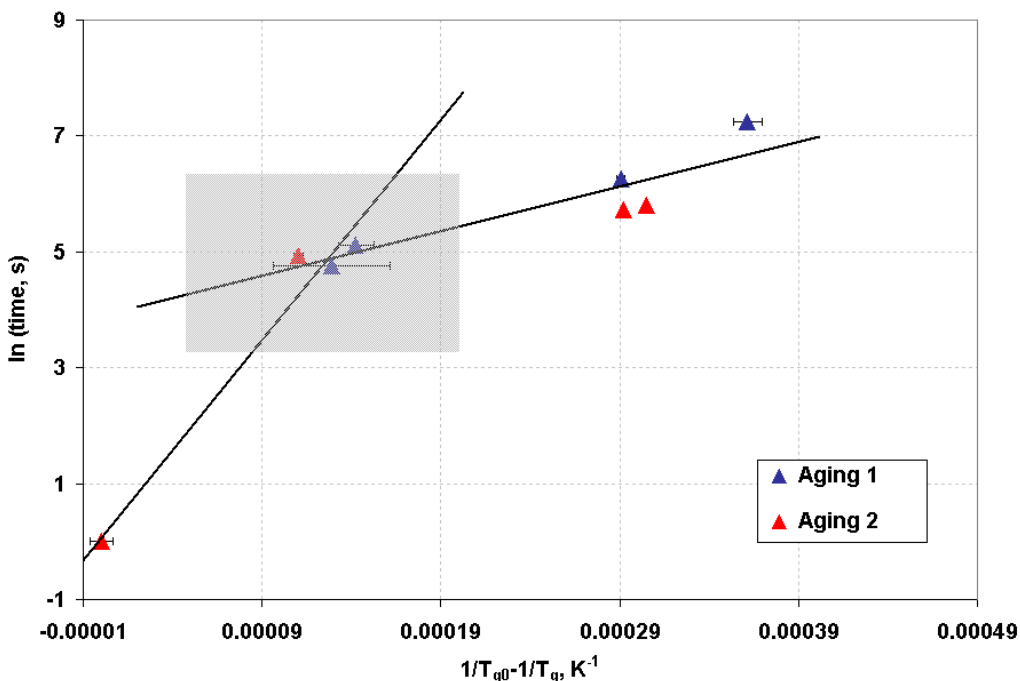


Figure 5.7.1 Results of 30% Sulfonated Dais<sup>®</sup> Aging Experiments

It was demonstrated in the previous sections that many properties of the Dais<sup>®</sup> membranes are directly linked to the formation and growth of ionic clusters. Since the

same relationships were established to apply to the Nafion<sup>®</sup> materials, it seems reasonable to draw similar conclusions about the nature of the processes controlling the “aging” of the Dais<sup>®</sup> membranes as the ones that were found for Nafion<sup>®</sup>. The diffusion properties of aged 30% sulfonated Dais<sup>®</sup> are summarized in Table 5.7.1 and material’s sorption and desorption isotherms are shown in Figure 5.7.2 and Figure 5.7.3. Diffusion coefficients show a moderate increase in the values as a function of aging, while the maximum water uptake of the aged membranes is more than two times higher than the one of virgin materials. The last findings confirm the idea that, similar to the “aging” of Nafion<sup>®</sup>, the mechanisms that control the changes of the materials properties in this case, are physical aging process in competition with the growth of the ionic clusters.

**Table 5.7.1 Diffusion Properties of Virgin and Aged Dais<sup>®</sup> Membranes**

	<b>30% Sulfonated Virgin Dais<sup>®</sup></b>	<b>30% Sulfonated Aged Dais<sup>®</sup></b>
Sorption	$(2.9 \pm 0.4) \times 10^{-8} \text{ cm}^2/\text{s}$	$3.9 \times 10^{-8} \text{ cm}^2/\text{s}$
Desorption	$(-4.2 \pm 0.04) \times 10^{-4} \text{ s}^{-1}$	$-1.4 \times 10^{-3} \text{ s}^{-1}$
Maximum Uptake	$27.2 \pm 0.2 \text{ wt}\%$	$85.8 \text{ wt}\%$

In the course of the aging study, it was possible to visibly monitor the changes in the mechanical properties of Dais<sup>®</sup> membranes as a function of “aging”. The materials, which were exposed to DI water at 90°C for a significant amount of time, were losing their structural integrity when handled in the saturated state. It was noticed that the membranes visibly deformed (the thickness decreased from 0.018cm to 0.013cm) and when dried, they felt coarse compared to the virgin films. The observed effects can be explained by both the aging and the growth of the ionic clusters. As the clusters grow, the amount of water absorbed by the membrane increases, leading to a drastic plasticization of the material resulting in the loss of the structural integrity of the saturated Dais<sup>®</sup> membranes. On the other hand, since the physical aging process results in the increase of the  $T_g$  of the dry material, the membranes are expected to become stiffer due to the collapse of the free volume leading to the decreased mobility of the chains.

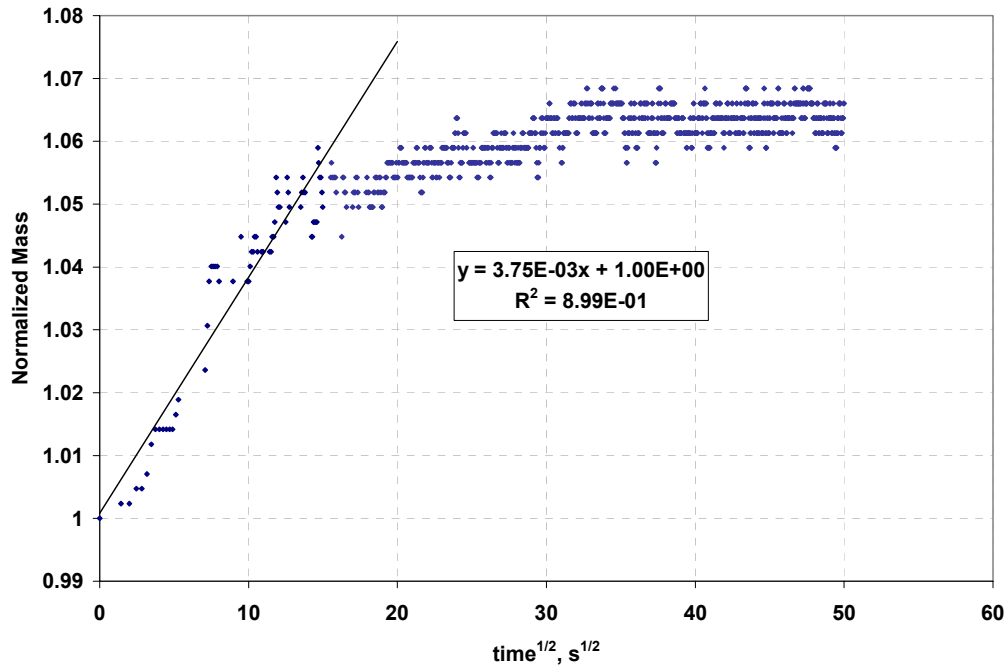


Figure 5.7.2 Vapor Phase Sorption Behavior of Aged 30% Sulfonated Dais<sup>®</sup> Membrane

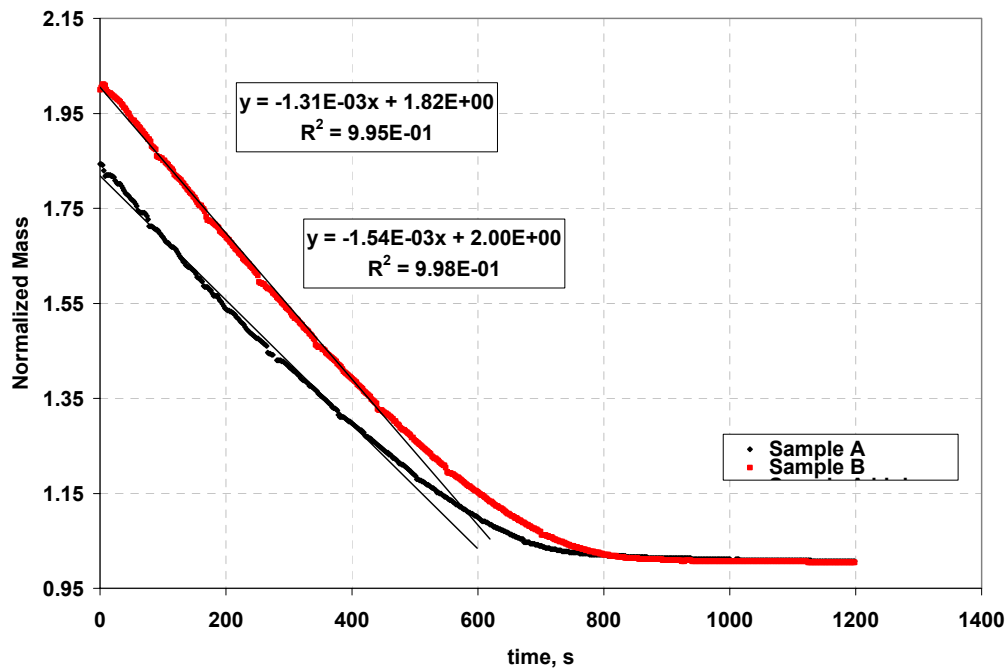


Figure 5.7.3 Water Desorption Behavior of Aged 30% Sulfonated Dais<sup>®</sup> Membrane

The possibility of chemical degradation of Dais<sup>®</sup> materials as a result of “aging” was also explored. The TGA analysis (Figure 4.4.6 and Figure 4.4.7) indicates that, although the peak of the derivative weight % curve of the “aged” specimen occurs 12°C lower than the that of the virgin membrane, the onset of the major weight loss for the aged sample is actually observed at a slightly higher temperature. Results of the FTIR analysis of the aged membranes are also inconclusive (Figure 4.5.8 and Figure 4.5.9). The intensity of the peaks through the whole spectrum decreases as a function of the aging time; however, the disappearance of the old peaks or the formation of the new peaks, indicative of the rupture or the formation of the chemical bonds, are not observed. The only feature that might signify that some changes do take place as a result of “aging” is the dissimilarity between the aged and unaged spectra in the 2900-2950 cm<sup>-1</sup> wavelength region; however it is unlikely that it is indicative of major variation in the chemical structure of the two membranes.

Additional experiments, which will be discussed in Chapter 7, might be conducted in order to conclude with certainty that the prolonged exposure of the 30% sulfonated Dais<sup>®</sup> membranes to DI water at elevated temperatures does not result in alteration of the chemical structure of this material. However, based on the data and the arguments presented in this work, it can be plausibly argued that sustained saturation of Dais<sup>®</sup> membranes at 90°C results not in chemical degradation, but in physical aging of the material counteracted by the growth of ionic clusters.

## 6 SUMMARY AND CONCLUSIONS

The purpose of this thesis was to investigate the effects of structure, humidity and aging on the properties of Nafion<sup>®</sup> and Dais<sup>®</sup> membranes. In the course of this work, electrical conductivity and structural integrity, the two crucial factors in the design and selection of the ionomers for fuel cell applications, were investigated. The changes in the structural integrity of the materials were related to the changes in the mechanical properties of the membranes as a function of aging and to the effects of saturation controlled by the level of sulfonation. Since electrical conductivity is related to proton and water diffusion through PEM, the water diffusion properties of the membranes were determined and found to depend on sulfonation levels, membrane pre-treatment methods and the time length of the exposure to high temperature saturated environments. It was found that a majority of the PEM properties were controlled by the formation and growth of ionic clusters that were the direct result of the ionic structure of these materials. The key conclusions of the study are summarized below.

In the process of this study, the structures of Nafion<sup>®</sup> and Dais<sup>®</sup> membranes were compared on the basis of the dynamic mechanical analysis, and the major differences in the mechanical response of Nafion<sup>®</sup> homopolymer and Dais<sup>®</sup> copolymers were discussed. The thermal degradation behavior of all three types of membranes was analyzed and found to be in agreement with the results reported in the literature.

As part of the structural properties examination of Dais<sup>®</sup> membranes, a mastercurve of 60% sulfonated Dais<sup>®</sup> material was constructed and a shift factor plot, associated with it, was created. The data from both can be utilized to predict the mechanical behavior of the membrane through a wide range of time and temperature.

The effects of sulfonation on the properties of the ionomers were investigated using Dais<sup>®</sup> membranes. The level of sulfonation was found to control the position of the upper glass transition temperature which moved from 140°C for 30% sulfonated Dais<sup>®</sup> membrane to 220°C for 60% sulfonated Dais<sup>®</sup> membrane. The sulfonation was also

determined to reduce the structural integrity of saturated Dais<sup>®</sup> membranes by increasing the amount of water absorbed by the material. This indicates that, in order to find the best balance of properties based on the particular application, the mechanical response of these ionomers can be controlled by the level of sulfonation of the membranes.

It was determined that saturation has a detrimental effect on the mechanical properties of the ionomers. The modulus of the saturated materials was found to decrease significantly as a result of plasticization by water. These findings are extremely important for several reasons. First, they raise the issue of structural integrity of the material as a result of the membrane exposure to saturated environments at elevated temperatures. Second, they demonstrate that in order to realistically predict the mechanical behavior of these membranes, tests should be performed in the environments similar to the ones that the materials will be exposed to during their use.

The effect of pre-treatment on the properties of Nafion<sup>®</sup> membranes was investigated. The glass transition temperature was determined to increase with an increase in the severity of the pre-treatment method. Based on the experiments performed as well as the literature analysis it was concluded that pre-treatment resulted in the facilitated growth of ionic clusters.

The diffusion properties of Nafion<sup>®</sup> and Dais<sup>®</sup> membranes were studied and the maximum water uptake and the diffusion coefficients for the vapor phase sorption at 100% RH for each membrane were determined. The sorption process was found to follow pseudo-Fickian type of behavior with  $n=0.6$ , while the movement of water out of the membranes during the desorption process was determined to be controlled by the mechanisms other than diffusion.

The aging studies of Nafion<sup>®</sup> and 30% sulfonated Dais<sup>®</sup> membranes generated several unexpected results. Prior to the experiments, it was anticipated that exposure of the membranes to DI water at elevated temperatures would result in an increase of the glass transition temperature and a drastic decrease in the values of the diffusion coefficients due to collapse of free volume. An Arrhenius type dependence was anticipated between aging time and the  $T_g$  of the membranes. However, it was determined that, although the  $T_g$ s of the membranes did increase, the expected linear dependence of the natural log of time on  $1/T_g$  did not exist. The shape of the

aforementioned plot suggested the existence of two competing mechanisms that were responsible for the changes in the properties of membranes as a function of “aging”. The results of diffusion properties studies of Nafion<sup>®</sup> and Dais<sup>®</sup> membranes were inconclusive; however, it was entirely possible that “aging” could increase the diffusion coefficients of these materials. Based on the results of this study and the literature review, it was concluded that two possible mechanisms responsible for the changes, observed as a result of exposure of Nafion<sup>®</sup> and Dais<sup>®</sup> to saturated environments at elevated temperatures, could be the process of physical aging and the growth of the ionic clusters. While the exact nature of the observed differences between virgin and “aged” membranes was not determined, this study clearly illustrated that the mechanical and diffusion properties of these ionomers changed as functions of time and exposure to elevated temperatures.

Although this thesis was aimed at investigating the PEM properties essential for fuel cell applications, the results of the study are also relevant to the other areas in which these types of ionic membranes are employed. For example, one of the research projects at Virginia Tech focuses on using Nafion<sup>®</sup> materials as actuators and sensors for a variety of applications. In that study, a Nafion<sup>®</sup> strip saturated by water or ion solution is clamped on one side and the electrical bias is applied. The strip bends in response to the bias and the bending mode and its extent are dependent on the water content of Nafion<sup>®</sup> material. The results of this thesis that address the effect of saturation on the mechanical behavior of ionic membranes and the nature of their diffusion properties can be used to better understand the dependence of the material bending mode, resulting from applied electrical potential, on the water content of Nafion<sup>®</sup>.

As a whole, this work reiterates the need to include the factor of time dependence of the mechanical properties of PEMs into predictions of the long-term performance of fuel cells, as well as demonstrates the importance of applying familiar theoretical concepts, such as the time-dependence of the viscoelastic polymers, plasticization and others, to the processes of material selection and performance prediction for different applications that involve the use of polymeric ionomers.

## 7 FUTURE WORK

This thesis has left many questions unanswered and a range of experiments can be conducted in order to prove unequivocally some of the ideas presented in this work and to clarify others.

The position of the  $\alpha$  transition in Nafion<sup>®</sup> and its sensitivity to water plasticization were determined by dynamic mechanical analysis. However, DMA was found to be an inefficient tool for studying the  $\beta$  relaxation of Nafion<sup>®</sup> and the effect of humidity on the position of the  $\beta$  peak. As shown by Yeo and Eisenberg<sup>12</sup>, the dielectric measurement techniques can be successfully employed to analyze the  $\beta$  transition. Additional experiments can be conducted using this method in order to better understand the nature of the  $\beta$  relaxation.

The mechanical responses of dry and saturated Nafion<sup>®</sup> and Dais<sup>®</sup> membranes were compared in this study and plasticization was determined to have a profound effect on the relaxation of these materials. The next logical step in this study would be the evaluation of the mechanical properties of the ionomers at intermediate water contents. Varying degrees of moisture content in the material can be established by either equilibrating the films over salt solutions to obtain the environments of different relative humidity or by building an environmental chamber around the DMA sample stage (this work is currently under way at Virginia Tech).

The diffusion properties of Nafion<sup>®</sup> and Dais<sup>®</sup> membranes were measured for the conditions of 100% RH for sorption isotherms and 10% RH for desorption isotherms at 25°C. The measurements at different levels of humidity and at a range of temperatures will result in a more systematic study of the diffusion kinetics of these ionomers. The activation energies for sorption process can also be obtained for a range of RH values for both Nafion<sup>®</sup> and Dais<sup>®</sup> membranes.

The benefits of pre-treating Nafion<sup>®</sup> membranes prior to use were addressed in this work and in the literature. It was demonstrated that the treatment procedures result in the growth of ionic clusters and ultimately in the increase of the water diffusion

coefficients and the overall conductivity of the membranes. However, the concept of pre-treatment was never applied to Dais<sup>®</sup> membranes. A study that would determine the feasibility of this procedure for Dais<sup>®</sup> material can prove to be useful from the application point of view.

Additional experiments could also be conducted in order to take a more detailed look into the effect of elevated temperatures on the structure of Dais<sup>®</sup> membranes. A technique, like solid state NMR, that is more sensitive than FTIR to the chemical changes in the polymer molecule, could more precisely explore potential alterations in the molecular structure of these ionomers. A modified thermal degradation study of Dais<sup>®</sup> material can also answer questions about the thermal stability of the membranes. The weight loss information, obtained by the use of conventional TGA, does not provide an insight into the nature of the chemical groups being broken off. However, if a mass spectrometer is connected to the TGA unit, it can help to determine precisely the onset of the decomposition of sulfonic groups and the boundaries of thermal stability.

Lastly, further investigation is required in order to understand the nature of the effects that exposure to saturated environments at elevated temperatures has on the properties of the ionomers. The preliminary findings attributed these effects to the counteractive actions of physical aging and the growth of ionic clusters. In order to verify the validity of these arguments, the diffusion kinetics should be measured as a function of “aging” for the samples exposed to the saturated environments for the range of temperatures. From the shapes of the plots of natural log of time as a function of  $1/T_g$ , it is apparent that whatever mechanisms are responsible for the observed differences between “aged” and virgin materials, there should be one dominating process for each of the two linear regions. If physical aging dominates the changes in the first time interval, there would be an observable decrease in the values of the sorption diffusion coefficients due to the collapse of free volume. When ionic cluster growth takes over, the values of the diffusion coefficients are expected to increase. If ionic cluster formation dominates the initial time periods, the opposite observation is expected. The change in the rate of increase or decrease of the diffusion coefficients as a function of time should correspond to the time interval associated with a transition (“gray box”) region of log time vs.  $1/T_g$  plot. The growth and/or the formation of the ionic clusters can be verified by performing

Small Angle X-ray analysis (SAXS) on the materials aged for different amounts of time and in the different temperature environments. This data can then be correlated to changes in the shapes of the log time vs.  $1/T_g$  plots in order to obtain a more accurate information about the processes controlling the material structure as a result of the exposure to high temperature saturated environments.

## 8 REFERENCES

- <sup>1</sup> M.W.Verbrugge, R.F.Hill, *J. Eletrochem. Soc.*, **137**, 3370 (1990)
- <sup>2</sup> T.E.Springer, T.A.Zawodzinski, S.Gottesfeld, *J. Eletrochem. Soc.*, **138**, 2334 (1991)
- <sup>3</sup> J.C.Amphlett, R.M.Baumert, R.F.Mann, B.A. Peppley, P.R. Roberge, *J. Eletrochem. Soc.*, **142**, 1 (1995)
- <sup>4</sup> J.C.Amphlett, R.M.Baumert, R.F.Mann, B.A.Peppley, P.R. Roberge, *J. Eletrochem. Soc.*, **142**, 9 (1995)
- <sup>5</sup> G.E.Wnek, S.G.Ehrenberg, J.M.Serpico, B.M.Sheikh-Ali, T.N.Tangredi. E.Zador, *Second International Symposium on New materials for Fuel Cell and Modern Battery Systems*, Canada
- <sup>6</sup> U.S. Fuel Cell Council, *Fuel Cell Glossary*, August 19, 1999
- <sup>7</sup> Energy Partners, Inc. Technical Information
- <sup>8</sup> Mark W. Verbrugge, Eric W. Shneider, Robert S. Conell, Robert F. Hill, *J.Electrochem. Soc.*, **139**, 3421 (1992)
- <sup>9</sup> M.W.Verbrugge, R.F.Hill, *J. Eletrochem. Soc.*, **137**, 886 (1990)
- <sup>10</sup> H.L. Yeager, *J. Eletrochem. Soc.*, **128**, 1880 (1981)
- <sup>11</sup> T.A.Zawodzinski, M.Neeman, L.O.Sillerud, S.Gottesfeld, *J. Phys. Chem.*, **95**, 6040 (1991)
- <sup>12</sup> S.C.Yeo, A.Eisenberg, *J. Appl. Polym. Sci.*, **21**, 875 (1977)
- <sup>13</sup> T.Kyu, A.Eisenberg, *Proceedings American Chemical Society*, ch 6, 1982
- <sup>14</sup> G.E.Wnek,B.M.Sheikh-Ali, J.M.Serpico, S.G.Ehrenberg,, T.N.Tangredi, C.Karuppaiah, Y.Ye, *Polym. Prepr.*, **39**, 54 (1998).
- <sup>15</sup> F.S.Bates, G.H.Fredrickson, *Physics Today*, 32 (Feb 1999)
- <sup>16</sup> L.H.Sperling, *Introduction to Physical Polymer Science*, 2<sup>nd</sup> ed., John Wiley & Sons Inc., New York, **8**, pp.303-382 (1992)
- <sup>17</sup> G.Odian, *Principles of Polymerization*, 3<sup>rd</sup>ed., John Wiley & Sons Inc., New York, **1**, p33(1991)
- <sup>18</sup> R.A.Weiss, A.Sen, C.L.Willis, L.A.Pottick, *Polymer*, **32**, n10, 1867 (1991).

- 
- <sup>19</sup> H.L.Yeager, A.Steck, *J. Elettrochem. Soc.*, **128**, n9, 1880 (1981)
- <sup>20</sup> S.H.DeAlmeida, Y.Kawano, *Eur. Polym. J.*, **33**, n8, 1307 (1997)
- <sup>21</sup> L.H.Sperling, *Introduction to Physical Polymer Science*, 2<sup>nd</sup> ed., John Wiley & Sons Inc., New York, **10**, pp.479-482 (1992)
- <sup>22</sup> I.M.Ward, D.W.Hadley, *An Introduction to the Mechanical Properties of Solid Polymers*, John Wiley & Sons Inc., New York, **6**, pp.91-102 (1998)
- <sup>23</sup> C.A.Daniels, *Polymers: Structure and Properties*, Technomic Publishing Company, Inc., Lancaster, PA, **2**, pp.21-22 (1989)
- <sup>24</sup> N.Sivashinsky, G.B.Tanny, *J. Appl. Polym. Sci.*, **26**, 2625 (1981)
- <sup>25</sup> M.W.Verbrugge, E.W. Schneider, R.S.Conell, R.F.Hill, *J. Elettrochem. Soc.*, **139**, n12, 3421 (1992)
- <sup>26</sup> T.A.Zawodzinski, C.Derouin, S.Radzinski, R.J.Sherman, V.T.Smith, T.E.Springer S.Gottesfeld, *J. Elettrochem. Soc.*, **140**, n 4, 1041 (1993)
- <sup>27</sup> T.A.Zawodzinski, T.E.Springer, J.Davey, R.Jestel, C.Lopez, J.Valerio, S.Gottesfeld, *J.Elettrochem. Soc.*, **140**, n 7, 1981 (1993)
- <sup>28</sup> J.Halim, F.N.Buchi, O.Haas, M.Stamm, G.G.Scherer, *Electrochimica Acta*, **39**, n 8/9, 1303 (1994)
- <sup>29</sup> J.T.Hinatsu, M.Mizuhata, H.Takenaka, *J. Elettrochem. Soc.*, **141**, n 6, 1493 (1994)
- <sup>30</sup> Yoshitsugu.Sone, Per Ekdunge, Daniel Simonsson, *J. Elettrochem. Soc.*, **143**, n 4, 1254 (1996)
- <sup>31</sup> H.S.Sodaye, P.K.Pujari, A.Goswami, S.B.Manohar, *J. Polym. Sci: Part B: Polym. Phys.*, **36**, 983 (1998)
- <sup>32</sup> R.Duplessix, M.Escoubes, B.Rodmacq, F.Volino, E.Roche, A.Eisenberg, M.Pineri, *Proceedings American Chemical Society*, ch 28, 469 (1980)
- <sup>33</sup> Takeji Hashimoto, Mineo Fujimura, Hiromichi Kawai, *Proceedings American Chemical Society*, ch 11, p217 (1982)
- <sup>34</sup> Klaus-Dieter Kreuer, T. Dippel, W. Meyer, J.Maier, *Mat. Res. Soc. Symp. Proc.*, **293**, p271 (1993)
- <sup>35</sup> Marcella Cappadonia, J. Wilhelm Erning, Ulrich Stimming, *J. Electroanalytical Chem.*, **376**, 189 (1994)

- 
- <sup>36</sup> D.R.Morris, Xiaodong Sun, *J. Appl. Polym. Sci.*, **50**, 1445 (1993)
- <sup>37</sup> T.Takamatsu, M.Hashiyama, A.Eisenberg, *J. Appl. Polym. Sci.*, **24**, 2199 (1979)
- <sup>38</sup> C.A.Edmondson, J.J.Fontanella, S.H.Chung, S.G.Greenbaum, G.E.Wnek, *Electrochim. Acta*, **46**, n 10/11, 1623 (2001)
- <sup>39</sup> P.G. Shewman, *Diffusion in Solids*, McGraw-Hill Publishing., New York, p.124 (1963)
- <sup>40</sup> R.McGregor, *Diffusion and Sorption in Fibers and Films*, Academic Press Inc., New York, (1974)
- <sup>41</sup> J.L.McPeak, PhD. Dissertation, “*Solvent-Induced Crystallization of Poly(Ether Ether Ketone)*”, Virginia Polytechnic Institute and State University, pp8-11, 1999
- <sup>42</sup> J.Crank, *The Mathematics of Diffusion*, Clarendon Press, Oxford, 2<sup>nd</sup> ed, (1975)
- <sup>43</sup> M.Hara, P.Jar, J.A.Sauer, *Polymer*, **32**, 9, 1622 (1991)
- <sup>44</sup> J.Suroweic, R.Bogoczek, *J. Therm. Analysis*, **33**, 1097 (1988)
- <sup>45</sup> S.R.Samms, S.Wasmus, R.F.Savinell, *J. Electrochem. Soc.*, **143**, n 5, 1498 (1996)
- <sup>46</sup> S.H.DeAlmeida, Y.Kawano, *J. Therm. Analysis and Calorimetry*, **58**, 569 (1999)
- <sup>47</sup> DuPont Technical Information Data Sheet, Jan 1998
- <sup>48</sup> J.L.McPeak, PhD. Dissertation, “*Solvent-Induced Crystallization of Poly(Ether Ether Ketone)*”, Virginia Polytechnic Institute and State University, pp37-38, 1999
- <sup>49</sup> R.S.Chen, J.P.Jayakody, S.G.Greenbaum, Y.S.Pak, G.Xu, M.G.McLin, J.J.Fontanella, *J. Electrochem. Soc.*, **140**, n 4, 889 (1993)
- <sup>50</sup> D.A.Skoog, J.L.Leary, *Principles of Instrumental Analysis*, 4<sup>th</sup> ed., Saunders College Publishing, **12**, pp.252-261 (1992)
- <sup>51</sup> D.A.Skoog, J.L.Leary, *Principles of Instrumental Analysis*, 4<sup>th</sup> ed., Saunders College Publishing, **16**, pp.394-399 (1992)
- <sup>52</sup> Mineo Fujimura, Takeji Hashimoto, Hiromichi Kawai, *Macromolecules*, **14**, 1309 (1981)
- <sup>53</sup> P.Krtil, A.Trojanek, Z.Samec, *J Phys. Chem.: Part B*, **105**, 7979 (2001)
- <sup>54</sup> R.J.Young, *Introduction to Polymers*, Chapman and Hall, New York, p204 (1983)
- <sup>55</sup> *Polymer Data Handbook*, Oxford University Press Inc., p344 (1999)

---

## VITA

Julie Uan-Zo-li, daughter of Tamara Golovach and Mikhail Dvorkin, was born on March 19, 1973 in Minsk, Belarus. She attended the city school of Minsk from 1980 to 1990 and the nursing school from 1990 to 1991. In December of 1991, Julie immigrated to the United States. In 1993 she graduated from Eagan High School in Eagan, MN after attending University of St. Thomas in St. Paul, MN as a part of the post-secondary program. In June of 1996, she graduated with a Bachelor of Science degree in Chemical Engineering from the University of Minnesota. While at the University of Minnesota Julie worked as a technical aide at 3M Science Research Laboratory. In August of 1996 Ms. Uan-Zo-li moved to Blacksburg, VA to pursue a graduate degree in Materials Science and Engineering at Virginia Polytechnic Institute and State University.